

# **Modelling of glacier and snow melt processes within the hydrological catchment model WaSiM-ETH**

Lisette Klok and Kees Roelofsma

Supervisors:

Ir. P.M.M. Warmerdam (WU)

Dr. J. Gurtz and Dipl.-Hydr. K. Jasper (ETHZ)

**RAPPORT 85**

Sectie Waterhuishouding  
Nieuwe Kanaal 11, 6709 PA Wageningen

ISSN 0926-230X

gbv 702

*There is a theory which states that if ever anyone discovers exactly what the Universe is for and why it is there, it will instantly disappear and be replaced by something even more bizarre and inexplicable.*

*There is another which states that this has already happened.....*

Douglas Adams

## Preface

Two Dutch students, coming from Wageningen Agricultural University, are going to the ETHZ (Eidgenössische Technische Hochschule Zürich) in Switzerland to study glaciers. They are interested in the effects of climate change on glaciers, but they are also fascinated by the processes of snow and glacier melt, and the hydrology of glacierized catchment areas. One of them is a hydrological student while the other is a student in meteorology. What has possessed them to study glaciers in Switzerland? Glaciers do not exist in the Netherlands and the annual snowfall in the Netherlands is also negligible. Dutch mountains only appear in songs or dreams. So, what do Dutch students actually know about glaciers and the hydrology of mountainous areas? In any case, mountains are attractive if you are living in a flat country. As are glaciers and snowfall. Besides, Zürich is a big city and the ETH a large university, compared to Wageningen.

Really, we have never regretted going to Zürich to study glacier melt processes within the hydrological model WaSiM-ETH (Waterbalance Simulation Model). The subject of our thesis was very interesting and a perfect combination of hydrology and meteorology. WaSiM-ETH is truly an amazing hydrological model to work with, taking into account many hydrological processes within a catchment area. It was very instructive to work with WaSiM-ETH. Further, we do not regret that we did this thesis together. Working together is so much nicer than working alone. The advantage of working together is the enthusiasm and encouragement you give each other.

We would like to thank numerous people, who made our stay and study in Zürich successful and unforgettable.

First of all, we would like to thank our supervisor Piet Warmerdam, who sent us to the ETH in Switzerland. When we informed him about our ideas of doing a thesis together, about climate change, glaciers, snow melt and hydrology, in a foreign country, he made contacts with Prof. Herbert Lang in Zürich. We always enjoyed the stimulating e-mails we got in Switzerland, which were typically more fatherly than scientific. Many thanks go to Joachim Gurtz, who was our supervisor in Switzerland and made our stay possible by organizing a working place in the institute, a room in Zürich and an 'Erasmus stipendium'. We will remember the tea breaks, and especially the (pine-) applecakes in the afternoon, the trip to the Titlis mountain, the cheese fondue and the nice stories about Joachim's sons. Special thanks also go to Karsten Jasper, who did the programming of the glacier model and supported us by understanding WaSiM-ETH. He often came up with some brilliant ideas when WaSiM-ETH did not work the way we wanted it to. We will not forget the pleasant times we had with him during the weekends.

We are very grateful to Alex Badoux for showing us around the university and Zürich. He was also working on his thesis and worked on a similar project. We enjoyed the co-operation with him and the games he invented during working time. Thanks to Raelene Sheppard, who checked the English grammar. She also made our period at the institute pleasant by the Mövenpick ice-cream and the nice talks we had with her. We would like to thank Massimiliano Zappa for helping us with the preparation of the geographical data and his always present excitements involving the simulation results of WaSiM-ETH.

Tomas Vitvar is acknowledged for preparing the meteorological data. We also would like to acknowledge Jörg Schulla the developer of WaSiM-ETH, who provided us with some useful information about WaSiM. Thanks are due to Prof. Herbert Lang for commenting on our thesis.

Kees Roelofsma and Lisette Klok  
April, 1999

## Summary

Glaciers play an important role in the hydrological processes of partly glacierized areas in mountainous or arctic areas. During the melt season, glaciers contribute significant quantities of melt water to the discharge of partly glacierized catchment areas. Glaciers store precipitation during winter. Until now, no hydrological models existed with the ability to simulate discharges of partly glacierized areas since glacier melt processes were not simulated within these models. Therefore, the water balance of many mountainous areas and the daily discharge fluctuations during the melt season could not be accurately calculated. The aim of this research was to incorporate a submodel, which simulates glacier melt processes, into the hydrological model WaSiM-ETH (Waterbalance Simulation Model), in order to apply WaSiM-ETH to partly glacierized catchment areas.

WaSiM-ETH is a spatial distributed model, developed by Schulla (1997). It simulates the hydrologically important components of the rainfall-runoff system. WaSiM-ETH contains several submodels for modifying meteorological input data according to exposition and topographic shading, and for spatial interpolation, as well as for simulating evapotranspiration, snow accumulation and melt, interception, infiltration, surface runoff, interflow and baseflow. The minimal meteorological input data are precipitation and air temperature. Further, a digital elevation model and grid information about soil type and land use are required to run WaSiM-ETH. The spatial resolution is given by a regular grid, which can be any size. The temporal resolution can vary from very short up to some days. WaSiM-ETH is able to complete simulations when only a few input data are available. However, additional and detailed data are needed to gain optimal simulation results.

Two temperature index methods are incorporated into WaSiM-ETH to simulate glacier melt processes. Both methods are based on a study of Hock (1998). The first method is called 'the classical degree day method'. The classical degree day method is based on the relationship between positive temperature sums and melt rate. The second temperature index method includes measured global radiation, aiming at a better simulation of diurnal melt cycles and spatial distribution of melt rates.

To calculate melt water quantities, the glacier is divided into three areas: snow, firn and ice. Firn, often covered by fresh snow, is defined as the area above the equilibrium line. At the equilibrium, glacier melt and snowfall are in balance. In WaSiM-ETH, the equilibrium line is defined by an input grid. Above the equilibrium line the amount of snowfall exceeds glacier melt. The mass balance is negative below the equilibrium line. The snow covered area below the equilibrium line is defined as snow area. Ice is defined as the area of exposed ice below the equilibrium line. The algorithms which calculate glacier melt contain different melt coefficients for ice, firn and snow.

The transformation of the melt water discharge of the snow, firn and ice areas to the glacier snout is simulated by three parallel linear reservoirs.

WaSiM-ETH, including the glacier melt model, is tested on the Gletsch catchment (Switzerland). 52% of this catchment area is glacierized. The total area of the Gletsch catchment is 39 km<sup>2</sup>. The temperature index method, including the radiation factor, was used for the simulations. A spatial resolution of 100 m and a temporal resolution of one hour are used. A parameter sensitivity is carried out to study the sensitivity and dependency of the new parameters and coefficients. The simulation results of WaSiM-ETH, including the glacier melt model, are compared to observed discharges. The results for the Gletsch catchment have improved considerably compared to the simulation results of WaSiM-ETH without the glacier model. The year 1992 is used for calibration ( $R^2 = 0.93$ ) and the years 1993 to 1996 for validation ( $R^2$  ranged from 0.91 to 0.94). Further, the results of the

## Summary

validation period show that WaSiM-ETH can now be successfully applied to partly glacierized catchment areas.

Simulation of 1992, applying the classical degree day method, yielded worse simulation results compared to the results simulated by the temperature index method including a radiation factor. The classical degree day method is not able to accurately simulate diurnal discharge fluctuations.

WaSiM-ETH, including the glacier model, is also applied to another catchment area, the Aletsch catchment (Switzerland), to test the consistency of the model. The Aletsch catchment is glacierized for 66% and has an area of 195 km<sup>2</sup>. The values for the parameters and coefficients were taken as for the Gletsch catchment. The good results for 1992 ( $R^2 = 0.86$ ) are indicators of the elasticity of the model.

## Samenvatting

Gletsjers spelen een belangrijke rol in de hydrologische processen van gedeeltelijk vergletsjerde gebieden in hooggebergtes of arctische gebieden. Tijdens het smeltseizoen leveren gletsjers een belangrijke bijdrage aan de afvoer van gedeeltelijk vergletsjerde stroomgebieden en in de winter wordt neerslag in gletsjers opgeslagen in de vorm van sneeuw en ijs. Tot voor kort waren er geen hydrologische afvoermodellen die in staat waren afvoeren van gedeeltelijk vergletsjerde gebieden te modelleren, omdat deze modellen niet beschikten over een module dat op een realistische wijze de processen van gletsjersmelt simuleert. Derhalve was het voor veel gebieden onmogelijk de waterbalans kloppend te krijgen en de dagelijkse variatie in afvoer te simuleren. Vooral stroomgebieden in hooggebergtes vielen hierdoor buiten de reikwijdte van model studies. Het doel van dit onderzoek was, het inbouwen van een module voor de berekening van het gletsjersmeltproces in het neerslag-afvoer model WaSiM-ETH (Waterbalance Simulation Model), waardoor de toepasbaarheid van dit model ook zou gaan gelden voor gedeeltelijk vergletsjerde gebieden.

Het ruimtelijk verdeelde, raster georiënteerde model WaSiM-ETH is ontwikkeld door Schulla (1997). Het model simuleert de belangrijkste processen van het neerslag-afvoer systeem. WaSiM-ETH omvat een aantal submodellen waarmee meteorologische gegevens worden gecorrigeerd en geïnterpoleerd over de ruimte, alsmede evapotranspiratie, sneeuwaccumulatie en -smelt, interceptie, infiltratie, oppervlakte afstroming, interflow en basisafvoer worden berekend. Het minimum aan input gegevens voor WaSiM-ETH bestaat uit de meteorologische gegevens temperatuur en neerslag, en grid gegevens voor topografische hoogte, landgebruik en bodemtype. De ruimtelijke resolutie van WaSiM-ETH kan elke grootte aannemen en de tijdstap waarmee gerekend wordt kan variëren van kort tot een aantal dagen. Het model is dusdanig opgezet dat bij een beperkte beschikbaarheid aan gegevens toch gerekend kan worden. Indien er meer gedetailleerde gegevens aanwezig zijn, kunnen deze bij de berekeningen worden betrokken, wat de betrouwbaarheid van de resultaten ten goede komt.

Om de gletsjersmeltprocessen te simuleren, zijn twee temperatuur index methodes ingebouwd in WaSiM-ETH. Deze methodes zijn gebaseerd op werk van Hock (1998). De eerste methode, 'the classical degree day method', is gebaseerd op de relatie tussen de positieve temperatuursom en de smeltsnelheid. De tweede methode bevat naast de temperatuur, ook een factor voor globale straling, waardoor de dagelijkse en ruimtelijke variatie in gletsjersmelt beter wordt gesimuleerd.

Om de hoeveelheid smeltwater in de tijd te berekenen, wordt de gletsjer onderverdeeld in drie verschillende gebieden: sneeuw, firn en ijs. Het gebied boven de evenwichtslijn, vaak bedekt met verse sneeuw, is gedefinieerd als firn. De evenwichtslijn is de lijn waarboven meer sneeuw valt dan smelt en wordt in WaSiM-ETH bepaald door een input grid. Beneden de evenwichtslijn is de massabalans negatief en smelt er meer dan dat er aan sneeuwval bijkomt. Voor dit laatste gebied wordt balansmatig bijgehouden welk gedeelte bedekt is met sneeuw (het sneeuwgebied) en welk deel met ijs (het ijsgebied). In de algoritmes die de hoeveelheid smeltwater in de tijd simuleren, verschillen de smeltcoëfficiënten voor ijs van die van sneeuw en firn.

De transformatie van de afvoer van het smeltwater van het sneeuw-, firn- en ijsgebied naar het eindpunt van de gletsjer wordt gesimuleerd door drie parallelle lineaire reservoirs.

WaSiM-ETH inclusief het gletsjermodel is getest op het stroomgebied waarin de Rhonegletsjer is gesitueerd (Zwitserland), het Gletsch gebied. Dit stroomgebied heeft een oppervlakte van 39 km<sup>2</sup> en is voor 52% vergletsjerd. Bij de berekeningen is gebruik gemaakt van de temperatuur index methode die de stralingsfactor bevat. Er is gerekend met een

ruimtelijke resolutie van 100 m en een tijdstap van een uur. Een gevoeligheids-analyse is uitgevoerd om de nieuwe coëfficiënten in het model op hun gevoeligheid en afhankelijkheid te testen. De modelresultaten van WaSiM-ETH inclusief het gletsjermodel zijn vergeleken met gemeten afvoeren en toonden een aanzienlijke verbetering ten opzichte van de resultaten van WaSiM-ETH zonder gletsjermodel. Het jaar 1992 is gebruikt voor calibratie ( $R^2 = 0.93$ ) en de jaren 1993 t/m 1996 voor validatie ( $R^2$  variërend tussen 0.91 en 0.94). Ook de goede resultaten voor de gevalideerde jaren tonen aan dat door dit onderzoek de toepasbaarheid van WaSiM-ETH is uitgebreid tot (gedeeltelijk) vergletsjerde gebieden.

Een vergelijking met de resultaten van 1992 waarbij de 'classical degree day' methode is gebruikt, liet zien dat deze methode minder geschikt is de dagelijkse variatie in afvoer te simuleren.

WaSiM-ETH inclusief het gletsjermodel is ook op een ander gebied, het Aletsch gebied, getest. Het Aletsch gebied ligt ook in Zwitserland, is voor 66% vergletsjerd en heeft een oppervlakte van 195 km<sup>2</sup>. De waarden van de parameters en coëfficiënten zijn gelijk genomen aan de waarden voor het Gletsch gebied. Voor een eerste run leverde WaSiM-ETH inclusief het gletsjermodel goede resultaten ( $R^2 = 0.86$ ). De goede resultaten geven de elasticiteit van het model aan.

# Contents

Preface .....	5
Summary .....	7
Samenvatting .....	9
Appendices .....	12
List of symbols .....	13
1 Introduction .....	17
2 Glaciers, the theory and their modelling .....	19
2.1 Introduction .....	19
2.2 The glacier water budget .....	19
2.3 Glacier melt .....	20
2.4 Glacier runoff .....	22
2.4.1 Runoff characteristics .....	22
2.4.2 Water transport through the glacier .....	23
2.5 Modelling of glacier melt and runoff .....	24
2.5.1 Glacier melt models .....	24
2.5.2 Glacier runoff models .....	28
3 The Waterbalance Simulation Model .....	31
3.1 Introduction .....	31
3.2 Structure of WaSiM-ETH .....	31
3.3 Preprocessing, processing and postprocessing .....	33
3.4 Submodels of WaSiM-ETH .....	34
3.4.1 Interpolation of input data .....	34
3.4.2 Precipitation correction .....	35
3.4.3 Radiation correction and temperature modification .....	35
3.4.4 Evapotranspiration .....	35
3.4.5 Interception .....	36
3.4.6 The soil water model .....	37
3.4.7 Discharge routing .....	39
3.5 Snow and glacier submodel .....	39
3.5.1 Introduction .....	39
3.5.2 Snow accumulation .....	40
3.5.3 Snow melt on unglacierized areas .....	40
3.5.4 Glacier melt and melt water transport .....	40
4 Application of the model .....	43
4.1 Introduction .....	43
4.2 Description of the Gletsch catchment .....	43
4.3 Acquisition of the required input data .....	45
4.3.1 Meteorological data .....	45
4.3.2 Geographical data .....	46
4.3.3 Hydrological data .....	47
4.4 Assessment of initial values .....	47
4.5 Parameter values .....	50
4.6 Spatial and temporal resolution .....	50
5 Calibration criteria and sensitivity analysis of parameters .....	53
5.1 Introduction .....	53
5.2 Efficiency criteria .....	53
5.3 Sensitivity Analysis .....	54
5.3.1 Melt Factor .....	55
5.3.2 Radiation coefficients for ice and snow .....	55
5.3.3 Storage constants .....	56



5.3.4 Degree Day Factor.....	58
5.3.5 Height of firm area .....	58
5.3.6 Spatial resolution.....	59
5.4 Interdependency between parameters.....	60
6 Results of simulations .....	63
6.1 Introduction .....	63
6.2 Calibration results of WaSiM-ETH.....	63
6.2.1 Without the glacier model .....	63
6.2.2 The glacier model included .....	65
6.3 Validation results of WaSiM-ETH.....	68
6.4 Comparison of two temperature index methods.....	70
6.5 Application on the Aletsch catchment .....	71
6.5.1 Description of the Aletsch catchment .....	71
6.5.2 Results of the Aletsch catchment .....	73
7 Discussion of the results.....	75
8 Recommendations .....	79
References .....	81

## Appendices

Appendix 1:	Meteorological data and discharge for the Gletsch catchment for 1992
Appendix 2:	Control-file for WaSiM-ETH including glacier model
Appendix 3:	Data flow of WaSiM-ETH
Appendix 4:	Retreat of Rhone glacier
Appendix 5:	Location of meteorological stations
Appendix 6:	Digital Elevation Model for the Gletsch catchment
Appendix 7:	Digital landuse grid for the Gletsch catchment
Appendix 8:	Time series for the validation years

## List of symbols

$\alpha$	Albedo	-
$\beta$	Local slope	°
$\Delta$	First derivative of the saturated vapour pressure curve	$\text{hPa}\cdot\text{K}^{-1}$
$\Delta S$	Storage change in the water balance	mm
$\Delta t$	Timestep	h
$\epsilon_a$	Emissivity of the atmosphere	-
$\epsilon_s$	Emissivity of the surface	-
$\gamma_p$	Psychrometric constant	$\text{mbar}\cdot\text{K}^{-1}$
$\eta$	Maximum relative soil water content at which processes are aerobic	-
$\lambda$	Latent heat of evaporation	$\text{kJ}\cdot\text{kg}^{-1}$
$\theta$	Angle of incidence between the normal and the solar beam	°
$\theta$	Potential air temperature	K
$\theta$	Actual soil water content	-
$\theta_{\text{veg}}$	Soil water content when actual equals potential evapotranspiration	-
$\theta_m$	Soil water content in layer m	-
$\theta_{\text{sat}}$	Saturated soil water content	-
$\theta_{\text{wp}}$	Soil water content at wilting point	-
$\rho$	Air density	$\text{kg}\cdot\text{m}^{-3}$
$\rho_w$	Density of water	$\text{kg}\cdot\text{m}^{-3}$
$\sigma$	Stefan-Boltzmann constant	$\text{W}\cdot\text{m}^{-2}\cdot\text{K}^{-4}$
$\Psi$	Hydraulic head	m
$\Psi_f$	Hydraulic head at the depth at which the water has infiltrated	m
a	Regression coefficient for interpolation of the meteorological data	°C
a	Correction factor for precipitation	-
$a_{\text{snow/ice}}$	Radiation melt coefficient different for snow and ice	$\text{mm}\cdot(\text{timestep}\cdot\text{°C}\cdot\text{W}\cdot\text{m}^{-2})^{-1}$
b	Regression coefficient for interpolation of the meteorological data	°C·m <sup>-1</sup>
b	Correction factor for precipitation	s·m <sup>-1</sup>
C	Specific heat of water	$\text{J}\cdot(\text{kg}\cdot\text{°C})^{-1}$
CRFR	Coefficient for refreezing	-
CWH	Coefficient for water retention within snow	-
$c_1$	Temperature dependent melt factor	$\text{mm}\cdot(\text{d}\cdot\text{°C})^{-1}$
$c_2$	Wind speed dependent melt factor	$\text{mm}\cdot(\text{d}\cdot\text{°C}\cdot\text{m}\cdot\text{s}^{-1})^{-1}$
$c_p$	Specific heat of dry air at constant pressure	$\text{kJ}\cdot(\text{kg}\cdot\text{K})^{-1}$
DDF	Degree-day factor for melt	$\text{mm}\cdot(\text{d}\cdot\text{°C})^{-1}$
$d_r$	Drainage density	m <sup>-1</sup>
E	Evapotranspiration	mm or $\text{kg}\cdot\text{m}^{-2}$
ETP	Potential evapotranspiration	mm
ETR	Actual evapotranspiration	mm
e	Water vapour pressure	mbar
$e_s$	Saturated water vapour pressure	mbar
F	Infiltrated amount of water until saturation	mm
$F_s$	Infiltrated depth of water	mm
G	Soil heat flux	$\text{W}\cdot\text{m}^{-2}$
h	height	m
$h_{\text{geo},0}$	Surface level above sea level	m
$h_{\text{GW}}$	Groundwater level above sea level	m

List of symbols

$h_{si}$	Maximum depth of water on a wet surface	mm
$I$	Slope	-
$I$	Potential clear sky direct solar radiation	$W \cdot m^{-2}$
$I_{corr}$	Radiation normal to the grid slope	$W \cdot m^{-2}$
$I_{norm}$	Incoming radiation normal to the horizontal	$W \cdot m^{-2}$
$i$	Index for each reservoir	-
$K^{\downarrow}$	Global radiation	$W \cdot m^{-2}$
$K_H$	Eddy diffusivity for the sensible heat flux	$m^2 \cdot s$
$K_L$	Eddy diffusivity for the latent heat flux	$m^2 \cdot s$
$k$	Storage constant	$s^{-1}$
$k(\Theta)$	Hydraulic conductivity	$m \cdot s^{-1}$
$k_B$	Recession constant for baseflow	m
$k_s$	Saturated hydraulic conductivity of the soil	$mm \cdot h^{-1}$
LAI	Leaf area index	-
$L_f$	Latent heat of fusion	$J \cdot kg^{-1}$
$l_s$	Soil depth to be saturated	mm
$M$	Melt rate	$mm \cdot timestep^{-1}$
$M$	Hydraulic resistance	$m^{1/3} \cdot s^{-1}$
$M_L$	Melt rate due to the latent heat flux	$mm \cdot timestep^{-1}$
$M_{neg}$	Negative melt rate	$mm \cdot timestep^{-1}$
$M_P$	Melt rate due to rainfall	$mm \cdot timestep^{-1}$
$M_R$	Melt rate due to radiation	$mm \cdot timestep^{-1}$
$M_S$	Melt rate due to the sensible heat flux	$mm \cdot timestep^{-1}$
MF	Melt factor	$mm \cdot (d \cdot ^\circ C)^{-1}$
$m_p$	Mass of liquid precipitation	kg
$n$	number of timesteps	-
$n_a$	Difference between saturated and actual soil water content	-
P	Precipitation	mm
$P_{corr}$	Corrected precipitation	mm
$P_{snow}$	Part of snow from total precipitation	-
PI	Precipitation intensity	$mm \cdot h^{-1}$
Q	Discharge	$m^3 \cdot s$
$Q_0$	Scaling factor for basflow	-
$Q_b$	Baseflow	$m \cdot s^{-1}$
$Q_G$	Heat flux into snow pack	$W \cdot m^{-2}$
$Q_H$	Sensible heat flux	$W \cdot m^{-2}$
$Q_L$	Latent heat flux	$W \cdot m^{-2}$
$Q_M$	Energy available for melt	$W \cdot m^{-2}$
$Q_N$	Net radiation	$W \cdot m^{-2}$
$Q_P$	Heat flux provided from precipitation	$W \cdot m^{-2}$
$q$	Specific humidity	-
$q$	Specific water flow	$m \cdot s^{-1}$
$q_{in}$	Incoming water flux in soil the layer	$m \cdot s^{-1}$
$q_{if}$	Interflow	$m \cdot s^{-1}$
$q_{if,max}$	Maximum interflow	$m \cdot s^{-1}$
$q_{out}$	Outgoing water flux in the soil layer	$m \cdot s^{-1}$
R	Rate of water inflow to a reservoir	$m^3 \cdot s^{-1}$
R	Runoff	mm
$R_h$	Hydraulic radius	m
$R_n$	Net radiation	$W \cdot m^{-2}$
RMF	Seasonally varied radiation melt factor	$mm \cdot (d \cdot ^\circ C)^{-1}$

$r$	Multiplicative factor for accelerated melt over ice compared to snow	-
$r_a$	Aerodynamic diffusion resistance	$s \cdot m^{-1}$
$r_s$	Internal canopy diffusion resistance	$s \cdot m^{-1}$
$SI_{max}$	Maximum storage capacity of the interception	mm
$T$	Air temperature	$^{\circ}C$
$T_0$	Threshold temperature for snow melt	$^{\circ}C$
$T_a$	Air temperature	$^{\circ}C$
$T_p$	Temperature of precipitation	$^{\circ}C$
$T_{R/S}$	Temperature at which 50% of the total precipitation is snow	$^{\circ}C$
$T_s$	Surface temperature	$^{\circ}C$
$T_{trans}$	Temperature range where bothe snow- and rainfall occur	$^{\circ}C$
$t$	Time	h or s
$t_I$	Timestep	s
$t_s$	Time needed to saturate the soil	h
$u$	Wind speed	$m \cdot s^{-1}$
$V$	Volume of a reservoir	$m^3$
$v$	Relative surface area covered with vegetation	-
$v_1$	Flow velocity	$m \cdot s^{-1}$
$w_j$	Weight of station j for interpolation of the meteorological data	-
$Z$	Local zenith angle	$^{\circ}$
$z$	Height	m
$z$	Interpolated meteorological value	depending on meteorological value
$z_j$	Measured meteorological value at station j	depending on meteorological value
$z_o$	Surface roughness length	m

# 1 Introduction

Glaciers exert an essential control on the hydrology of mountainous and polar areas since they store significant quantities of water. During the melting season, glaciers contribute large amounts of melt water to the stream flow, which also influence the hydrology of lowland areas. In contrast to flatland hydrology where rainfall and evapotranspiration are the most important input variables for runoff modelling, slope, exposure and the occurrence of snow and glaciers are also important input factors for runoff of precipitation in mountainous areas. Melting of snow and glaciers often occur during dry and warm weather periods. Discharge of rivers which contain melt water of snow and glaciers therefore show distinctive annual and diurnal fluctuations.

The significant interaction between glaciers and the atmosphere implies both the influence of the atmosphere on the glaciers, and the impact of glaciers on the climate system. As climate changes, glaciers grow or retreat, and sea level respectively falls or rises. Glacier fluctuations constitute important information about the variability of the climate, because they are highly sensitive to climate. Glaciers are natural large-scale and representative indicators for the energy-balance of the earth's surface in polar or high-altitude areas. An example of the impact of glaciers on the climate is the lowering of the temperature of the earth's surface, due to an increase in albedo. This is followed by reduced absorption of radiation when fresh snow covers the glacier, or the snow covered area or glacier area increase (Guisan et al., 1995).

Since the processes of water storage by glaciers and glacier melt play an important role in the water balance of partly glacierized catchment areas, hydrologic models applied to these areas should be able to simulate glacier melt processes. These hydrological models can be used to predict streamflow for water supply, hydropower facilities, flood forecasting, and to deal with questions concerning the impact of climate change on hydrological systems. The International Commission for the Hydrology of the Rhine Basin (CHR) studied the impacts of climate change on the hydrology of the Rhine river based on the results of different hydrological models (Grabs, 1997). However, glacier melt processes were not simulated or investigated within that CHR-study.

There is a lack of models accomplishing glacier melt modelling within a hydrological catchment area. There are models which simulate glacier melt or discharge, but not as a component of hydrological processes in a hydrological model. Models simulating glacier melt range from simple temperature index methods to more fundamental energy balance methods. A temperature index method is based on the positive relationship between air temperature and melt rate. Such a method was first used by Finsterwalder and Schunk (1887). A few of these melt models are coupled to discharge models, which involve the routing of melt water and rain through the glacier. Generally, a concept of linear reservoirs is used to simulate the glacier melt water outflow (Baker et al., 1982). The present study is concerned with the modelling of glacier melt processes within the Waterbalance Simulation Model, in order to simulate the water balance of catchment areas including glacierized areas and establish a first hydrological model which simulates discharges of partly glacierized catchment areas.

WaSiM-ETH is a model to simulate the hydrological processes of a river basin, and is developed by Schulla (1997). This spatial distributed model is developed to answer questions concerning the influences of climate change on hydrologic regimes in large regions on a physically sound basis. WaSiM-ETH can be run with a small quantity of meteorological and geographical data and a high spatial and temporal resolution. The model contains modules for spatial interpolation of meteorological data taken at a relatively small amount of meteorological stations. A digital elevation model, soil properties, land use information, temperature and precipitation are required to run WaSiM-ETH. However, for an optimal simulation, global radiation, sunshine duration, wind speed and vapour pressure are necessary additional data.

WaSiM-ETH consists of several model components, which carry out the spatial interpolation of meteorological data of various stations and the modification of air temperature and radiation according to exposition, slope and topographic shading. The model calculates interception, snow accumulation and melt, evapotranspiration, infiltration and generates surface runoff, interflow and baseflow. Schulla (1997) tested this model in the basin of the river Thur (north-east Switzerland) and for the Wernersbach (Germany). WaSiM-ETH was also used within the CHR study to investigate the impact of climate change on the Thur basin by applying climate change scenarios to the climate data (Grabs, 1997).

It was not possible to apply this model to glacierized areas while glacier melt processes were not simulated by WaSiM-ETH. Therefore, WaSiM-ETH could not simulate the hydrological processes and the annual, as well as diurnal, variation in discharge of many mountainous catchment areas accurately. In order to apply WaSiM-ETH to partly glacierized areas, two temperature index methods to simulate glacier melt, based on work of Hock (1998), were incorporated into WaSiM-ETH in this study. One method is a simple temperature index method and the second is a temperature index method including a radiation factor. The transformation of melt and rain water to the glacier snout is simulated by three parallel linear reservoirs.

WaSiM-ETH including the glacier model is tested on a basin in Switzerland in which the Rhone glacier is situated, the Gletsch catchment. At the time of this study, Badoux (1999) incorporated a glacier model into the rainfall-runoff model PREVAH. He also applied PREVAH to the Gletsch catchment. This catchment area is glacierized for 52%. Meteorological data and discharge measurements at the catchment outlet in Gletsch were available for 1990 to 1996. The years 1990 and 1991 are used to calculate starting values for 1992, which is used for calibration. The years 1993 to 1996 are used to validate the model. The model results of this catchment area are compared with the simulation results of WaSiM-ETH without the glacier melt model, in order to study the impact of the glacier melt. Furthermore, the two temperature index methods are compared and the model is tested on a second catchment area, the Aletsch area including the Aletsch glacier.

Chapter 2 starts with a description of the theory of glaciers, the mass balance of a glacier, glacier melt, glacier discharge and some methods to simulate glacier melt and discharge. The next chapter contains a comprehensive description of WaSiM-ETH including the glacier model. The application of WaSiM-ETH is explained in Chapter 4. Chapter 5 describes the parameter sensitivity and the interdependency between model parameters. The calibration and validation results of the model are described in Chapter 6. Chapter 6 also contains the comparison of results with the results of WaSiM-ETH without a glacier model as well as between the two glacier melt methods. Further, it discusses the application of the model on the Aletsch catchment. Chapter 7 describes the discussion of the results and conclusions. The last chapter contains the recommendations.

## 2 Glaciers, the theory and their modelling

### 2.1 Introduction

A glacier is a reservoir which stores snow, ice and firn, but also liquid water. Glaciers occur in the polar latitudes and in mountainous areas, where the climatic conditions are cold. A glacier has its origin in mountainous areas which are above the climatic snow line (Röthlisberger and Lang, 1987). In winter most glaciers are totally covered by snow, including the area below the climatic snow line. During the melting period the snow line retreats upglacier (see Figure 2-1). The highest position of the snow line occurs at the end of the melting period. During an exceptionally dry and warm year the snow line can retreat to an extreme high position, exposing the firn layers. Firn is wetted snow that has survived one summer without being transformed into ice. It is old granular snow and gradually changes into ice depending on the temperature. Firn becomes ice when the interconnecting air passages between the grains are sealed off (Paterson, 1981).

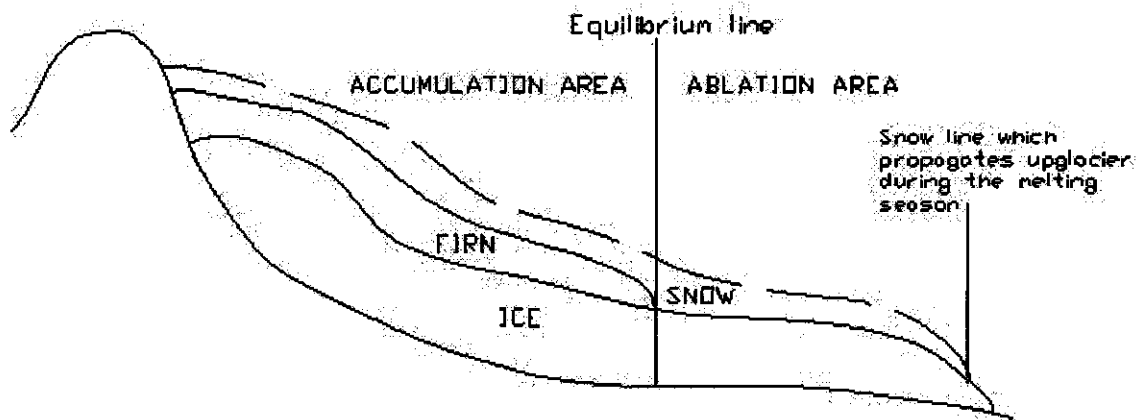


**Figure 2-1: Cross section of a glacier.**

The influence of glaciers on the world's environment is much greater than one might expect. Glaciers cover 10 per cent of the total land area and contain 3 per cent of the earth's water volume (Sharp, 1960). Discharge from glaciers can cause floods. The melt water is sometimes used for water supply and hydropower facilities. Glaciers are major contributors to streamflow, even in many lowlands.

Glaciers are very sensitive to climatic change. They grow and shrink with changing climatic conditions. The largest glaciers in the world are the ice sheets of Greenland and Antarctica. Their behaviour is of world-wide interest because of the effect on sea level, mankind and its shoreline operations under possible climate change (Sharp, 1960).

This chapter describes the mass balance of a glacier (Section 2.2), the theory of glacier melt (Section 2.3) and the transport of melt and rain water through the glacier (Section 2.4). Section 2.5 describes different methods to simulate glacier melt and glacier runoff.

### 2.2 The glacier water budget

A glacier can be divided into two parts: an accumulation area at the upper part of the glacier and an ablation area at the lower part of the glacier. During an average year, more snow is accumulated than ablated in the accumulation area and the annual mass balance is positive.

The mass balance is negative in the ablation area, where on average more ice and snow is ablated than rebuilt. Accumulation includes processes in which water is added to the glacier, like snowfall, avalanches, rime formation and freezing of rain within the snowpack. Ablation is the loss of ice and snow from a glacier caused by melting, evaporation, wind and calving of ice parts (Paterson, 1980).

The line between the accumulation and ablation area is called the equilibrium line (see Figure 2-1). This line is equal to the climatic snow line. At this line, enough heat is available to bring ablation and accumulation into balance. The storage change component ( $\Delta S$ ) in the water balance of a glacierized area is defined by

$$\Delta S = P - R - E$$

2-1

where P is precipitation, R is runoff and E is evaporation.  $\Delta S$  is positive for the accumulation area and negative for the ablation area.

Gravity and physical ice characteristics cause movement of glacier masses from the accumulation area to the ablation area. Under stationary conditions, this movement of the glacier would compensate for the positive mass balance in the accumulation area and the negative mass balance in the ablation area. The storage change component for the whole glacier,  $\Delta S$ , is then zero. However, stationary glaciers do not exist, because of the inherent variability of climate. Climatic variations occur over all timescales, from day to day fluctuations in weather to long-term variations as a result of cyclic changes in the Earth-Sun orbital system (Röthlisberger and Lang, 1987).

This storage change component of the entire glacier is called the glacier budget. The time over which the glacier budget is determined is called the budget year. The beginning of a budget year is defined as the time in autumn when the accumulation of new snow by precipitation exceeds the melt of snow and ice (Sharp 1960). At that time the accumulation season begins. This is shown in Figure 2-2. If the glacier budget is balanced, the area between the two lines of the accumulation season equals the area between the two lines of the ablation season.

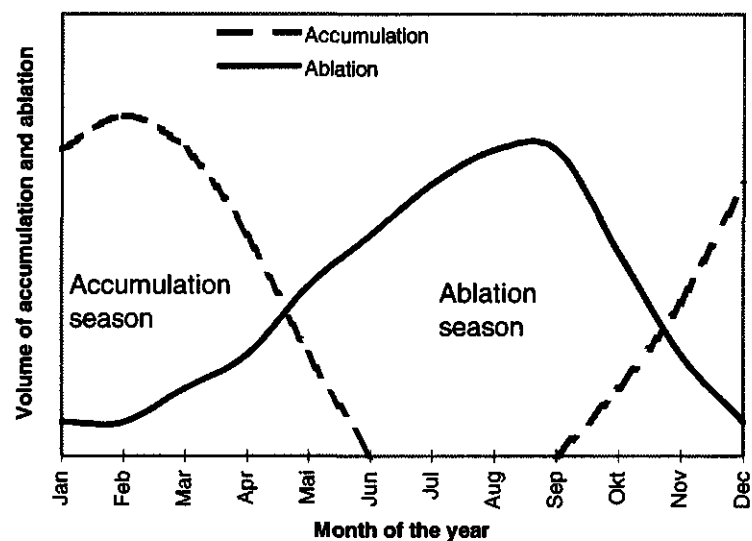


**Figure 2-2: Volume of glacier accumulation and ablation during a year.**

### 2.3 Glacier melt

Sources which cause glacier melt are radiation, latent and sensible heat fluxes, liquid precipitation, friction and geothermal heat. Other types of glacier melt are basal melt due to



the air temperature in cavities and melt due to the passage of melt water over the surface of ice masses (Menziés, 1995).

During the ablation season, the temperature at the surface of the glacier increases to 0 °C and the glacier begins to melt. The melt water infiltrates the snow and may be frozen again, resulting in an evolution of heat which warms the surrounding snow or ice. The melt water saturates the snow and the glacier surface. If the temperature of the total snow and firn area is around 0 °C, the melt water and the rain water percolate through the glacier ice (Noetzli, 1996).

The melting process at the glacier surface can be estimated by using the energy balance of the glacier surface. The energy available for melt ( $Q_M$ ) is determined by

$$Q_M = Q_N + Q_H + Q_L + Q_P + Q_G \quad 2-2$$

where  $Q_N$  is the net radiation,  $Q_H$  is the sensible heat,  $Q_L$  is the latent heat,  $Q_P$  is the heat provided from precipitation and  $Q_G$  is the heat from heat conduction in the snow pack.

The net radiation is the incoming minus the outgoing shortwave and longwave radiation. The outgoing shortwave radiation is determined by the albedo of the glacier ice or snow (Röthlisberger and Lang, 1987). Typical albedo values are 0.7 to 0.9 for fresh snow, 0.4 to 0.6 for firn and 0.2 to 0.4 for glacier ice (Paterson, 1981). This means glacier ice absorbs more incoming shortwave radiation than snow, resulting in more available energy for glacier melt. Albedo values also change because of the changing angle of incidence of solar radiation. Snow and ice behave almost as perfect black bodies in the infra-red part of the spectrum and the emissivities range from 0.98 to 0.99 for snow and 0.97 for ice (Müller, 1985).

The heat provided from precipitation is proportional to the mass and temperature of the rain drops falling on a melting glacier surface, and the specific heat of water. The contribution of heat from rain drops to the energy available for melt is small, but it influences the surface albedo. If the liquid water content of snow increases and snow gets older, the albedo is reduced. Therefore, the albedo normally decreases in summer, while sudden snowfall events enhance the albedo, resulting in reduced melt and runoff (Warren, 1982).

Radiation, cloud cover, air temperature, humidity and wind speed are important factors for glacier melt. Direct radiation accounts for more than 80 per cent of the glacier melt in some areas and is the main source of melt energy. The contribution of direct radiation to glacier melt increases with altitude due to clearer air and lower temperatures. Also, wind speed exerts a major effect on melting, since it creates turbulence. Turbulence removes the thin layer of cold air next to the ice or snow and brings a new supply of warmer air into contact with the glacier. However, stable atmospheric conditions above the glacier normally suppress turbulence. The stable atmospheric conditions are created by the surface temperature of ice which cannot exceed 0 °C and can cause a temperature inversion above the glacier (Hock, 1998).

The vapour pressure is also significant for glacier melt. If the air is almost saturated, the water vapour will condense as soon as the air temperature reaches dew point. While the air is cooled in contact with the glacier, condensation of the water vapour occurs, which results in a large evolution of heat ( $2.501 \cdot 10^6 \text{ J} \cdot \text{kg}^{-1}$  at 0 °C). While the specific heat of evaporation is 7.5 times larger than the heat of fusion required for melting snow and ice ( $0.334 \cdot 10^6 \text{ J} \cdot \text{kg}^{-1}$ ), condensation of water vapour is an important source of glacier melt (Sharp, 1960).

## **2.4 Glacier runoff**

### **2.4.1 Runoff characteristics**

Annual variations in glacier runoff approximately follow the reverse pattern of a rain dominated runoff regime. A rain dominated runoff regime is characterized by high discharges during periods with high precipitation. Such low glacierized areas are characterized by a positive relationship between precipitation and runoff, but runoff is delayed when precipitation exists of snow.

Snowfall has a negative influence on the runoff of especially highly glacierized areas, because incoming solar radiation is reduced when the sky is covered by clouds, and fresh snow has a higher albedo. Both factors play an important role in the energy balance of the glacier and result in less glacier melt during periods with snowfall.

The hydrograph of outflow from a highly glacierized area shows distinctive annual variations, since snow is stored in winter and released by melting in summer. In winter the discharge of a highly glacierized catchment area is at minimum level and at maximum in the melting season. The ratio of melt water runoff to total runoff rises with increasing glacierized area. For instance, the runoff regime of the Gletsch catchment, which is glacierized for 52 per cent, is mainly determined by melt water from the glacier. Appendix 1 shows the annual variation in runoff for the Gletsch catchment for the year 1992. During the melting season, the discharge increases, but runoff is at minimum during winter. The runoff peaks in the summer are a result of the daily variations in radiation and temperature. The runoff of the summer months (June, July and August) of 1990 contributed to 68 per cent of the total annual runoff.

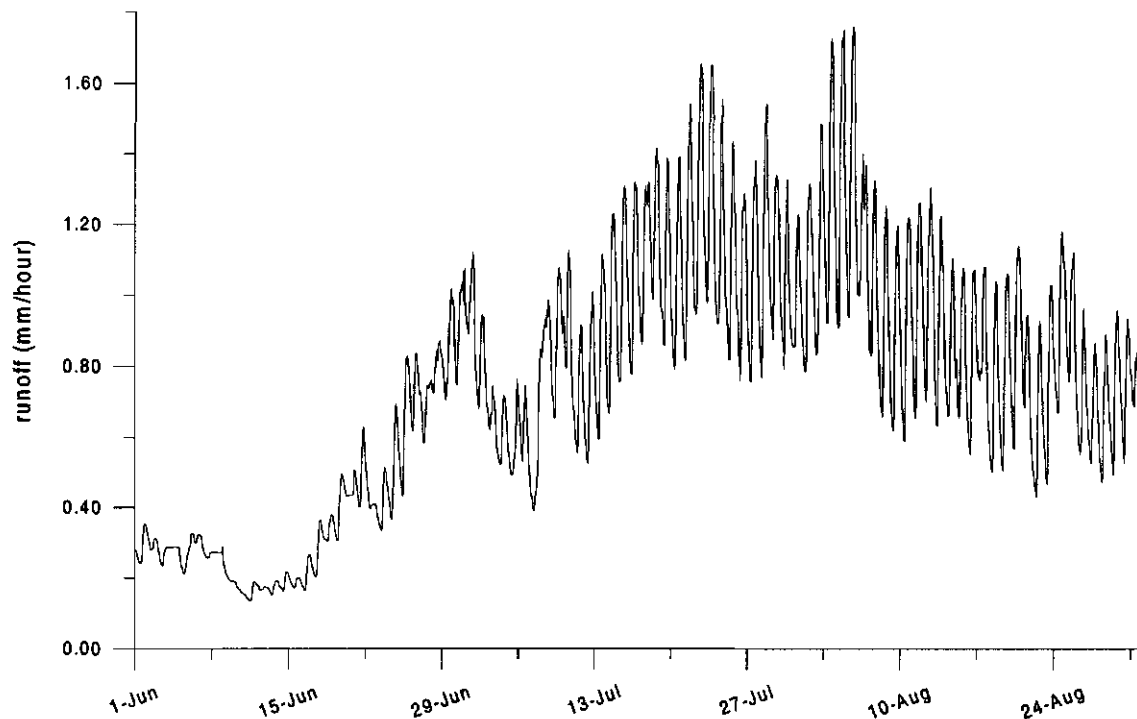
The variability of yearly runoff is reduced when a catchment area contains a glacier, because during a dry and warm summer the low flow from the rain-dominated parts of the catchment is compensated by the melt water from the glacier in the upper part of the catchment area. During a cold and wet year, low glacier melt rates are compensated by the storm runoff of the unglacierized area of the catchment basin (Röthlisberger and Lang, 1987).

Figure 2-3 shows a hydrograph of Gletsch for the summer of 1990. During the day, melt rates show a variation due to the daily change in meteorological factors. In particular the amount of incoming solar radiation influences the production of melt. During the night, when the incoming solar radiation is zero, the production of melt water is minimized, resulting in a minimum runoff. The diurnal variation of discharge is superimposed on the baseflow. When the melt season ends, the diurnal variation in discharge decreases and the base flow declines. During winter, there is no diurnal variation (Paterson, 1981).

Occasionally sudden runoff variations occur which cannot be explained by the daily variations of radiation and temperature. It was found that these variations are caused by sudden high amounts of precipitation or by the release of water from water pockets within the glacier and outbursts of stored water from ice-dammed lakes (Hock, 1998). However, high amounts of snowfall increase the albedo and reduce solar radiation and thus reduce melt rates. Therefore, high amounts of precipitation (snow) do not always result in a high runoff volumes.

At the end of a warm summer day, heavy rain storms may occur. The runoff of this heavy rain storm is superimposed on the high melt rate of the day and an extreme runoff rate occurs. Such extreme melt rates and rainfall events can cause floods in a glacier basin.

The highest melt rates occur when the glacier is not covered by snow at all, which means a low albedo, together with high values for incoming radiation and low values for the latent heat flux and sensible heat flux (Röthlisberger and Lang, 1987).



**Figure 2-3: Observed runoff volumes (mm/h) at Gletsch for June, July and August 1990.**

#### 2.4.2 Water transport through the glacier

The way melt water and precipitation is transported through the glacier, depends on the glacier conditions. Percolation of water through snow or firn is like percolation through an unsaturated porous medium. Water storage and movement in snow and firn can therefore be described according to Darcy's law. The hydraulic properties of snow and firn change rapidly during the melt season, because of the metamorphosis of snow and changes in snow distribution and percolation conditions. During the melt season, the snow and firn layers act as a reservoir and can contain a considerable amount of free water.

Also glacier ice contains appreciable quantities of melt water during the melt season. Glacier ice has a considerably lower permeability than firn and snow. Therefore, percolation is smaller through glacier ice than through firn and snow. When melt and rain water reaches the ice surface, it flows through channels on the ice surface and disappears into crevasses or moulins in the ice or it seeps into the glacier ice (small pores) and is transported to the glacier outlet. Crevasses are open linear cracks in a glacier. The walls of a crevasse have separated and are often many metres apart (Sharp, 1960). Moulins are vertical passages in a glacier, which are usually formed where melt water flows into a crevasse (Paterson, 1981). Figure 2-4 shows the passageways of water through the glacier. The moulins, crevasses and passageways within the glacier are called the englacial drainage system. The subglacial conduit is the drainage system at the glacier bed. Surface channels on the ice which transport water to the outlet of the glacier are an exception. Most of the water is transported by moulins and crevasses and a limited amount seeps into the ice (Röthlisberger and Lang, 1987).

The size of the passageways within the glacier ice (moulins and crevasses) is influenced by many processes and changes throughout the year. Two processes which influence the size of the passages are heat transfer between the water flowing through the passage and the surrounding ice and the deformation of ice. The evolution of passages does not only change throughout the year, but also varies in space. Passageways can be distinguished in large passages called tunnels or channels, and small passages called small tubes or veins (Röthlisberger and Lang, 1987). Some of these are isolated, while others are connected with

each other. During the winter, the passages are closed, but are reopened during the melt season by melt water. As long as enough water flows through the moulin and crevasses, they will not be closed. If the passageways are too small to carry off the water, water is stored. During the melt season, new passageways are opened, old passageways are enlarged by an increasing amount of melt water and isolated moulin become connected to other passageways. Therefore, the time that water spends within the glacier ice reduces during the melt season (Paterson, 1981).

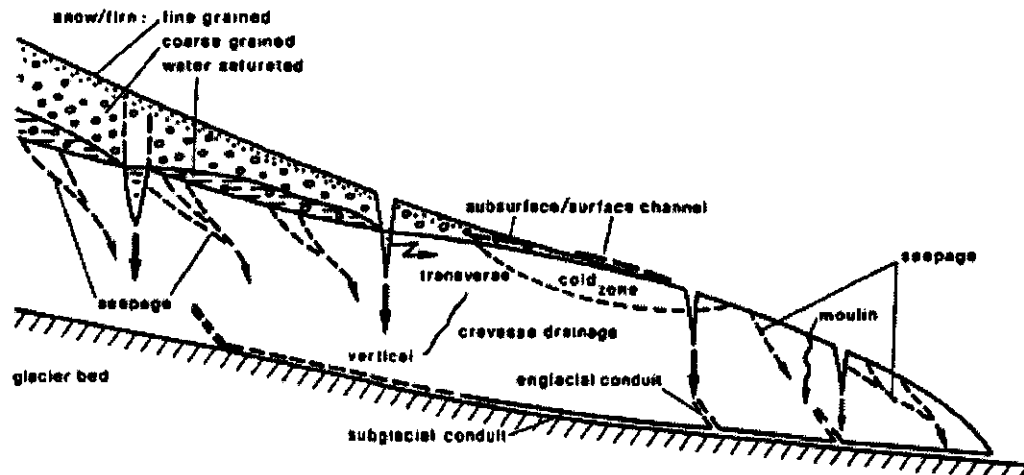


Figure 2-4: The drainage system of a glacier.

After a period of heavy rain or heavy melt, more water might reach the glacier bed than can drain away, because the time is too short to allow passageways to enlarge. Water pressure builds, which partly counteracts the glacier's weight. This water pressure reduces the glacier's shear strength and is important for glacier sliding. During the winter, the water pressure is higher than in the summer, because of the restricted amount and size of the passageways.

Once the water reaches the glacier bed, it can either flow through channels or as sheet flow towards the glacier outlet (Röthlisberger and Lang, 1987). The subglacial drainage system depends on the existence of overburden water pressures and the topography of the glacier bed. The subglacial system is able to move vast quantities of sediment and cut down sediments into bedrock, which influence the ice-bed interface and the hydraulic system. For instance, if the glacier bed is covered with a high permeable sediment, it is possible that little or no melt water will flow between the bed and the ice. So the glacier bed varies within time and location depending on the glaciodynamic changes, which are important for the subglacial drainage system (Menzies, 1995).

Summarily, a glacier can be divided into three aquifers, owing to the different properties: snow, firn and ice. The firn and the snow aquifer correspond to a porous groundwater aquifer through which water percolates, depending on the permeability. The ice aquifer is similar to a karst aquifer, defined by subglacial and englacial channels.

## 2.5 Modelling of glacier melt and runoff

### 2.5.1 Glacier melt models

There are different methods to calculate the melt rate of a glacier. While a glacier also contains snow, snow melt must also be modelled. Two methods often used to calculate the

melt rate at the glacier surface are: temperature index methods and surface energy balance methods. Both methods can be applied in distributed models (Lang, 1986).

Temperature index methods are sometimes called degree-day models. Degree-day models are based on the assumed relationship between air temperature and melt rates. The strong relationship between melt and air temperature depends on the high correlation of temperature with other parameters, in particular short- and longwave radiation, which influence the melting of snow and ice. The air temperature depends on the global radiation and affects the turbulent heat fluxes, which are important for snow and ice melt (Hock, 1998). The meteorological input data for a temperature index method is air temperature, but sometimes a degree-day method is extended by more meteorological data such as wind speed and global radiation.

#### *Classical degree day method*

The most simple degree day method used is to take the positive hourly or daily mean temperature and compute the melt rate with a factor of proportionality, the degree-day factor, according to

$$M = \frac{1}{n} \cdot DDF \cdot T$$

2-3

where M is the melt rate of snow or ice [mm·timestep<sup>-1</sup>], DDF is the degree-day factor different for snow and ice surfaces [mm·(d·°C)<sup>-1</sup>], T is the positive mean temperature [°C] and n is the number of timesteps per day. Daily melt rates are calculated using daily mean temperatures and n=1. If the mean temperature equals zero or is below zero, the melt rate is zero. This method will be called the classical degree-day method and is a strong simplification of the melt processes. It does not evaluate the processes as exactly as an energy balance method. Therefore, the degree-day factor (DDF) shows large variations. Degree-day factors for snow melt are less than for ice, because of the high albedo of snow. On average, the degree-day factors for snow range from 3 to 6 mm·(d·°C)<sup>-1</sup> and for ice the degree-day factors range from 6 to 20 mm·(d·°C)<sup>-1</sup> (Hock, 1998).

#### *Temperature threshold method*

At higher temperatures, the temperature index method seems to be more reliable, because at temperatures below zero, the melt rate is assumed to be zero. Although, sometimes some snow or ice melts at temperatures below 0 °C. Therefore, it is suggested to replace the temperature, T, by (T - T<sub>0</sub>), where T<sub>0</sub> is a threshold temperature above which melt is assumed to occur (Lang, 1986). Below the temperature T<sub>0</sub> the snow or ice melt is zero. The classical degree-day method including this threshold temperature is given by

$$M = \frac{1}{n} \cdot DDF \cdot (T - T_0)$$

2-4

The degree-day factor also varies seasonally due to the variation in the snow and ice properties. Therefore, a temperature index method can be improved by using a seasonally variable degree day factor (Lang, 1986).

A higher time resolution for the temperature input data, for example hourly means instead of daily means, will also improve calculations. For instance, daily mean temperatures can cause inaccurate melt rate calculations during days with temperatures around zero degrees. Temperature fluctuations around freezing point can result in a mean temperature below zero, while snow and ice melt could have occurred.

*Braun wind method*

The classical degree-day method only uses air temperature as input data. This means that the temperature represents an index for all processes which influence the energy available for snow and ice melt. By incorporating more meteorological variables which influence the energy balance, calculations will improve. Variables which can be introduced are vapour pressure, wind speed, global radiation, net radiation, albedo, or a combination of these.

Braun (1985) incorporated wind speed into the classical temperature index method according to

$$M = \frac{1}{n} \cdot (c_1 + c_2 \cdot u) \cdot (T - T_0) \quad 2-5$$

where  $c_1$  is a temperature dependent melt factor [ $\text{mm} \cdot (\text{d} \cdot ^\circ\text{C})^{-1}$ ],  $c_2$  is a wind speed dependent melt factor [ $(\text{mm} \cdot (\text{d} \cdot ^\circ\text{C} \cdot \text{m/s})^{-1})$ ] and  $u$  is the wind speed [ $\text{m} \cdot \text{s}^{-1}$ ].

*Hock radiation method*

Hock (1998) included a radiation index and the potential clear sky solar radiation in the classical degree-day method to overcome the shortcomings of the classical degree-day method, which does not accurately simulate the diurnal variability in melt rate. The potential clear sky radiation determines, to a large extent, melt rates and is affected by atmospheric conditions, slope, exposure and shading, and is subject to pronounced daily cycles. The inclusion of potential clear sky radiation improves the simulation of the diurnal melt rate fluctuations and the spatial distribution of melt rates. Melt rates are calculated following

$$M = \left( \frac{1}{n} \cdot MF + a_{\text{snow/ice}} \cdot I \right) \cdot T \quad 2-6$$

where MF is a melt factor [ $\text{mm} \cdot (\text{d} \cdot ^\circ\text{C})^{-1}$ ],  $a_{\text{snow/ice}}$  is a radiation coefficient different for snow and ice surfaces [ $\text{mm} \cdot (\text{timestep} \cdot ^\circ\text{C} \cdot \text{W} \cdot \text{m}^{-2})^{-1}$ ] and  $I$  is the potential clear sky direct solar radiation at the ice or snow surface [ $\text{W} \cdot \text{m}^{-2}$ ]. The potential clear sky solar radiation can be calculated as a function of the top of the atmosphere solar radiation, atmospheric transmissivity and topographical characteristics.

Instead of using calculated potential clear sky solar radiation, measured global radiation can be used.

*Anderson combination method*

Anderson (1973) introduced the so called combination method. This method uses a seasonally varied simple degree-day method during dry periods and a simplified empirical energy balance method during periods with precipitation. In principle, this method was used to calculate snow melt in lowland and lower alpine regions. Braun (1988) incorporated a multiplicative factor,  $r$ , to account for accelerated melt over ice as compared to snow and vapour pressure as a new input variable into Anderson's method. He applied the Anderson method to the glacierized basin of the Aletsch glacier.

When the temperature exceeds a threshold temperature,  $T_0$ , and the rainfall rate is zero, radiation melt occurs, which is described by

$$M = \frac{1}{n} \cdot r \cdot \text{RMF} \cdot (T - T_0) \quad 2-7$$

where RMF is a seasonally varied radiation melt factor [ $\text{mm} \cdot (\text{d} \cdot ^\circ\text{C})^{-1}$ ], which is interpolated sinusoidal between a minimum value for RMF on December 21<sup>st</sup> and a maximum value on

June 21<sup>st</sup>. When precipitation occurs and the temperature is above the threshold temperature total melt is the sum of radiation melt ( $M_R$ ), melt due to the sensible heat flux ( $M_S$ ), melt due to the latent heat flux ( $M_L$ ) and melt due to rain ( $M_P$ ), which are described by Braun (1988) as

$$M_R = \frac{1}{n} \cdot 1.2 \cdot T \quad 2-8$$

$$M_S = \frac{1}{n} \cdot r \cdot (c_1 + c_2 \cdot u) \cdot (T - T_0) \quad 2-9$$

$$M_L = \frac{1}{n} \cdot r \cdot (c_1 + c_2 \cdot u) \frac{e - 6.11}{\gamma_p} \quad 2-10$$

$$M_P = \frac{1}{n} \cdot 0.0125 \cdot P \cdot T \quad 2-11$$

where  $e$  is the water vapour pressure [mbar],  $\gamma_p$  is the psychrometric constant [mbar·K<sup>-1</sup>] and  $P$  is the precipitation [mm]. If the temperature is below the threshold temperature, refreezing of possible present liquid water in the snow pack is calculated following

$$M_{neg} = \frac{1}{n} \cdot CRFR \cdot RMF \cdot (T - T_0) \quad 2-12$$

where  $M_{neg}$  is the negative melt rate [mm·timestep<sup>-1</sup>] and CRFR is a coefficient of refreezing [-].

#### *Energy budget method*

A more fundamental method to calculate the melt of ice and snow is the energy budget method, which calculates the energy fluxes to and from the glacier surface. The energy available for melt rate can be calculated from the formula of the surface energy balance of a glacier (Equation 2-2). The melt rate is calculated following

$$M = \frac{Q_M}{\rho_w L_f} \quad 2-13$$

where  $M$  is the melt rate [m·s<sup>-1</sup>],  $Q_M$  is the energy available for melting [W·m<sup>-2</sup>],  $\rho_w$  is the density of water [kg·m<sup>-3</sup>] and  $L_f$  is the latent heat of fusion [J·kg<sup>-1</sup>]. There are different types of methods to calculate the components of the energy balance. The methods used depend on the available data. Energy balance models require a lot of meteorological measurements like air temperature, humidity, wind speed and global radiation. Reflected shortwave radiation, net radiation and cloud cover are desirable data. The major problem of an energy balance method is the calculation of the turbulent heat fluxes. Roughness lengths need to be calculated or estimated, or they can be treated as tuning parameters. Hock (1998) describes two energy balance methods.

The different components of the energy balance can be calculated using the following formulas:

$$Q_N = K^\downarrow \cdot (1 - \alpha) + \epsilon_a \sigma T_a^4 - \epsilon_s \sigma T_s^4 \quad 2-14$$

$$Q_H = c_p \cdot \rho \cdot K_H \frac{d\theta}{dz} \quad 2-15$$

$$Q_L = \lambda \cdot \rho \cdot K_L \frac{dq}{dz} \quad 2-16$$

$$Q_P = C \cdot m_p \cdot (T_p - T_0) \quad 2-17$$

where  $K^\downarrow$  is the global radiation [ $\text{W}\cdot\text{m}^{-2}$ ],  $\alpha$  is the albedo [-],  $\epsilon_a$  is the emissivity of the atmosphere [-],  $\epsilon_s$  is the emissivity of the surface,  $\sigma$  is the Stefan-Boltzmann constant [ $\text{W}\cdot\text{m}^{-2}\cdot\text{K}^{-4}$ ],  $T_a$  is the air temperature [K],  $T_s$  is the temperature of the snow or ice surface [K],  $c_p$  is the specific heat of dry air at constant pressure [ $\text{kJ}\cdot(\text{kg}\cdot\text{K})^{-1}$ ],  $\rho$  is the air density [ $\text{kg}\cdot\text{m}^{-3}$ ],  $K_H$  is the eddy diffusivity for sensible heat [ $\text{m}^2\cdot\text{s}^{-1}$ ],  $\theta$  is the potential air temperature [K],  $z$  is the height [m],  $\lambda$  is the latent heat of evaporation [ $\text{kJ}\cdot\text{kg}^{-1}$ ],  $K_L$  is the eddy diffusivity for latent heat flux [ $\text{m}^2\cdot\text{s}^{-1}$ ],  $q$  is the specific humidity [-],  $C$  is the specific heat of water [ $\text{J}\cdot(\text{kg}\cdot^\circ\text{C})^{-1}$ ],  $m_p$  is the mass of the rainwater falling on the snow cover [ $\text{kg}\cdot\text{m}^{-2}$ ],  $T_p$  is the temperature of the rain drops [ $^\circ\text{C}$ ] and  $T_0 = 0^\circ\text{C}$ .

The heat conduction in the snow pack ( $Q_G$ ) is usually of minor importance and need not to be taken into account during the main melt period (Lang, 1986). However, during the pre- and postmelt periods, the heat conduction in the snow pack is important since the surface temperature of the glacier may be below zero. If the surface temperature is below zero, snow and ice melt does not occur. The temperature must be raised to  $0^\circ\text{C}$  by a snow or ice heat flux before surface melting takes place. Therefore, an energy balance method is restricted to the melt period when the heat conduction of the snow pack is neglected (Hock, 1998).

### 2.5.2 Glacier runoff models

When snow and ice are melting, melt water is transported through the glacier. The routing of melt water through snow and ice and the way it reaches the glacier outlet is already described in Section 2.4.2. Because of the complexity and the yearly and spatial variability of the water flow through the glacier, only a few models exist which describe the routing of water through the glacier. More often, the concept of linear reservoirs is used. A linear reservoir approach assumes that at any time,  $t$ , the discharge is proportional to the reservoir's volume, following

$$V(t) = k \cdot Q(t) \quad 2-18$$

where  $V(t)$  is the reservoir's volume [ $\text{m}^3$ ],  $t$  is time [s],  $k$  is a storage constant [ $\text{s}^{-1}$ ] and  $Q(t)$  is the discharge [ $\text{m}^3\cdot\text{s}^{-1}$ ]. The factor of proportionality, the storage constant, is sometimes called the recession constant. The continuity equation for a reservoir is given by

$$\frac{dV}{dt} = R(t) - Q(t) \quad 2-19$$

where  $R(t)$  is the rate of water inflow to the reservoir [ $\text{m}^3\cdot\text{s}^{-1}$ ]. Combining the storage equation and the continuity equation results in

$$k \frac{dQ}{dt} = R(t) - Q(t) \quad 2-20$$

Because firn has different hydraulic properties than ice or snow, the glacier should be divided into different reservoirs, for instance the accumulation and ablation reservoir, with different storage constants. The reservoirs can be coupled in series or parallel.



Hock (1998) used a linear reservoir approach in her study on a small valley glacier in northern Sweden, called Storglaciären. This linear reservoir approach, which is based on the work of Baker et al. (1982), uses three reservoirs: firn, snow and ice. For each reservoir, a storage constant must be estimated. The firn reservoir is defined as the area above the equilibrium line and the ice reservoir is defined as the area of exposed ice below the equilibrium line. The snow reservoir is the snow covered area below the equilibrium line. When Equation 2-20 is solved, the discharge can be calculated. The total discharge per timestep at the glacier snout is the sum of the three discharges for firn, snow and ice and is given by

$$Q(t) = \sum_{i=1}^3 \left( Q_i(t-1) \cdot e^{-\frac{1}{k_i}} + R_i(t) \cdot (1 - e^{-\frac{1}{k_i}}) \right) \quad 2-21$$

where  $Q(t)$  is the discharge at the end of the glacier snout [ $\text{mm} \cdot \text{timestep}^{-1}$ ],  $i$  is an index for each reservoir,  $Q_i(t-1)$  is the discharge of reservoir  $i$  at the previous timestep ( $t-1$ ),  $k_i$  is the storage constant of reservoir  $i$  and  $R_i(t)$  is the rate of water inflow to reservoir  $i$  during the timestep and equals the sum of melt and rain water.

Rain can be distinguished from solid precipitation by using a threshold temperature. Above this temperature, precipitation is liquid, while snow falls below this threshold temperature.

During the transport of melt and rain water through the glacier, melt water can refreeze or can be retained by capillary forces. To account for this delay, a water reservoir in the glacier can be applied, which retains water until a certain threshold value is exceeded. This threshold value can be a percentage of the total snow pack on the glacier.



## **3 The Waterbalance Simulation Model**

### **3.1 Introduction**

The Waterbalance Simulation Model (WaSiM-ETH) has been developed to simulate the runoff hydrograph and the water balance of a catchment area. Such a water balance model should not be specific to one region, and should run with a minimum amount of geographical and meteorological data, with a reasonably high spatial and temporal resolution. The spatial resolution of WaSiM-ETH is given by a regular grid, which can vary in size. The temporal resolution can range from one minute to a few days, depending among others on the time resolution of the meteorological data. The minimum amount of input data required to run the model is precipitation and temperature and grid information about soil properties, land use and elevation. Before the glacier model was incorporated into WaSiM-ETH, runoff simulation studies could not be done in (partly) glacierized catchment areas. In general, WaSiM-ETH was only applicable in regions with low and high mountains without glaciers (Schulla, 1997).

At present, there are two versions of WaSiM-ETH. Version I includes a submodel considering the soil moisture regime, which is based on the Topmodel after Beven and Kirkby (1979). This Topmodel is a conceptual model, describing flow components between and within the saturated and unsaturated zone by fluxes to and out of several reservoirs. Due to its conceptual base, several parameters which have no physical meaning are used. Their values must be adjusted during calibration. Version II comprises a soil moisture method which is based on the more physical Richards equation. In this study, WaSiM-ETH version II is used.

A submodel accounting for groundwater flow using the finite difference method has recently been built in WaSiM-ETH. This means that WaSiM-ETH can now be used in regions where groundwater flow is dominant in the river flow regime. The combination of the Richards equations and the submodel for the groundwater flow enables the user to perform calculations on issues as solute transport in the soil.

The description of WaSiM-ETH, which is given in this chapter, will focus on the background of version II. First, the structure of WaSiM-ETH will be explained. Section 3.3 discusses preprocessing, processing and postprocessing of WaSiM-ETH while Section 3.4 explains the components and the theory of the several submodels of WaSiM-ETH. The description of the glacier/snow submodel will be given at the end of this chapter in Section 3.5. A full description of the parameterizations, input and output files, format requirements and the theory of the submodels is given in Schulla (1999).

### **3.2 Structure of WaSiM-ETH**

WaSiM-ETH is partly based on physical methods, such as the evapotranspiration model after Penman-Monteith, but also uses conceptual approaches.

The water balance of a region which is simulated by WaSiM-ETH includes the components of surface runoff, interflow, groundwater flow and channel flow and the storage of water such as interception, snow accumulation, depression storage and storage of water in the unsaturated and saturated soil. The snow, firn and ice accumulation as well as melt are important for the water balance of glacierized areas.

In order to simulate the water balance of a catchment area, the area must be divided into grid cells. WaSiM-ETH performs calculations for each grid cell, although the interflow and the groundwater flow are simulated for the whole catchment. Interactions between grid cells are not calculated. Figure 3-1 shows the structure of WaSiM-ETH with the glacier submodel.

Each element in this flow chart represents a submodel. The submodels indicated in the large grey element are the submodels which complete calculations per grid cell.

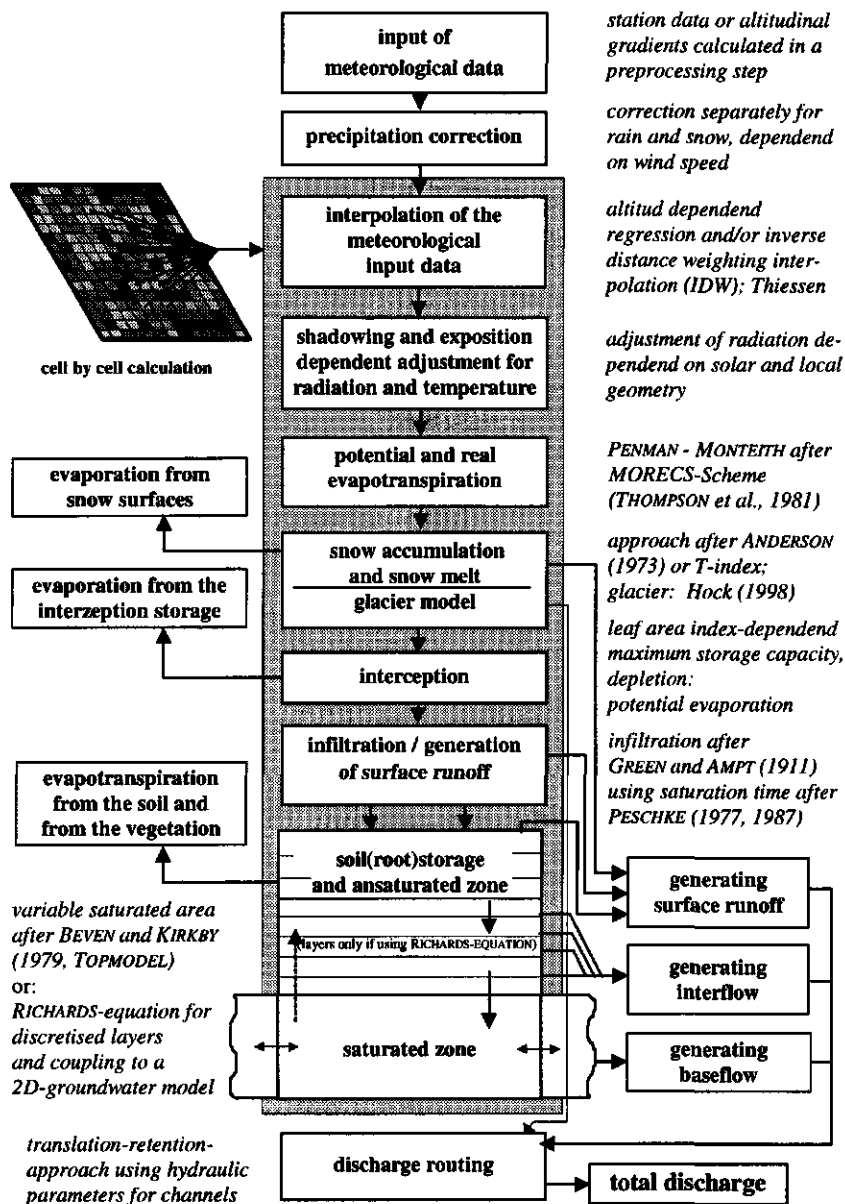


Figure 3-1: Structure of WaSiM-ETH (Source: Schulla, 1999).

WaSiM-ETH carries out the interpolation of meteorological data obtained at various meteorological stations. These stations can be situated outside the catchment area. The submodel that adjusts radiation and temperature modifies the radiation and the air temperature according to exposition and topographic shading of the grid cells (Schulla, 1997).

It is not always necessary to run all the submodels of WaSiM-ETH. The submodels which must be run are found in a control-file. The file names, model parameters, calculation period, output options, and available meteorological, hydrological and geographical data are also defined in the control-file. Additionally, the methods which are used to calculate the different components of the water balance are defined. For instance, to interpolate a meteorological parameter, a choice must be made out of the methods of altitude dependent regression, inverse distance weighting and a combination of both regression and inverse distance

weighting. Appendix 2 shows an example of a control-file for WaSiM-ETH. An advantage of using a control-file is that the source code remains the same when applying the model to another area.

### **3.3 Preprocessing, processing and postprocessing**

During the preprocessing stage, the meteorological, geographical and hydrological data are prepared for use by WaSiM-ETH while also estimates are made for various model parameters, for example the degree day factor for snow melt. The control-file is also prepared to run WaSiM-ETH.

Meteorological input data such as air temperature, relative humidity, wind speed, global radiation, precipitation, sunshine duration and vapour pressure must be given in the appropriate format and units. They can be taken from an automatic meteorological station, operating on hour intervals, or from a conventional station with measurements three times a day. Precipitation data from stations where only daily sums are measured can also be used. Time interpolation is needed to adjust the meteorological data to the time resolution used in WaSiM-ETH. For instance, daily precipitation measurements must be changed into hourly data when the time resolution of WaSiM-ETH is one hour. For spatial interpolation of the meteorological data according to the height dependent regression, regression coefficients are needed. These coefficients must be assessed during the preprocessing stage by the programs REGR or REGRESS, which are described in the WaSiM-ETH manual (Schulla, 1998). WaSiM-ETH uses these regression coefficients, meteorological data and the digital elevation model to calculate meteorological data for every grid cell.

In order to calibrate the model the discharge at the outlet of the basin is needed. The units of the discharge must be similar to the discharge units as defined in the control-file.

The minimum amount of spatially distributed data as grids are elevation, soil properties and land use. Other grid information which is necessary, and can be generated by using the digital elevation model are the catchment boundary, the slope, the exposition and the flow times. All grids must be of the same size and the same spatial resolution. Different programs are available to resize grids, build grids, visualize grids and to change the resolution. The program TANALYS (= Topographical Analysis) calculates for each grid cell exposition, slope, flow direction, flow time and other important hydrological parameters as well as the catchment boundary. This program uses only the digital elevation model as input. TANALYS consists of many submodels. When no GIS tools are available, TANALYS is essential to work with WaSiM-ETH.

The processing of the model follows according to the control-file. Appendix 3 shows the data flow of WaSiM-ETH version II, when all submodels are used. Firstly, WaSiM-ETH opens and reads the meteorological, geographical and hydrological input files, which are defined in the control-file. It generates grids such as albedo, soil water storage and hydraulic conductivity using the land use and soil type grids as well as the land use and the soil type tables which are defined in the control-file. Secondly, the spatial interpolation of meteorological data observed at various locations and the execution of the submodels are carried out for each grid cell at the first time step. The predefined output data are written to output files for the first time step before interpolating and calculating the data for the next time step. The output data of each time step are usually spatial averages of the total catchment area or different subcatchment areas. These time series stored in files reveal the temporal variation of, for instance, discharge or evaporation. Apart from these files, WaSiM-ETH generates for every grid cell sums and outputs with average, maximum or minimum values of any output data for any time period. This output information reveals spatial variations. Any combination of averages over time and area can be requested, and must be defined in the control-file. When the submodel 'Routing of discharge' is executed, WaSiM-

ETH creates a file with the total discharge, compares the simulated discharge with the observed discharge and calculates efficiency criteria between these time series.

Postprocessing includes the visualisation and interpretation of the output data. Graphical programs such as Graphics or Excel can be used to show the simulated time series. These programs are also used to interpret the output data and to calculate, for instance, correlation coefficients between two time series and total evaporation for the seasons. Combining several output files allows to check the water balance of a catchment area. During the postprocessing also model parameters are verified and changed in order to improve the simulation.

#### **3.4 Submodels of WaSiM-ETH**

The submodels of WaSiM-ETH version II are: Interpolation of input data, Precipitation correction, Radiation correction and temperature modification, Evapotranspiration, Snow and Glacier model, Interception, Soil water model (including infiltration) and Discharge routing. The submodels will be described briefly in this section. The Snow and Glacier submodel will be described separately in Section 3.5, because this is the newly incorporated submodel.

##### **3.4.1 Interpolation of input data**

Meteorological data are normally measured at some locations or stations, which can be situated outside the catchment area. Two interpolation methods frequently used to obtain values for each grid cell are the altitude dependent regression and inverse distance weighting interpolation method. A combination of these two methods can also be applied. A third interpolation method uses the Thiessen Polygons method.

The air temperature, vapour pressure and wind speed depend strongly on altitude and should be interpolated by using the altitude dependent regression. When using the altitude dependent regression, a number of two meteorological stations is sufficient to calculate the regression coefficients. During winter, stable weather conditions cause temperature inversions. These inversions are taken into account during the regression. The top and bottom height of the possible inversion layer are defined in the control-files of the programs REGR or REGRESS. During the calculations the program checks whether there is an inversion within the defined layer.

WaSiM-ETH calculates, for example, the temperature as a function of height following

$$T(h) = a + b \cdot h \quad 3-1$$

where T is the temperature [°C], h is the height [m] and a [°C] and b [°C·m<sup>-1</sup>] are regression coefficients.

The inverse distance weighting interpolation method is used for horizontal interpolation. This method is often used to interpolate precipitation or sunshine duration and is based on the assumption that every grid cell can be described by a weighted average of surrounding station measurements following

$$z = \sum_j (w_j \cdot z_j) \quad 3-2$$

where z is the interpolated value, w<sub>j</sub> is the weight of station j and z<sub>j</sub> is the measured value at station j.

The Thiessen Polygon method is similar to the inverse distance weighting interpolation method used for horizontal interpolation. Using this method, the value of a grid cell is determined by the value of the nearest station.

### 3.4.2 Precipitation correction

Precipitation measurements do not normally represent the true value of precipitation. Errors in measurements always contain a random error and a systematic error. Raingauge measurements are influenced by wind, evaporation and absorption of water by the gauge itself. In particular, snow measurements are sensitive to wind exposure and are systematically underestimated. Therefore, the measurements should be corrected. The systematic error of the precipitation measurements is corrected using

$$P_{corr} = P \cdot (a + b \cdot u) \quad 3-3$$

where  $P_{corr}$  is the corrected precipitation [mm],  $P$  is the measured precipitation [mm],  $u$  is the wind speed [ $m \cdot s^{-1}$ ] and  $a$  [-] and  $b$  [ $s \cdot m^{-1}$ ] are correction factors.  $a$  and  $b$  are different for liquid and solid precipitation.

### 3.4.3 Radiation correction and temperature modification

Radiation and temperature are influenced by topography, especially in hilly areas. The temperature at a north slope can differ significantly from the temperature at a south slope. The exposure (north, south, east, west), the slope (0-90°) and the shading influence the amount of incoming shortwave radiation. Both temperature and radiation are important factors to estimate evaporation, sensible heat flux, soil temperature and snow melt.

The incoming solar radiation perpendicular projected to the horizontal plane can be calculated as a function of the top of the atmosphere radiation, atmospheric transmissivity and solar geometry, or it can be measured at a meteorological station. The radiation perpendicular projected to the horizontal plane must be corrected for the slope of a grid cell following

$$I_{corr} = I_{norm} \cdot \frac{\cos \theta}{\cos Z} \quad 3-4$$

where  $I_{corr}$  is the radiation normal to the grid slope [ $W \cdot m^{-2}$ ],  $I_{norm}$  is the incoming radiation perpendicular to the horizontal [ $W \cdot m^{-2}$ ],  $\theta$  is the angle of incidence between the normal to the grid cell and the solar beam [°] and  $Z$  is the local zenith angle [°]. Whether a grid cell is shaded can be estimated for every time step using the zenith angle and the solar azimuth angle.

The temperature is corrected for incoming solar radiation. This correction depends on the relative sunshine duration. If the sunshine duration is zero, the temperature is not corrected. In case the sunshine duration exceeds zero, the temperature is corrected according to an empirical function using relative sunshine duration, an empirical parameter, the angle of incidence between the normal to the grid cell and the solar beam, and the local zenith angle.

### 3.4.4 Evapotranspiration

The potential evapotranspiration can be calculated using the Penman-Monteith method (Monteith, 1975). The Penman-Monteith method uses many meteorological variables and coefficients. In case these meteorological data are not available, the potential evapotranspiration can be assessed using the method of Wendling (Wendling, 1975) or Hamon (Federer and Lash, 1983). The method of Wendling uses global radiation, albedo and daily temperature to calculate the daily potential evapotranspiration. This method cannot be

used for hourly simulations. The method of uses day length and the daily temperature with matching saturated water vapour pressure.

The calculation of evapotranspiration according to the Penman-Monteith method follows

$$\lambda E = \frac{\frac{\Delta}{\gamma_p} \cdot (R_n - G) + \frac{\rho \cdot c_p}{\gamma_p \cdot r_a} (e_s - e) \cdot t_i}{\frac{\Delta}{\gamma_p} + 1 + \frac{r_s}{r_a}} \quad 3-5$$

where  $\lambda$  is the latent heat of evaporation [ $\text{kJ} \cdot \text{kg}^{-1}$ ],  $E$  is the evapotranspiration [ $\text{kg} \cdot \text{m}^{-2}$ ],  $\Delta$  is the first derivative of the saturated vapour pressure curve [ $\text{hPa} \cdot \text{K}^{-1}$ ],  $\gamma_p$  is the psychrometric constant [ $\text{hPa} \cdot \text{K}^{-1}$ ],  $R_n$  is the net radiation [ $\text{kJ} \cdot \text{m}^{-2}$ ],  $G$  is the soil heat flux [ $\text{kJ} \cdot \text{m}^{-2}$ ],  $\rho$  is the air density [ $\text{kg} \cdot \text{m}^{-3}$ ],  $c_p$  is the specific heat of dry air at constant pressure [ $\text{kJ} \cdot (\text{kg} \cdot \text{K})^{-1}$ ],  $r_a$  is the aerodynamic diffusion resistance [ $\text{s} \cdot \text{m}^{-1}$ ],  $r_s$  is the internal canopy diffusion resistance [ $\text{s} \cdot \text{m}^{-1}$ ],  $e_s$  is the saturated vapour pressure at the actual temperature [ $\text{hPa}$ ],  $e$  is the actual water vapour pressure [ $\text{hPa}$ ] and  $t_i$  is number of seconds per time step [-].

The net radiation is the sum of incoming and outgoing short- and longwave radiation. The value can be calculated and estimated in different ways. The aerodynamic diffusion resistance ( $r_a$ ) depends on the wind speed and the surface roughness length ( $z_0$ ). The internal canopy diffusion resistance ( $r_s$ ) depends on the type of crop, the solar radiation, the temperature, the leaf area index and the soil moisture properties.

The actual evapotranspiration depends on the soil water content. In case the soil water content is below wilting point, the actual evapotranspiration is zero. If the soil water content is between wilting point and saturated soil water content the actual evapotranspiration is calculated by

$$ETR = ETP \cdot (\theta - \theta_{wp}) / (\theta_{\psi_g} - \theta_{wp}) \quad \theta_{wp} \leq \theta \leq \theta_{\psi_g} \quad 3-6$$

$$ETR = ETP \quad \theta_{\psi_g} \leq \theta \leq \eta \cdot \theta_{sat} \quad 3-7$$

$$ETR = ETP \cdot (\theta_{sat} - \theta) / (\theta_{sat} - \eta \theta_{sat}) \quad \eta \cdot \theta_{sat} \leq \theta \leq \theta_{sat} \quad 3-8$$

where  $ETR$  is the actual evapotranspiration [ $\text{mm}$ ],  $ETP$  is the potential evapotranspiration [ $\text{mm}$ ],  $\theta$  is the actual soil water content [-],  $\theta_{wp}$  is the soil water content at wilting point [-],  $\theta_{\psi_g}$  is the soil water content at which actual evapotranspiration equals potential evapotranspiration [-],  $\eta$  is the maximum relative water content at which processes in the soil are aerobic [-] and  $\theta_{sat}$  is the saturated soil water content.

### 3.4.5 Interception

Interception is defined in WaSiM-ETH as the storage of precipitation and melt water on vegetation and the soil surface. The storage capacity depends on the type of vegetation, the leaf area index and the area which is covered by vegetation. The storage capacity is calculated according to

$$SI_{max} = v \cdot LAI \cdot h_{si} + (1 - v) \cdot h_{si} \quad 3-9$$

where  $SI_{max}$  is the maximal storage capacity of the interception [ $\text{mm}$ ],  $v$  is the surface area covered by vegetation [ $\text{m}^2 \cdot \text{m}^{-2}$ ],  $LAI$  is the leaf area index [-] and  $h_{si}$  is the maximum depth of water on a wet surface [ $\text{mm}$ ]. As long as the interception reservoir contains water, the actual



evaporation equals potential evaporation and water evaporates from the interception storage. During this time, no water evaporates from the soil. Evaporation from the soil begins when the interception reservoir is empty. In contrast with evaporation from the interception reservoir, evaporation from the soil does not always equal potential evaporation, depending on the soil water content.

### 3.4.6 The soil water model

The soil water model is used to calculate the vertical flow of water in the unsaturated zone. In WaSiM-ETH version II it is based on the Richards equation. Each grid cell represents a soil column, which is divided in several horizontal layers. Between these layers, the flux is calculated by the discrete Richards equation following

$$\frac{\Delta\theta}{\Delta t} = \frac{\Delta q}{\Delta z} = q_{in} - q_{out} \quad 3-10$$

where the  $\theta$  is water content [-],  $t$  is the time [s],  $q$  is the specific flow [ $\text{m}\cdot\text{s}^{-1}$ ],  $z$  is the height [m],  $q_{in}$  is the incoming flux in the soil layer [ $\text{m}\cdot\text{s}^{-1}$ ] and  $q_{out}$  is the outgoing flux in the soil layer [ $\text{m}\cdot\text{s}^{-1}$ ].

This equation is based on the continuum equation for one dimensional flow in a vertical soil column under unsaturated conditions, given by

$$\frac{\partial\theta}{\partial t} = \frac{\partial q}{\partial z} = \frac{\partial}{\partial z} \left( -k(\theta) \frac{\partial\Psi(\theta)}{\partial z} \right) \quad 3-11$$

where  $k(\theta)$  is the hydraulic conductivity [ $\text{m}\cdot\text{s}^{-1}$ ] and  $\Psi(\theta)$  is the hydraulic head which is the sum of the pressure head and elevation head [m].

Within the model, the dependency of the hydraulic conductivity with changing water content is considered. This can be done by implementing two methods. The first uses measured values for conductivity and water content [ $\theta$ ,  $h_h(\theta)$ ] and [ $\theta$ ,  $k_{rel}(\theta)$ ]. Values used for model calculations are obtained by interpolating the measured values.

Another approach is to use the parametrization after Genuchten (1976) that also includes the process of hysteresis.

Equation 3-11 is solved for each layer, by using a 1-dimensional vertical numerical scheme. Numerical problems are avoided by using a restriction parameter and the condition that every zone within the catchment area should have the same number of layers.

For each time step, the boundary condition for the first layer is determined by the amount of infiltrating water, calculated by the methods of Green and Ampt (1911) and Peschke (1977, 1987), respectively.

The infiltration model is incorporated into the soil model. Melt water and rain infiltrate into the soil depending on soil water content, infiltration capacity and some other soil properties. The time needed to saturate the soil ( $t_s$ ) [h] is calculated according to

$$t_s = \frac{l_s \cdot n_a}{PI} \quad 3-12$$

where  $l_s$  is the soil depth to be saturated [mm],  $n_a$  is the difference between the saturated soil water content and the actual soil water content [-] and PI is the precipitation intensity [ $\text{mm}\cdot\text{h}^{-1}$ ]. The water volume that can infiltrate into the soil until the soil is saturated,  $F_s$  [mm], follows

$$F_s = l_s \cdot n_a = t_s \cdot PI \quad 3-13$$

Although the soil is saturated after  $t_s$ , water still infiltrates into the soil during the remaining time  $(t - t_s)$  ( $t$  is the time step [h]) according to

$$F = \frac{A}{2} + \left[ \frac{A^2}{4} + A \cdot B + F_s^2 \right]^{\frac{1}{2}} \quad 3-14$$

with

$$A = k_s (t - t_s)$$

$$B = F_s + 2 \cdot n_a \cdot \psi_f$$

where  $F$  is the infiltrated amount of water when the soil is saturated [mm],  $k_s$  is the saturated hydraulic conductivity of the soil [ $\text{mm} \cdot \text{h}^{-1}$ ] and  $\psi_f$  is the hydraulic head at the depth at which the water has infiltrated [mm].

Water which does not infiltrate into the soil,  $PI \cdot \Delta T - F - F_s$ , is defined as surface runoff. This surface runoff is calculated per grid cell and is transformed afterwards, together with the direct runoff from the snow model, into total direct runoff, using a linear reservoir.

The numerical calculations for vertical unsaturated flow start in the layer beneath the layer that is saturated by the process of infiltration. When no upper layers are saturated, calculations start at the first top layer. The lower boundary for the calculations is the layer in which the groundwater level is present. The calculations are done in an iterative way and terminate when a numerical threshold value is reached. In this iterative approach, a complete water balance for the layers in the vertical soil column is calculated, including the processes of infiltration and exfiltration from rivers and channels. An extended description of the calculation is given in Schulla and Jasper (1998).

Interflow is calculated in two steps. For this calculation a threshold value is used for the hydraulic head ( $\Psi$ ) which must be smaller than 3.45. First a maximum rate of interflow is calculated according to

$$q_{ifl,max} = \frac{(\theta(\Psi) - \theta_{\Psi=3.45}) \cdot \Delta z}{\Delta t} \quad 3-15$$

where  $q_{ifl,max}$  is the maximum interflow [ $\text{m} \cdot \text{s}^{-1}$ ],  $\theta(\Psi)$  is the water content at the actual hydraulic head [-],  $\theta_{\Psi=3.45}$  is the water content at the hydraulic head  $\Psi = 3.45$  [-],  $\Delta z$  is the layer thickness [m] and  $\Delta t$  is the time step [s].

Besides the maximum interflow, a value for interflow which is based on conductivity, channel density and gradients is calculated, according to

$$q_{ifl} = k_s (\theta_m) \cdot \Delta z \cdot d_r \cdot \tan \beta \quad 3-16$$

where  $q_{ifl}$  is the interflow [ $\text{m} \cdot \text{s}^{-1}$ ],  $k_s$  is the saturated hydraulic conductivity [ $\text{m} \cdot \text{s}^{-1}$ ],  $\theta_m$  is the water content in layer  $m$  [-],  $d_r$  is the drainage density [ $\text{m}^{-1}$ ] and  $\beta$  is the local slope [ $^\circ$ ].

When both values for interflow are calculated, the smallest value is chosen as the actual interflow. Then, all grid cell values are summarized and transformed into a total interflow rate by using a linear reservoir approach while spatial distribution is no longer considered.

After the water balance for ground water is calculated, base flow for each grid cell is calculated according to

$$Q_b = Q_0 \cdot k_s \cdot e^{(h_{GW} - h_{geo,0})/k_B} \quad 3-17$$

Where  $Q_b$  is the base flow rate [ $m \cdot s^{-1}$ ],  $Q_0$  is a scaling factor for the base flow [-],  $k_s$  is the saturated hydraulic conductivity [ $m \cdot s^{-1}$ ],  $h_{GW}$  is the groundwater level above sea level [m],  $h_{geo,0}$  is the surface level above sea level [m] and  $k_B$  is a recession constant for base flow [m]. This formula, which is based on the linear reservoir approach, is related to the groundwater level rather than to time. Total base flow is obtained by adding all values for all grid cells.  $Q_0$  and  $k_B$  are parameters to be optimized.

### 3.4.7 Discharge routing

The 'discharge routing' submodel is used for calculations on larger catchment areas in which several subbasins are present. For each subbasin the discharge at its outlet is calculated, by the submodels mentioned above. The discharge at the outlet of the entire catchment area is then calculated by routing the discharges of the individual subbasins through the interconnecting rivers and channels. In this study, discharge routing is used to route the discharge of the glacier to the outlet of the catchment area.

In this routing method, the equation for flow after Manning-Strickler is used, which follows

$$v_l = M \cdot R_h^{2/3} \cdot I^{1/2} \quad 3-18$$

in which  $v_l$  is the flow velocity [ $m \cdot s^{-1}$ ],  $M$  is the hydraulic resistance [ $m^{1/3} \cdot s^{-1}$ ],  $R_h$  is the hydraulic radius [m] and  $I$  is the slope of the river bed [ $m \cdot m^{-1}$ ].

Values for the hydraulic radius can be obtained by using TANALYS and some predefined relationships between river depth and width. The width is related to the size of the area of which the river transports runoff. Slope is also taken into account. TANALYS calculates a set of values for these flow parameters which are used in WaSiM-ETH for the discharge routing. It is also possible to use data obtained by measurements.

## 3.5 Snow and glacier submodel

### 3.5.1 Introduction

Before the glacier submodel was incorporated into WaSiM-ETH, a snow submodel existed in WaSiM-ETH. This submodel calculated accumulation of snow and snow melt, and contained different temperature index methods to calculate snow melt, which are described in Section 3.5.3. Melting of snow, which does not cover a glacier, is calculated by one of these methods. Section 2.5.1 describes some glacier melt models. Two temperature index methods were chosen to insert into WaSiM-ETH to calculate glacier melt instead of an energy balance method, because of four reasons. Firstly, a temperature index method is the most widely used approach. Secondly, energy models require large quantities of meteorological data. Thirdly, there is large uncertainty about the parameterization of the turbulent heat fluxes. Finally the energy balance methods which were used by Hock are restricted to use in the main melt season, because the heat content of the glacier is not taken into account (Hock, 1998).

Section 3.5.4 describes the two temperature index methods chosen and the discharge model, which calculates the transport of melt water to the glacier snout. The methods which are used to simulate snow melt on unglacierized areas are explained in Section 3.5.3. Section 3.5.2. describes how snow accumulation on glacierized and unglacierized areas is calculated.

### 3.5.2. Snow accumulation

Snow accumulation caused by snowfall is calculated for the glacierized and unglacierized parts of a catchment area. Whether snowfall or rainfall occurs depends on the air temperature. Two threshold temperatures are used to discriminate solid precipitation from liquid precipitation according to

$$P_{\text{snow}} = \frac{T_{R/S} + T_{\text{trans}} - T}{2 \cdot T_{\text{trans}}} \quad \text{for } (T_{R/S} - T_{\text{trans}}) < T < (T_{R/S} + T_{\text{trans}}) \quad 3-19$$

where  $P_{\text{snow}}$  is the part of snow from total precipitation [-],  $T_{R/S}$  is defined as the temperature at which 50% of the total precipitation is snow [ $^{\circ}\text{C}$ ],  $T$  is the current air temperature [ $^{\circ}\text{C}$ ] and  $2 \cdot T_{\text{trans}}$  is the temperature range where both snow- and rainfall occur. Below  $T_{R/S} - T_{\text{trans}}$  only snowfall occurs. Above  $T_{R/S} + T_{\text{trans}}$  precipitation consists of rain.

### 3.5.3 Snow melt on unglacierized areas

WaSiM-ETH contains three different methods to calculate snow melt on the unglacierized areas. The first and simplest method is the classical degree-day method, which is described by Equation 2-4. The second method is the degree-day method, which is extended by a wind speed dependent melt factor and follows Equation 2-5 (Braun, 1985). The combination method by Anderson (1973) that was extended by Braun (1985), is the third method, which calculates snow melt. This method has been described in Section 2.5.1. The saturated water vapour pressure at air temperature is used instead of the actual water vapour pressure to calculate the melt rate due to the latent heat flux.

Within the model a CWH factor determines the amount of water that is stored within the snow pack of the unglacierized area. It determines the amount of water that is stored within the snow on the unglacierized area as a percentage of the total snow reservoir. The melt water which is not retained by snow either infiltrates into the soil or is discharged as surface runoff. The occurrence of snow melt, together with the accumulated amount of snowfall determine the snow storage and the area covered with snow. If the snow storage is calculated as zero, the area is not covered by snow and snow melt does not occur.

### 3.5.4 Glacier melt and melt water transport

Besides the melting of snow, melting of firn and ice must be calculated for glacierized areas. The two methods, which are incorporated in WaSiM-ETH to calculate glacier melt are based on the work of Hock (1998).

The first method is the classical degree-day method following Equation 2-5. Three different degree-day factors are used to calculate snow, ice and firn melt. The glacierized area covered by snow is determined by a snow storage grid. This snow storage grid is calculated for every time step and changes due to the accumulation and melting of snow. The firn area is defined as the glacier area above the equilibrium line. The ice area is defined by the glacier area below the equilibrium line which is not covered by snow. The snow area is defined as the area below the equilibrium line which is covered by snow. The equilibrium line and the glacier area are defined by a grid which is constant in time. This means, the glacier area does not vary in time and the glacier does not retreat. The firn area and the ice area are not defined by a storage grid, like for snow, because the accumulation and the storage of firn and ice is not calculated.

The second method is similar to the classical degree-day method including a radiation index according to Equation 2-6. However, measured global radiation is used instead of potential clear sky solar radiation. This method uses one degree-day factor, called the melt factor, and two radiation coefficients for snow and ice. Here, the snow area is defined as the glacier area covered with snow, including the firn area. The ice area is the area with exposed ice.

Melt water from the glacier is transported through the glacier to the glacier snout according to the linear reservoir approach of Hock (1998), which has been described in Section 2.5.2. The discharges of each reservoir, firn, snow and ice, are calculated and summarized to get the total discharge of the glacier. Therefore, three storage constants must be estimated. The sum of the discharges of the snow, ice and firn reservoir at the glacier snout is treated as the discharge of a subcatchment and is routed by the submodel 'discharge routing' to the catchment outlet.

### 3 The Waterbalance Simulation Model

## 4 Application of the model

### 4.1 Introduction

In this study, the WaSiM-ETH model is used to calculate the runoff of the Gletsch catchment, which contains the Rhone-glacier. This catchment area has been chosen while up to 50 percent of its area is glacierized. Therefore, it is an appropriate catchment basin to test the performance of the new built glacier model and to compare the results of model runs with and without the glacier submodel.

The spatial distributed modelling of runoff requires large quantities of temporal and spatial data. The availability of these data largely determine the quality of the results of the model calculations. For this reason, data acquisition is one of the most important aspects of modelling. Obtaining a high quality data set for calculations in mountainous areas is even harder since meteorological data do not only vary in space and time but also in altitude. Therefore, it is not only necessary to use algorithms as Inverse Distance Weighting, but also height dependent regression techniques.

In this chapter, the acquisition and preparation of the required input data will be described. A description of the Gletsch catchment will be given in Section 4.2. The acquisition of meteorological, geographical and hydrological data is described in Section 4.3. The following two sections describe the initial values and list all input parameters, respectively. The last section contains the background of spatial and temporal resolution.

### 4.2 Description of the Gletsch catchment

The Gletsch catchment area is located in Central-Switzerland and is part of the Swiss Central Alps (46°37' N, 8°24' E), situated between the Aare- and Gotthard massif. The Rhone River originates in this catchment area. Its altitude ranges from 1755 m (outlet at Gletsch) to 3629 m (Dammastock) above sea level and covers an area of 38.87 km<sup>2</sup>. The valley has an orientation of NNW to SSW, and is surrounded by peaks which all exceed an altitude of 3000 m (Weilenman, 1979). In the catchment area, four glaciers are present: The Rhone glacier which covers most of the northern part and three (much smaller) glaciers in the middle and south eastern part.

In the Gletsch catchment it is possible to distinguish three different zones hydrological as well as topographical.

- The south-west directed chalk area of Gletsch (non-glacierized)
- Muttbachtal in the Northwest direction (including the Mutt glacier)
- The catchment area of the Rhone glacier (including the Rhone glacier)

A visualisation of the catchment area is given in Figure 4.1.

The Rhone glacier which is the most dominant source for the runoff from the area, has a length of 10.2 km and ranges in height from 2125 to 3620 m with an average height of 2940 m. The total area of the glacier is approximately 17.38 km<sup>2</sup>. Together with the three smaller glaciers, the Gerstenhorn glacier (0.8 km<sup>2</sup>), the Mutt glacier (0.57 km<sup>2</sup>) and the Galen Glacier (0.4 km<sup>2</sup>), this results in a percentage glacierized area of 52% (Bernath, 1991). While the Galen and the Gerstenhorn glacier are part of the Rhone glacier, they will not be discussed further but will be addressed to as Rhone glacier.

Discharge measurements for the Gletsch area are completed by the 'Landeshydrologie Bern'. There is one measurement station at the Gletsch settlement, where discharge is measured on a hourly basis. The snout of the Rhone glacier is approximately two kilometres to the north east of Gletsch.

The runoff of the Mutt glacier is transported by the Muttbach and reaches the Rhone about 1.5 km upstream of Gletsch.

The yearly mean temperature at an altitude of 2300 m is 0.5 °C, while the averaged precipitation amounts to approximately 2000 mm per year (Bernath, 1991).

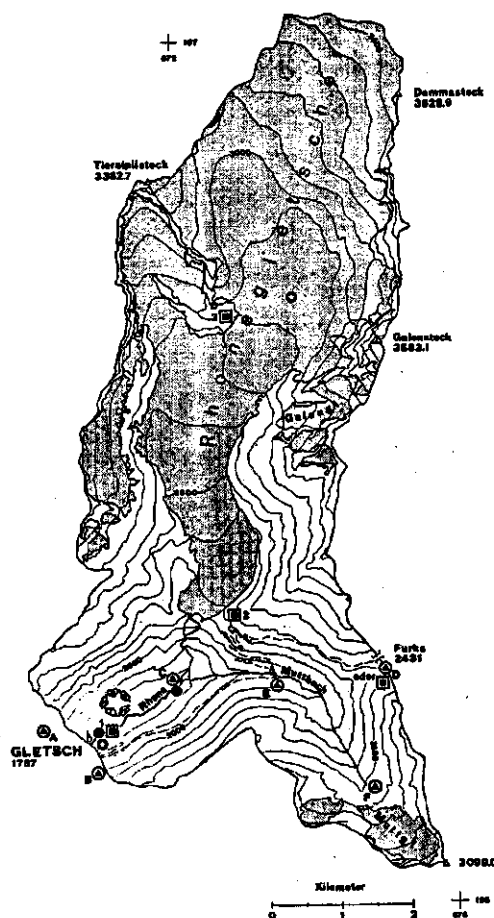


**Figure 4-1: The Gletsch catchment. (Source: Bernath, 1991)**

The geological proportions are set by the Aare- and the Gotthard massif. The Rhone glacier is mainly positioned in the area of the Aare granite, while the Mutt glacier is situated in the paragneisen of the Gotthard massif. Between these two, there is a zone of Amphibolites, Paragneis, Gneiss, Perm, Dogger and Malm. The valley is filled by fluvio-glacial processes. This debris originates from the Quaternary. The moraine banks of 1602, 1640, 1818, 1856 and 1920 are still visible (Bernath, 1991). From a hydrological point of view this valley is very important. In the underground near Gletsch the valley is closed off by rock. This means that (almost) no water is leaving the catchment area as subsurface flow.

The vegetational cover is diverse due to the fact that the area's altitude ranges from higher subalpine regions to the main alpine regions. In the lower part of the catchment area, the growing season lasts for about 4 months, of which two are mostly without frost. With increasing altitude, the vegetation cover decreases until it ceases completely, leaving just snow, ice and rock.

As a consequence of the glacier's retreat which mainly took place in the last 300 to 400 years, the soil in front of the snout is still young from a geological point of view. For centuries the glaciers volume was smaller than the present volume. The small ice age of the 16<sup>th</sup> century, which lasted some decades, resulted in a clear increase of volume of all the Alpine glaciers. In 1602, the glacier snout was at Gletsch, indicating that the glacier is still adjusting to the climatic conditions of the period after this last small Ice Age (Kümmerly and Frey Bern, 1980). The glacier's retreat over the years is shown in Appendix 4.

The hydrograph of outflow for 1992 of the Gletsch catchment is shown in Appendix 1, which shows the response of the catchment to varying meteorological conditions.

In summer, snow melt, induced by temperature and radiation, is the main contributing factor to runoff. The hydrograph in the Appendix shows this clearly: increasing temperature and radiation results in a higher runoff, which is barely effected by the precipitation.

A part of the snow melt water will infiltrate into the soil, resulting in interflow or baseflow, while the other part of the melt water will transform to direct runoff. A time delay may occur while a reasonable amount of water can be stored in the snow reservoir. When the snow in the valley and on the south facing slopes has melted, rainfall will become a more dominant



factor in the outflow. Nevertheless, there may still be snow melt in the higher regions. In summer, the glacier melt will contribute to the runoff, leaving its marks on the hydrograph by large diurnal variations and, in comparison with winter and spring times, large baseflow rates. The hydrograph mentioned before show that the effects of, for instance, temperature, radiation and precipitation are changing throughout the year.

Within WaSiM-ETH, the catchment boundary is determined during preprocessing by the program TANALYS. When the co-ordinates of the outlet are given, this program calculates the boundary of the catchment area, based on the Digital Elevation Model. By doing so, a boundary at the surface is determined. The actual catchment boundary is probably slightly different due to neglected hydro-geological processes. However, the deviation is small. When using a resolution of 100 x 100 m, an area size of 39.68 km<sup>2</sup> is calculated, which is 2.1% larger than the value given by Bernath (1991). When extended hydro-geological research results are available, WaSiM-ETH enables the user to use this data for optimising the water balance.

### **4.3 Acquisition of the required input data**

The required input data can be divided into three different categories, which are meteorological data, geographical data and hydrological data.

#### **4.3.1 Meteorological data**

For the calculations on the Gletsch catchment, meteorological data is used from six automatic, so called, ANETZ (Automatisches Netz) stations, where all six parameters are measured on hourly basis. Furthermore data was used of three conventional stations and ten locations where only precipitation is measured on a daily basis. At a conventional station, precipitation (sum value for the corresponding time step), temperature, wind speed and air humidity (not used) is measured three times a day at 7.00 am, 1.00 pm and 7.00 pm. The stations, mentioned, are not located in the model area but in the surroundings up to 35 km from the Gletsch area. It is assumed that these data are representative for the purpose of this study in the Gletsch area. The locations and characteristics of these several stations are shown in Appendix 5.

Although these stations were not active for the complete period 1990 - 1996, a combination of the results leads to a reliable source of input data. The data which is not measured on an hourly basis (conventional and daily stations), is divided over the day to gain the same temporal resolution as the ANETZ stations. Therefore, the data is not just divided into 24 pieces, but is divided over the day according to the time series of the nearest ANETZ station.

In order to get optimal results the meteorological input data is interpolated in various ways (Table 4-1), depending on the specific parameter. When using the combination of inverse distance weighting (IDW) and height dependent regression (HDR) it is possible, by using a defined parameter in the control-file, to change the contribution of the interpolation methods to the final result. The Thiessen method is a special form of the IDW and should be used only when the data of the nearest measurement station is taken into account.

For precipitation a combination of 75 % IDW and 25 % height dependent regression is used. The relative importance of the HDR in the interpolation follows from the dependency between altitude and precipitations sums in alpine regions. Since there are no meteorological measurement stations within the catchment area, IDW is not enough to obtain reliable meteorological data. More information about precipitation in alpine regions and the height dependency of precipitation amounts can be found in Sevruk et al. (1985).

**Table 4-1: The interpolation methods which are used to calculate grid values of variables.**

	<i>Inverse Distance Weighting (IDW)</i>	<i>Height Dependent Regression (HDR)</i>	<i>Combination of IDW and HDR</i>	<i>Thiessen</i>
Temperature		X		
Precipitation			X	
Global radiation		X		
Wind speed		X		
Vapour pressure		X		
Sunshine duration	X			

The meteorological data should be given in a text-format and should replicate the example given in Figure 4-3. The data is organised in columns. Each column represents a measurement station, in which data is stored. The first four columns are reserved for the year, month, day and hour declaration. The first data begins in the fifth column. The first row is for optional comments. The second row gives the altitude of the measurement station, the third and fourth give the *x* and *y* co-ordinates, respectively. The fifth row shows the names of the several stations.

Temperature (0.1 °C.)

YY	MM	DD	HH	1442	1055	1505
YY	MM	DD	HH	688500	665280	681180
YY	MM	DD	HH	165340	167550	130000
YY	MM	DD	HH	Anderm	Guttan	Bosco-
90	1	1	07	-118	-60	-52
90	1	1	13	-99	29	-27
90	1	1	21	-88	-40	-34
90	1	2	07	-126	-53	-32
90	1	2	13	-98	24	1

**Figure 4-3: Text format of meteorological input data.**

#### 4.3.2 Geographical data

For a reliable modelling of the runoff, geographical data is required. In mountainous areas, the Digital Elevation Model (DEM) offers the most important data source. For runoff modelling of the Gletsch catchment, the DEM of Switzerland (Bundesamt für Landestopografie, 1991) was used with a resolution of 100 x 100 meters. This resolution was gained by interpolation while the original version has a resolution of 250 x 250 meters. In Appendix 6 an example of the DEM for the Gletsch catchment is given.

In order to diminish the calculation time in WaSiM-ETH, it is possible to lower the resolution, resulting in less grid cells. In the Thur catchment Schulla (1997) used a grid size of 500 x 500 meters. In this study, the highest resolution of 100 x 100 meters is used because a lower resolution will probably not calculate the snow line retreat in a correct way. This snow line is very important, especially on the glacier, because it determines the transition between snow and ice melt. The parameter sensitivity (Section 5.3) shows the effect of changing the grid size. During preprocessing the DEM is also used to calculate spatially distributed data as grids for exposure and slope.

The information of the different land use types was obtained by using the 'Arealstatistik der Schweiz' (Bundesamt für Statistik, 1993). In this data bank, which is already in a GIS format, 67 land use types are distinguished based on economic criteria. These economic criteria are summarized in ten, from hydrological point of view, important land use types. The land use grid is showed in Appendix 7. The characteristics (albedo, root depth, resistance, LAI and others) of these types are declared in the land use table in the control-file.

The third important source of geographical data is the 'Digitale Bodeneignungskarte der Schweiz' (Bundesamt für Statistik, 1995). This map contains qualitative information about the soil characteristics. Together with the data regarding land use, these values are converted to values for the available soil moisture content at field capacity and hydraulic conductivity. The digital maps for soil type and land use both have a resolution of 100 x 100 meters. In contrast to the DEM, interpolation of the latter two is of no use, while no extra accuracy will be obtained.

#### 4.3.3 Hydrological data

For the Gletsch area, hydrological flow data was available for the period 1981 - 1997. The source of this data is the 'Landeshydrologie und Geologie' in Bern. This flow data is archived on a hourly basis in  $m^3/s$  and must be transformed into mm/time step before implementation into WaSiM-ETH. The format, as well as the time step, should be the same as the meteorological data (see Figure 4-3).

The available meteorological and hydrological data do not cover the same period therefore the data from 1990 to 1997 is used. In Version II of the model these data are only used for the calibration and the validation of the model.

While the gauging station is situated in Gletsch, only the total runoff of the complete area is measured. Therefore, it is not possible to distinguish between the runoff of the glacier and that of the unglacierized area.

#### 4.4 Assessment of initial values

In order to make a reliable model run also several initial values are necessary. These values can be given in two different ways. Firstly, a percentage can be given which is valid for the whole area. For instance the saturation deficit of the unsaturated zone at the beginning of the model run. Secondly, spatially distributed values can be given by making a grid in which every grid cell has a specific initial value, such as the snow grid.

These initial values mainly describe the amount of water present in the storage reservoirs at the beginning of the calculation period. In most cases these values are not known due to the fact that no measurements were available. In this study a grid with initial snow storage, a grid in which the Rhone glacier and the Mutt glacier are declared as a subcatchment, and a grid describing the firm area were needed.

Dependent on the time at which the calculation begins, initial values can have a great impact on the results because erroneous initial values can influence the result for a long period. The length of time that is influenced is determined by the reaction time of the reservoir. At each time step, the effect of the erroneous initial value is further reduced. When starting the calculation in winter, no problems will arise for the initial value for the unsaturated zone because this will most likely be on field capacity. However, the content of the snow reservoir is not known.

Although there is a (simple) numerical scheme (Section 3.4.6) for the calculations of vertical groundwater flow in WaSiM-ETH Version II, errors will not evolve into great instability, such as may occur by modelling flows in open water.

To obtain a reliable value of the content of the snow reservoir at the 1<sup>st</sup> of January 1990, the catchment area Dischma (near Davos) is used. This catchment area is used while it is more or less influenced by the same meteorological conditions as the Gletsch area and has already been the subject of research. Results of calculations of the Dischma area were available for the period 1990 - 1996 (Badoux, 1997). The water equivalent of the snow reservoir at 01-01-

1990 is compared with the subsequent years. The same water equivalent could be seen on the 1<sup>st</sup> December 1991 and 1994 as on the 1<sup>st</sup> January 1990.

Two test runs were then made with WaSiM-ETH starting at 01-01-1990 (no snow) and terminating 01-12-1991 and 01-12-1994. The assumption is that, like the Dischma area, the content of the snow reservoir in the Gletsch Catchment on 01-12-1991 and on 01-12-1994 is the same as on 01-01-1991.

The grid values of the snow reservoir are stored at the end of the model run. The results of both runs are compared and checked against values from the 'Hydrologischen Atlas'. The grid of the run that lasted until 01-12-1991 is then used as the initial value for the snow storage at 01-01-1990 in order to obtain an adequate estimation for the content of the snow reservoir at the beginning of the model run. The grid values of 01-12-94 is not used because a large snow reservoir evolved while no melt occurred in the accumulation zone.

An ice grid in which the glacierized area is defined is extracted out of the land use grid. It is used to distinguish the area on which the 'old' snow model and the new glacier and snow model is applied. Further, the equilibrium line of the glacier is defined in this ice grid. The position of the equilibrium line is based upon information of the Bundesamt für Landestopographie (1980) and Verlag Schweizer Lexikon Mengis and Ziehr (1993). A height of 2900 m for the south directed Rhone glacier and 2800 m for the north directed Mutt Glacier are chosen. The sensitivity analysis will show the effect of changing this height on the model efficiency. The ice grid is a stationary grid, which means that it does not change in time.

As mentioned in the previous chapter, the runoff from the glaciers is routed towards the catchment outlet. Therefore, a choice must be made in the preprocessing whether the runoff of the Mutt Glacier and Rhone glacier are routed together or are kept separately. In this study, the total runoff of the Mutt glacier is superimposed on the total runoff of the Rhone glacier and then routed towards the outlet near Gletsch.

**Table 4-2: Model parameters, units, remarks and method of assessment.**

<i>Submodel</i>	<i>Parameter</i>	<i>name</i>	<i>Unit</i>	<i>Remarks</i>
Precipitation correction	a <sub>liquid</sub>	correction factors for liquid precipitation	-	values from literature or experience otherwise calibrate
	b <sub>liquid</sub>	correction factors for solid precipitation	mm/(ms <sup>-1</sup> )	
	a <sub>solid</sub>	threshold temperature for rain ↔ snow	-	
	b <sub>solid</sub>	threshold temperature for rain ↔ snow	mm/(ms <sup>-1</sup> )	
	T <sub>RS</sub>	threshold temperature for rain ↔ snow	°C	
Interpolation of meteorological input data	d <sub>max</sub>	maximum distance to meteorological station	km	values from literature (2 .. 3) area dependent
	p	distance weighting in IDW	-	
	igo	upper and lower limit for inversion	m	
Temperature modification Glacier / Snow model	igu	scaling factor	m	calibrate using measurements (± 5 K) values from literature
	c <sub>T</sub>	scaling factor	°C	
	T <sub>R/S</sub>	threshold temperature for rain ↔ snow	°C	
	T <sub>trans</sub>	transition zone for rain ↔ snow	°C	
	T <sub>0,m</sub>	threshold temp. for melt	°C	
	c <sub>0</sub> (= DDF)	Degree Day Factor	mm·(°C·d) <sup>-1</sup>	literature; calibrate using measurements calibrate

	MF	melt factor (for glacierized areas)	$\text{mm}\cdot(\text{d}\cdot^{\circ}\text{C})^{-1}$	calibrate
	CWH	storage capacity for water within the snow	-	relative value
	$k_{\text{ice}}$	storage constant for ice	hour	Determined from time series or calibrated
	$k_{\text{snow}}$	storage constant for snow	hour	idem
	$k_{\text{firm}}$	storage constant for firm	hour	idem
	$a_{\text{snow}}$	radiation factor for snow	$\text{mm}\cdot(\text{time-step}\cdot^{\circ}\text{C}\cdot\text{W}\cdot\text{m}^{-2})^{-1}$	calibrate
	$a_{\text{ice}}$	radiation factor for ice	$\text{mm}\cdot(\text{time-step}\cdot^{\circ}\text{C}\cdot\text{W}\cdot\text{m}^{-2})^{-1}$	calibrate
Land use table used for evapotranspiration and interception	$r_c$	resistance	$\text{s}\cdot\text{m}^{-1}$	literature
	LAI	leaf area index	-	measurements, literature
	$v (=1-A)$	percentage which is covered by vegetation	-	literature
	$z_0$	surface roughness length	m	measurements; literature
	$\alpha$	albedo	-	measurements; literature
	$z_w$	root depth	m	measurements; literature
	$d_{1,400 - 44,400}$		Jul. Day	
extra for RICHARDS (Version II)	$\rho$	root distribution	-	measurements; literature
	$\psi_g$	hydraulic head	m	threshold for which ETR is reduced in connection with ETP
Interception	$h_{\text{SH}}$	max. thickness of water layer on vegetation	mm	calibrate
Infiltration	$x_f$	fraction of re-infiltrating water	-	$K_s$ , and $\psi_f$ used from soil table
soil table	$\Theta_{\text{sat}}$	water content at saturation	-	measurements, literature
	$\Theta_{\text{wp}}$	water content at wilting point	-	measurements, literature
	$K_s$	saturated hydraulic conductivity	$\text{m}\cdot\text{s}^{-1}$	measurements, literature
	$\alpha$	Genuchten parameter	$\text{m}^{-1}$	literature
	$n$	Genuchten parameter	-	literature
	$k_{\text{rec}}$	recession of $K_s$ with depth	-	$K_{s,t} = K_{s,t=0} \cdot (k_{\text{rec}})^t$ with t is depth
	$l_v$	number of soil layers	-	
	$d_z$	thickness of layer	m	
	$c_k$	threshold value for $K_s$ relationship		dependent on time step used
	Soil model	$k_D$	storage constant for direct runoff	hour
$k_H$		storage constant for	hour	determined from time

	$d_r$	interflow flow density (#channels per km)	-	series; calibrate measurements
	$k_B$	recession parameter for baseflow	m	calibrate
	$Q_0$	scaling factor for baseflow	-	calibrate
	$QD_{\text{snow}}$	fraction of snow melt which is transformed to direct runoff	-	
Runoff routing	$B_h, B_v$	width of river bed	m	these parameters can be calculated by the program TANALYS or taken from measurements
	$T_h$	depth of river	m	
	$M_h, M_v$	Manning value	$m^{1/3} \cdot s^{-1}$	
	$I$	slope	$m \cdot m^{-1}$	
	$L$	length of channel	m	
	$A_E$	size of the subcatchment of which discharge is transported by channel	$km^2$	
	$k_h, k_v$		hour	

#### 4.5 Parameter values

Not all values of parameters and coefficients used in the model run are obtained by field measurements. Mainly for two distinct reasons.

In order to obtain reliable values, a large measurement program is needed. Normally, these measurements will only take place in research catchment areas like the Rietholzbach (Switzerland) or the Hupselse Beek (the Netherlands). When no research is completed the values should be assessed from literature or experience. However, values in literature can vary in a wide range.

Besides this, some coefficients used by WaSiM-ETH do not have a physical background, and as such can not be measured. These parameters have to be adjusted during the calibration.

Former research (Schulla, 1997) shows that some parameters and coefficients are area independent. This means that calibrated values, which are found in other studies for other areas, can be used for the modelling of the Gletsch area.

An overview, based on Schulla and Jasper (1998), of the different parameters, their meaning in the model and the assessment is listed in Table 4-2.

#### 4.6 Spatial and temporal resolution

When hydrological modelling issues are concerned, problems of scale and scaling will become important. Questions about scaling will focus on space and time. There is a growing awareness in hydrology, that problems of scale and scaling of hydrologic processes are among the most critical tasks to be addressed today. A typical statement of the scale problem is: 'How can local observations be transferred to larger regions?' (Blöschl, 1996). While this issue of regionalisation is not unique for hydrology, literature dealing with scaling problems can be found in a wide spectrum of environmental studies. The main problem is that increasing (upscaling) as well as decreasing (downscaling) scales result in a shift between the most important processes. This means that optimal parameter values may no longer be correct when changing the scale (Blöschl, 1996).

In general one can distinguish three kinds of scales. These are the *process* scale, the *measurement* scale and the *model* scale. The process scale deals with scales in natural processes: convective rainfall events are of a smaller scale than synoptic events. This scale is important when field studies are done to investigate unknown or partly known processes. The measurement scale is about the scale on which the real process is measured.

Blöschl (1996) introduces 'hydrologic scale concepts'. In space, these concepts are: the local scale, the hillslope scale, the catchment scale and the regional scale. In time, these concepts are: the event scale, the seasonal scale and the long term scale. When the scale for the modelling is chosen, the boundaries are also determined. In most calculations, only one scale is considered, making the larger or smaller scale a boundary condition. For instance, in studies where only the seasonal scale is taken into account, it is possible to take the long term fluctuations as a constant value. For the Gletsch catchment, this means that when only seasonal runoff fluctuations are desired, long term fluctuations in the glacier mass balance (due to climatic fluctuations) can be neglected. So on closer inspection, these scale concepts are, in fact a prudent way of choosing the system boundaries. An overview is given in Table 4-3 (after Blöschl, 1996).

**Table 4-3: Overview of space and time scale concepts.**

<i>In space</i>	<i>scale concepts</i>	<i>typical lengths</i>
	local scale	1 m
	hillslope scale	100 m
	catchment scale	10 km
	regional scale	1000 km
<i>In time</i>	<i>scale concepts</i>	<i>typical times</i>
	event scale	1 day
	seasonal scale	1 year
	long term scale	100 years

Modelling with WaSiM-ETH needs some special consideration while all three time scales are embedded in the model. On a hourly basis, precipitation, evapotranspiration and (un)saturated flow are calculated to obtain seasonal runoff characteristics. Besides that WaSiM-ETH can be used to calculate the effects of climate change on hydrological catchment areas. Time scales can either be too small or too large. A time step which is too small will not result in inaccurate model results, but will demand a huge capacity of the hardware used.

A time step which is too large however, can result in incorrect answers, since some processes will not be calculated correctly. In general, the time step used in the calculations should be much smaller than the reaction time of the modelled processes.

In the present study, a time step of one hour is used, resulting from the available meteorological data. For obtaining seasonal runoff patterns in hydrological catchment studies, a larger time step of, for instance a day, should also yield good results. However, this study does not only focus on the seasonal runoff pattern, but also on the diurnal fluctuations induced by snow and glacier melt. Diurnal fluctuations will not be reflected in the model when using a time step of one day.

In this study, the time resolution is mainly determined by the availability of meteorological data. The spatial resolution has to be chosen by the modeller. As mentioned, parameters may change by up- and downscaling. In this study, these processes are neglected. In order to find an appropriate spatial resolution, the parameter sensitivity is investigated, to show the effect of decreasing spatial resolution on the  $R^2$  efficiency criteria. This is mere a result-orientated than a process-orientated approach.





## 5 Calibration criteria and sensitivity analysis of parameters

### 5.1 Introduction

By implementing the glacier model into WaSiM-ETH, some new model parameters and coefficients are introduced (see Section 4.5). In order to get a clear impression how these parameters influence the simulated results, an extended sensitivity analysis is completed. The model performance is based on several efficiency criteria. These criteria are described in Section 5.2. The sensitivity analysis will be described in Section 5.3. Section 5.4 contains the interdependency between model parameters. Using the results of this analysis the calibration of the model for 1992 is completed.

### 5.2 Efficiency criteria

In order to judge the model performance for a particular model run, its prediction error has to be defined using the errors associated with the individual readings in the output sequence. A measure of error is to be expressed mathematically, that is, an objective function ( $F^2$ ) has to be defined. Clearly, the magnitude of the objective function depends on the data set used and consequently a comparison of  $F^2$  between various data sets is meaningless. An expression of the error estimate which allows comparison between sets of data is the modelling efficiency (Stuyt, 1978).

To estimate the model's performance, WaSiM-ETH calculates several efficiency criteria. Observed runoff data is required for these calculations. These calculations can be done for each subcatchment for which runoff data is available. The efficiency criterion  $R^2$  is calculated according to:

$$R^2 = 1 - \frac{\sum_i \varepsilon_i^2}{\sum_i (x_i - \bar{x})^2} = 1 - \frac{\sum_i (y_i - x_i)^2}{\sum_i x_i^2 - \frac{1}{n} \left( \sum_i x_i \right)^2} \quad 5-1$$

where  $y_i$  is the simulated value,  $x_i$  is the measured value,  $\bar{x}$  the mean measured value,  $\varepsilon_i$  is the difference between the measured and simulated value and  $n$  is the number of time steps for which  $R^2$  is calculated.

The value of  $R^2$  can range from  $-\infty$  to 1. A negative value indicates that the model produces a worse estimate of the output than simply using the mean observed value. An efficiency of 1 indicates that there is no difference. The output of the model is then exactly equal to the observed values (Douglas, 1974).

When using this formula, errors in high water peaks have a considerably larger influence on the value of  $R^2$  than errors in periods with lower discharges. This is due to the fact that absolute differences between measured and simulated discharges are used in the calculations. To smooth the effect of high water peaks in the  $R^2$  value, a logarithmic efficiency is also calculated. In this calculation a logarithmic difference between measured and simulated discharge is used instead of the absolute difference. The  $R^2(\log)$  value can be used to estimate the model's overall performance, while errors in both dry and wet periods have the same relative influence on the  $R^2(\log)$  value.

In order to determine whether there is a shift in time of the simulated discharge in regard with the measured discharge, the efficiency criteria  $R^2(\text{lin})$  and  $R^2(\log)$  are calculated for 21 time

steps. Firstly, the simulated discharge is compared to the measured discharge resulting in a central  $R^2$  value. This central value corresponds with a time shift of 0 hours. The simulated discharge is shifted 1, 2, 3 ... 10 hours for- and backwards. For each case the new  $R^2$  value is determined. When the central value for  $R^2$  is not the optimal fit, it is concluded that a shift has occurred, probably as a consequence of incorrect parameters in the routing model or by the model itself.

Besides the  $R^2(\text{lin})$  and  $R^2(\text{log})$  values an explained variance coefficient (EV) is calculated. In contrast to the efficiency criteria the algorithm used for EV is able to recognise systematic shifting. Comparing both criteria allows to detect systematic errors (Schulla and Jasper, 1998).

### 5.3 Sensitivity Analysis

To retrieve the model reaction to changing values of parameters, a sensitivity analysis is essential. In this analysis test runs are made in which only one coefficient or parameter is changed, keeping the others at a constant value. The results of this analysis is used in twofold. Firstly, the results are used to make statements about the required accuracy for the coefficients involved. If a coefficient has a great impact on the simulated results, efforts to find an optimal value should be larger than when the coefficient is less sensitive. A schematic example of a sensitive and an insensitive coefficient is given in Figure 5-1.

Secondly, the results of the analysis are used in the process of calibration. When the reaction of the model to changing coefficients is known, it is easy to find the optimal value. A calibration based on trial and error can then be avoided. Difficulties may arise when the optimal value of a coefficient is

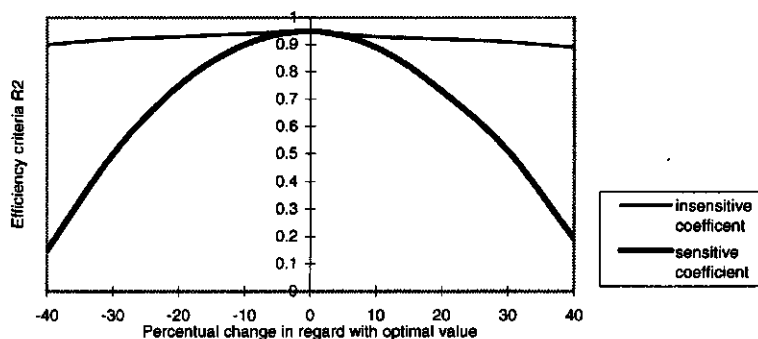


**Figure 5-1: Example of sensitive and insensitive coefficients.**

dependent on other coefficients. In such cases many test runs should be completed to find the optimal combination of coefficients.

The executed sensitivity analysis mainly focused on the coefficients, which are used within the new glacier model. The coefficients and parameters of the other submodels have already been investigated by Schulla (1997) and will therefore not be investigated again. Only the degree day factor used in the calculation for snow melt in unglacierized areas is tested again. Besides the four coefficients used in the new glacier model, the effect of increasing the the grid size and the height of the firm area is investigated. Not only the sensitivity of the individual parameters is tested within this analysis but also the interdependency between several coefficients and parameters. Interdependency is found in the calculation of glacier melt.

### 5.3.1 Melt Factor

The influence of temperature in total glacier melt volume is controlled by the melt factor (MF), as shown in Equation 2-6. Within the model the melt factor is assumed to be constant in time. The value for this melt factor is the same for ice and snow. Hock (1998) found an optimised value for the melt factor of 1.8 for Storglaciären (Sweden). The effect of the chosen melt factor for the Gletsch catchment, is shown in the Figure 5-2.

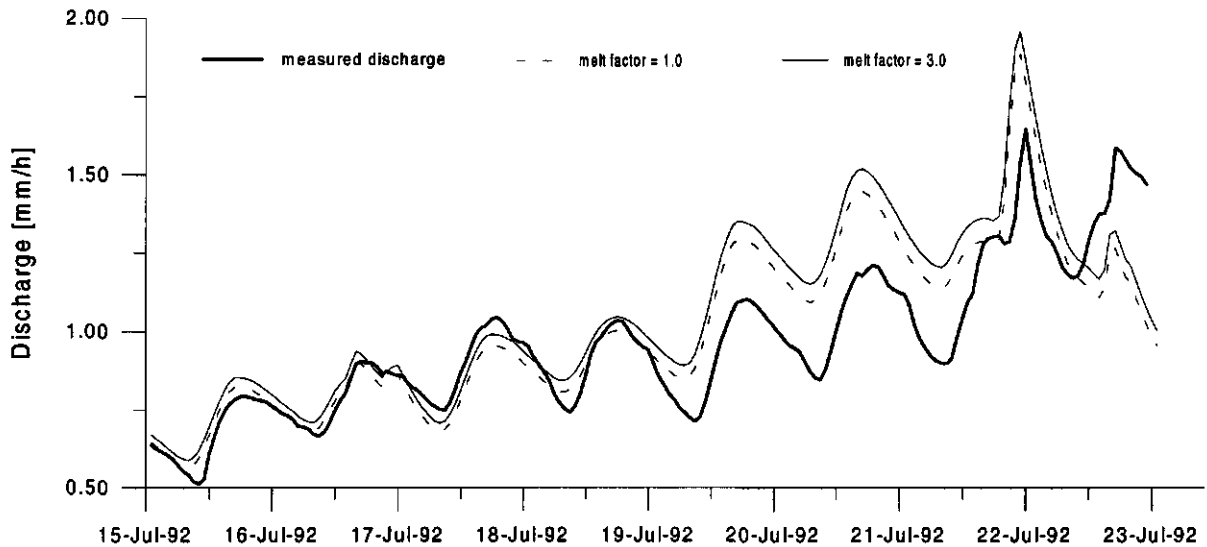


**Figure 5-2: Effect of changing the melt factor (MF) on the discharge at Gletsch.**

The figure shows that the effect on total discharge of increasing (or decreasing) the melt factor is only a moderate. Because the relative daily temperature fluctuations are not as large as the relative daily radiation fluctuations, the effect of changing the melt factor can be addressed as linear. This means that increasing (decreasing) the melt factor will result in a general shift upwards (downwards). When simulated results show a daily fluctuation which is too small, changing the melt factor is not of much use.

Besides this direct effect on discharge, an indirect effect on ice melt may also occur. A higher melt factor will result in a higher snow melt at the beginning of the melt period, exposing the ice earlier to radiation. Due to different albedo values, ice melt is larger than snow melt, and consequently, summer melt rates are overestimated.

### 5.3.2 Radiation coefficients for ice and snow

To control the calculated melt rates for glacierized areas, not only the melt factor, mentioned above, but also two different radiation coefficients,  $\alpha$ , for snow and ice (Equation 2-6) are used. These two coefficients take into account the effect of radiation to total melt. The coefficients are different for ice and snow, reflecting the differences in albedo for ice and snow. Figures 5-3 and 5-4 show the effect of changing the values for the radiation coefficients for ice and snow respectively.

Both figures clearly show that, when the values of the coefficients are lowered, melt volumes are lowered too while simulated daily amplitudes are also lowered. Both coefficients are therefore ideal parameters to adjust simulated daily fluctuations. Within the analysis, both values are varied in a range between  $0.1 \cdot 10^{-4}$  and  $0.9 \cdot 10^{-4}$ . This range corresponds with values found by Hock (1998). The same discussion about early ice exposure, as described for the melt factor, is also valid for the radiation coefficients.

When using the algorithms described in Section 3.5.3, calculated total glacier melt consists of two terms: melt induced by temperature and melt induced by radiation. As global radiation is

changing throughout the day, the contribution to total melt is also changing. Assuming, that global radiation varies roughly between 0 and  $1000 \text{ W}\cdot\text{m}^{-2}$ , the contribution of radiation to total melt changes from 0 to 85 % (melt factor = 2.0 and  $a_{\text{ice/snow}} = 0.0005$ ). The large contribution of radiation also explains the small effect of changing the melt factor, described in the previous section.

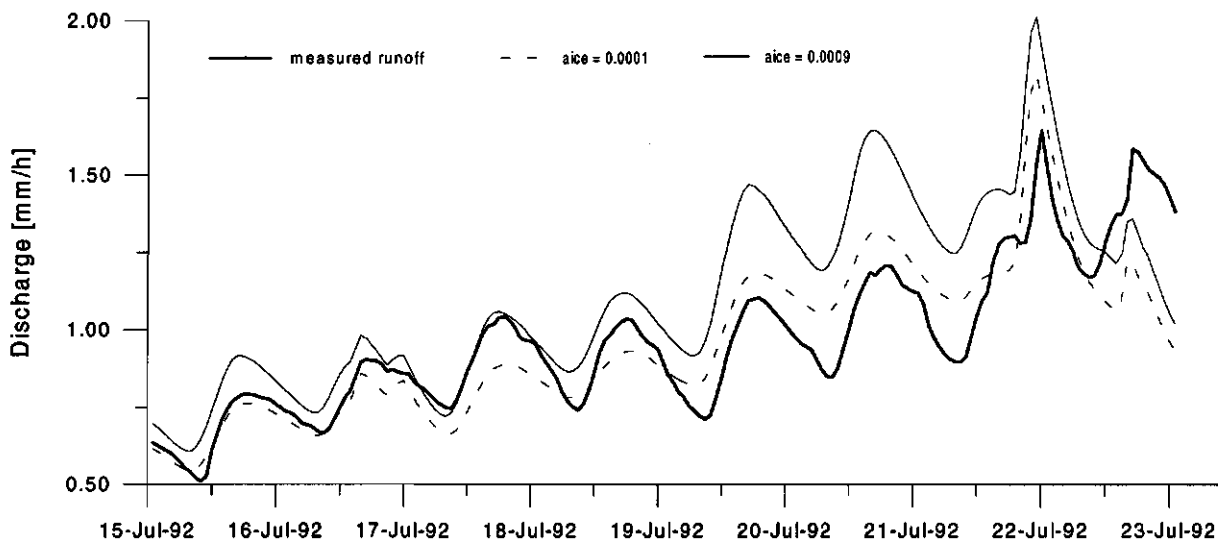


**Figure 5-3: Effect of changing the radiation coefficient,  $a$ , of ice on the discharge at Gletsch.**

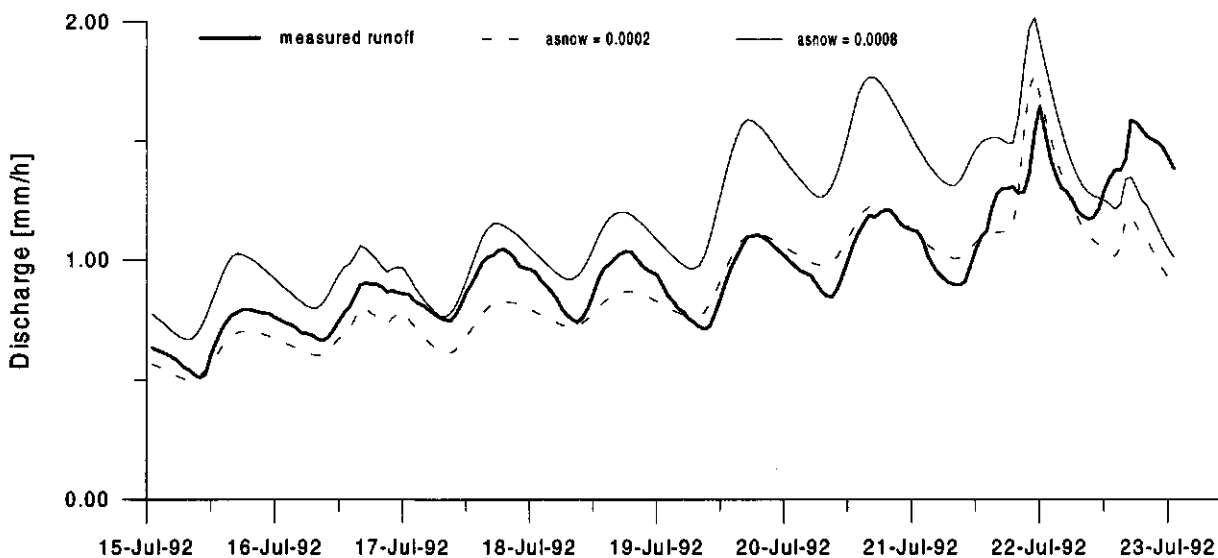


**Figure 5-4: Effect of changing the radiation coefficient,  $a$ , of snow on the discharge at Gletsch.**

### 5.3.3 Storage constants

Within the new glacier model, three reservoirs are incorporated to transform the glacier discharge (melt and rainfall) towards the glacier snout. These reservoirs for snow, ice and firn have different storage constants. Determining these parameters from the measured time series is hardly possible, because measured runoff in Gletsch is the sum of a combination of several reservoirs. Former research gives ranges in which these parameters can vary, dependent on the glacier involved. Within this given range, an optimal combination for the parameters is determined. The optimal fit is based on the statistical efficiency criteria.

Table 5-1 shows values for storage constants found by Hock (1998) for Storglaciären (Sweden) and by Baker et al. (1982) for Vernagtferner (Austria).

**Table 5-1: Storage constants in hours for the linear reservoirs of firn, snow and ice for Storglaciären (Hock, 1998) and Vernagtferner (Baker et al., 1982).**

	$k_{firn}$	$k_{snow}$	$k_{ice}$
Storglaciären	350	30	16
Vernagtferner	430	30	4

Additionally, the variable storage constants in time and space, during the year should be considered. In this study, an effort is made to simulate discharge for the whole year around. Optimal values for the reservoir coefficients are mean yearly values, without considering seasonal variation. Hock (1998), however, only simulated for the summer period.

The reaction of simulated discharge to changing values for the reservoir coefficients, are in principal, the same. When values for these coefficients increase, the buffering capacity increases and consequently the reservoirs react slower, resulting in smaller daily fluctuations. An example of such a response is given in Figure 5-5, showing the results when  $k_{snow}$  is increased from 40 to 80.

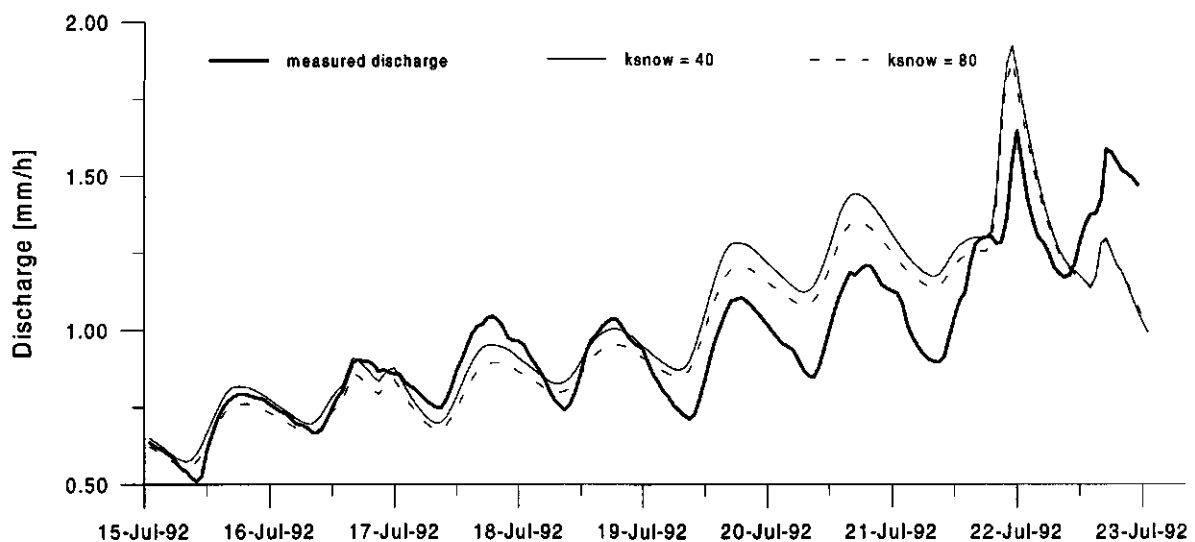


**Figure 5-5: Effect of changing the storage constant of snow reservoir on the discharge at Gletsch.**

Generally, if the storage coefficient is lowered, discharge peaks increase and amplitudes will become larger. Measured discharge reveals that the decrease of discharge during the night as a result of reduced melt water is not always the same.

The peak on the 22nd of July is probably induced by rainfall. Meteorological data show that there was 10 to 15 mm precipitation on the evening of the 21st. This rainfall is probably transformed to direct runoff. Therefore it is not possible to distinguish any differences between simulated runoff for  $k_{snow}$  is 40 and  $k_{snow}$  is 80. The process responsible for the peak on the 22nd of July is not influenced by the coefficient  $k_{snow}$ .

Although Figure 5-5 clearly shows that variation of the storage constants affects the simulated discharges, statistical fits are only slightly affected. Table 5-2 shows the effect of the variation of the different storage constants on the efficiency criteria  $R^2(\text{lin})$  and  $R^2(\text{log})$ . All values are varying in a range between 0.914 and 0.935. The storage constants considerably affect daily amplitudes, but regarding seasonal simulations, the model is almost insensitive to changing storage constants.

Looking at the  $R^2(\text{log})$  values no optimal values are found for  $k_{snow}$  and  $k_{firn}$ . This is probably the consequence of the baseflow simulation which show rather great deviation with the observed flow. Larger values for these constants result in simulated discharges which decrease less rapidly. Deviations are therefore smaller and the  $R^2(\text{log})$  value is larger.

**Table 5-2: Results of discharge simulations of Gletsch (1992) for different values for the storage constants of ice, snow and firn.**

$k_{ice}$	10	20	30	40	60
$R^2(\text{lin})$	0.9263	0.9295	0.9316	0.9321	0.9311
$R^2(\text{log})$	0.8320	0.8323	0.8330	0.8327	0.8138
$k_{snow}$	40	100	140	200	300
$R^2(\text{lin})$	0.9264	0.9337	0.9337	0.9328	0.9306
$R^2(\text{log})$	0.8119	0.8199	0.8228	0.8269	0.8329
$k_{firn}$	100	200	300	400	500
$R^2(\text{lin})$	0.9308	0.9339	0.9316	0.9279	0.9225
$R^2(\text{log})$	0.8116	0.8214	0.8301	0.8359	0.8391

### 5.3.4 Degree Day Factor

Instead of a melt factor, a degree day factor (DDF) is used for the modelling of snow melt on unglacierized areas (see Section 3.5.3). The DDF is a constant value. Therefore the difference in melt between fresh and old snow (different albedo values) is not considered.

The influence of DDF on total generated runoff changes throughout the year. In summer, the unglacierized area is mainly without snow. In that period, only a modest contribution to total melt can be expected from the unglacierized area. When, based on the efficiency criteria, a comparison is made between the simulated results for different DDF values, the influence of the DDF will be smooth, due to this small contribution. However, in spring and autumn, the influence can be large. Table 5-3 shows the effect of varying the DDF factor on the efficiency.

The effect is clear: increasing the value for DDF results in a larger snow melt volume. The larger the snow melt, the better the results for  $R^2(\text{log})$ . For  $R^2(\text{lin})$ , an optimum is found when DDF is 2.2.

**Table 5-3: Results of discharge simulations of Gletsch (1992) for different values for the degree day factor (DDF) of snow and the simulated volume of snow melt on the unglacierized area (mm).**

DDF	1.3	1.6	1.9	2.2	2.5	2.8	3.1	3.4	3.7
$R^2(\text{lin})$	0.906	0.916	0.922	0.923	0.922	0.919	0.914	0.908	0.902
$R^2(\text{log})$	0.797	0.799	0.801	0.819	0.828	0.830	0.837	0.840	0.843
$\Sigma$ snow melt	740	818	880	928	968	1001	1030	1056	1079

### 5.3.5 Height of firn area

Within the analysis, not only coefficients and parameters are tested. Some runs are made to test the sensitivity of the chosen height of the firn area. Normally, this input data can be obtained by field observations. In this study, however, the altitude of the equilibrium line was not precisely known. Further, the equilibrium line is not a fixed line, but changes in altitude over the years. Based on data found in the literature and geographic maps, an average altitude for the Rhone glacier is chosen of 2900 m. For the Mutt glacier, an altitude is chosen of 2800 m. A distinction is made because the Mutt glacier is north directed. This means that the glacier is more shaded than the south directed Rhone glacier. The shading will result in lower

temperatures and therefore a lower equilibrium line. This 100 m difference between the two glaciers is considered fixed and is therefore not changed. Table 5-4 shows the results of the different runs. The altitudes mentioned are those for the Rhone glacier.

**Table 5-4: Results of discharge simulations of Gletsch (1992) and the simulated volume of firn, ice and snow melt (mm) for different heights of the equilibrium line.**

Altitude equilibrium line [m]	2800	2850	2900	2950	3000
$R^2(\text{lin})$	0.924	0.928	0.931	0.933	0.934
$R^2(\text{log})$	0.807	0.806	0.808	0.808	0.808
$\Sigma$ firn melt	766	674	534	434	348
$\Sigma$ ice melt	410	445	494	524	544
$\Sigma$ snow melt	370	432	530	604	672

Although the statistical fit for 2900 m is not the best one, this altitude is chosen for further simulations. Differences in  $R^2(\text{lin})$  are only modest and, from the literature, it is found that an altitude of 2900 m is a more realistic value than 3000 m. With increasing altitude for the equilibrium line, the size of the firn area, by definition, decreases and therefore the total firn melt decreases. Total snow melt logically increases since the area on which snow melt is calculated increases when the firn area decreases. With increasing altitude of the equilibrium line the area of "ice possibly covered by snow" increases. Therefore, total ice melt also increases, showing that the simulated snow retreat line ranges over 3000 m in summer. Statements about the differences in total melt between the height steps, due to increasing or decreasing area sizes, can only be made if data are available regarding the slope and the shape of the glacier.

### 5.3.6 Spatial resolution

To discover, which spatial resolution is required to obtain good results, several runs with varying resolutions have been completed. Results of these runs are particularly important when larger catchment areas are involved, because calculation time may then become a problem. Results are shown in Figure 5-6. These results are not fully comparable because of the differences in percentage glacierized area. These differences arise when grid cells are aggregated. At a resolution of 5000 m the catchment area is completely covered with glacier and calculated baseflow becomes zero. In spite of the differences in glacierized area, it is concluded that results are not badly affected when the resolution is decreased to 500 x 500 m.

Schulla (1997) found, that for the Thur area, satisfying results still can be obtained if the spatial resolution decreases to 2000 m or even up to 5000 m. For the alpine, though unglacierized, subcatchment Stein, however, the quality of the results decrease quickly when the resolution exceeds 1500 m.

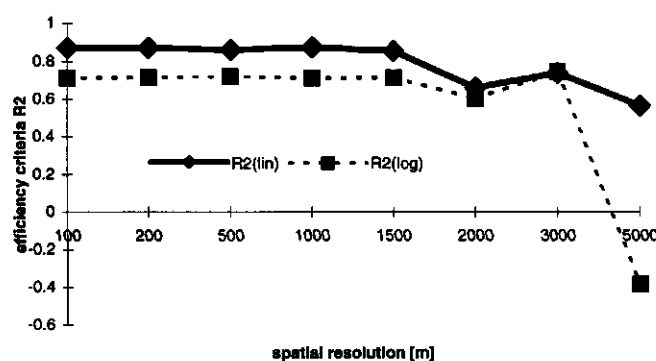


**Figure 5-6: Results of discharge simulations of Gletsch (1990) for different spatial resolutions.**

### 5.4 Interdependency between parameters

Parameters in algorithms used for conceptual modelling often show some kind of dependency. When calibrating such a model, these coefficients can not be considered separately because the optimal value for one parameter may change when the values of the other parameters are changed. Test runs can be made to find an optimal value for both coefficients. When statistical efficiency criteria are calculated, these can be used to make plots, showing the degree of dependency. Figure 5-7 gives an example of two parameters which are dependent (B) on each other and two parameters that are independent (A).

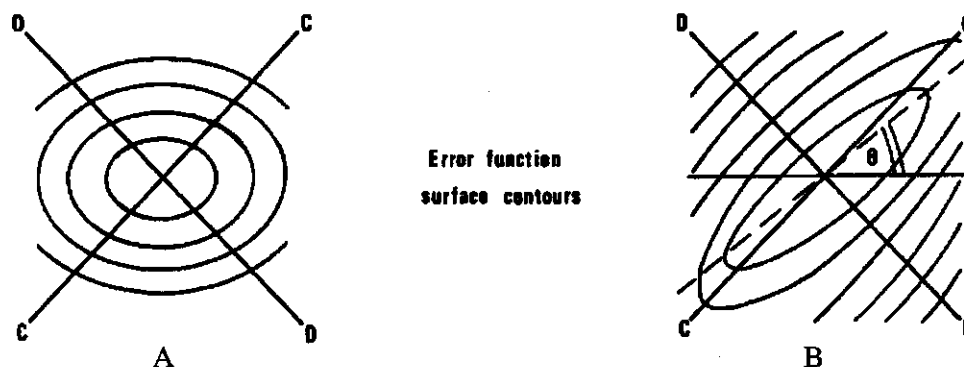


**Figure 5-7: A: Independent coefficients, B: Dependent coefficients.**

When a parameter is dependent on only one other parameter, calibrating is possible without too many efforts. However, when this specific parameter is dependent on three or four other parameters, the amount of test runs increases exponential and visualising the optimal set of parameters is not possible.

As mentioned before, a dependency exists between the parameters of the new glacier model. Ice melt is not only influenced by the value chosen for  $a_{ice}$ . A high value for both the melt factor (MF) and radiation coefficient  $a_{snow}$  will result in a high melt rate for snow and subsequently result in a quicker exposure of the underlying ice in spring.

These coefficients, however are not based on a physical background, and the optimal value can only be assessed by completing the process of calibration. To find the optimal set of values, a considerable number of test runs are made with different combinations of these values for  $a_{ice}$ ,  $a_{snow}$  and the melt factor. For each test run, an efficiency criterion ( $R^2$ ) is determined. The results are shown in Figure 5-8.

This figure clearly shows that the optimal combination for  $a_{ice}$ , and  $a_{snow}$  is changing with changing values for the melt factor. Comparing the shape of the figure with the examples given in Figure 5-7 shows that the rate of dependency between values for  $a_{ice}$ , and  $a_{snow}$  is significant.

Besides this dependency, which originates from the algorithm used, a dependency between the coefficients mentioned and the time constants for the linear reservoirs for snow and ice can be expected. This dependency is not based on a theoretical background but rather on the effect of the coefficients on simulated results. Each reservoir has its own specific storage constant which are, theoretical, determined from time series. This, however, becomes impossible when the contribution of the individual reservoirs to total generated runoff can no longer be separated. Time series then show a combined effect of several parallel reservoirs. When these values cannot be determined exactly, generated runoff (and especially daily fluctuations) depends not only on the three melt coefficients ( $a_{ice}$ ,  $a_{snow}$  and MF), but on the storage constants of the reservoirs as well, resulting in some kind of dependency.



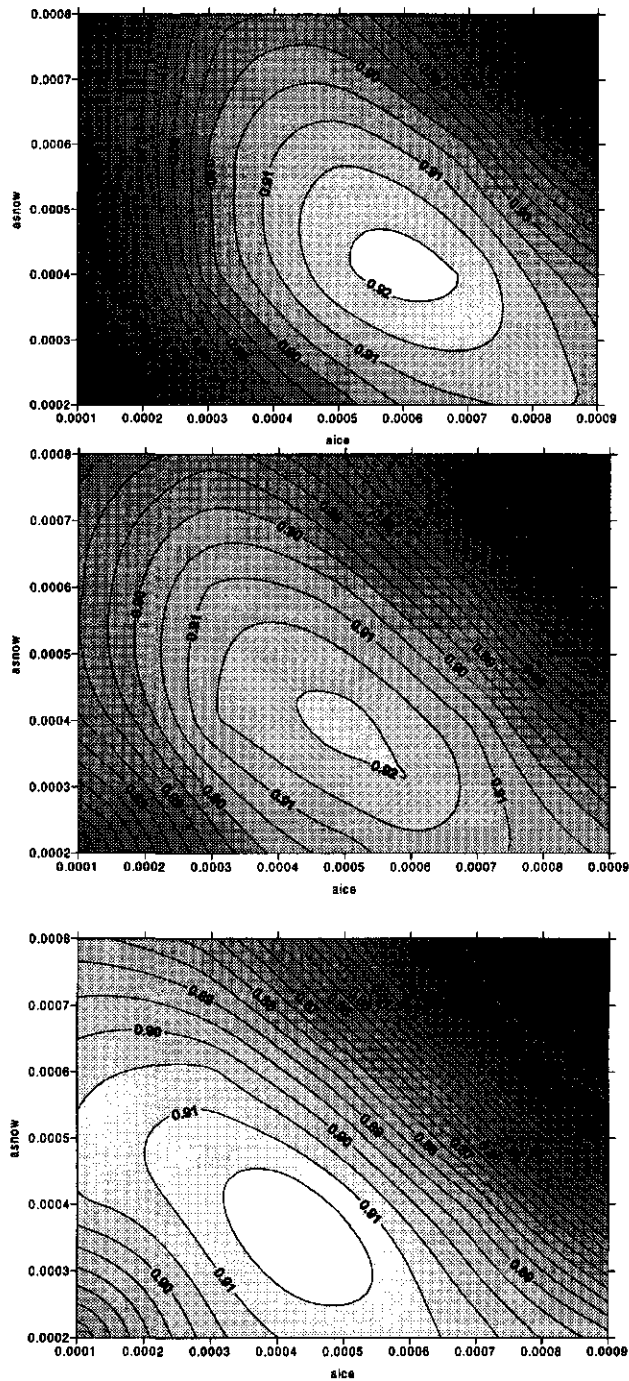


**Figure 5-8: Interdependency between the radiation coefficients of snow and ice at different values for the melt factor. Top: MF = 1.0, Middle: MF = 2.0, Bottom: MF = 3.0.**



## **6 Results of simulations**

### **6.1 Introduction**

In order to test the new embedded glacier model, two different catchment areas were used. Firstly, the Gletsch catchment, which is already described in Chapter 4. Calculations mainly focus on this area. Besides this, the Aletsch catchment is used. This area is used to test the consistency and the area dependency of the new model.

The results for the calibration period are written down in Section 6.2. Section 6.3 describes the results for the validation period. A comparison between the two different melt models is described in Section 6.4. The last Section, 6.5 gives a description of the Aletsch catchment and the results of the simulations that were proceeded for this area.

### **6.2 Calibration results of WaSiM-ETH**

In this study the outflow of the Gletsch catchment area is simulated in WaSiM-ETH, with and without the glacier model. Both models are calibrated for the year 1992. In this way, it is possible to compare the results of both simulations and to make statements about the effect of incorporating the glacier model into WaSiM-ETH.

#### **6.2.1 Without the glacier model**

Initial values for 1992 were obtained by starting the simulation in 1990 and using 1990 and 1991 to diminish the effect of incorrect starting values. At the end of 1991, the output data was stored and used as input data for the following year. Most of the initial values for 1990 were set to 0, besides the initial values for the groundwater reservoir and snow reservoir. While WaSiM-ETH without glacier model does not calculate glacier discharge, a snow input grid with a large snow storage is created in the preprocessing for those grid cells that are covered by the glacier. In this way glacier melt is simulated by snow melt from the large reservoir. The snow reservoir is chosen large enough that snow is still present after four or five melt seasons. Results of the calibration run are shown in Figure 6-1. Initial values for 1992 are obtained by simulating 1990 and 1991 first. The  $R^2(\text{lin})$  is 0.751 and the  $R^2(\text{log})$  is 0.843.

The figure shows that most of the peak values in spring and autumn are overestimated. Reason for this deviation is the constant value for the DDF. In practise, this value varies throughout the year, due to the physical differences between fresh snow, old snow, ice and firn. A varying value for the DDF throughout the year cannot be defined within the model. Therefore an average value for the DDF is used. The optimal DDF value for one year is determined during calibration and results in discharges which are too high in spring and autumn and too low in summer.

Another problem that arises is caused by the so called CWH factor. This factor determines the amount of water (rainfall as well as melt water) that can be stored within the snow as a percentage of the total snow reservoir. When using the eternal snow storage on glacierized areas, this percentage results in the fact that all the water is stored within the snow without being transformed to runoff. When the factor is set to 0, (no storage) melt peaks are simulated which do not correspond with observed discharge.

## 6 Results of simulations

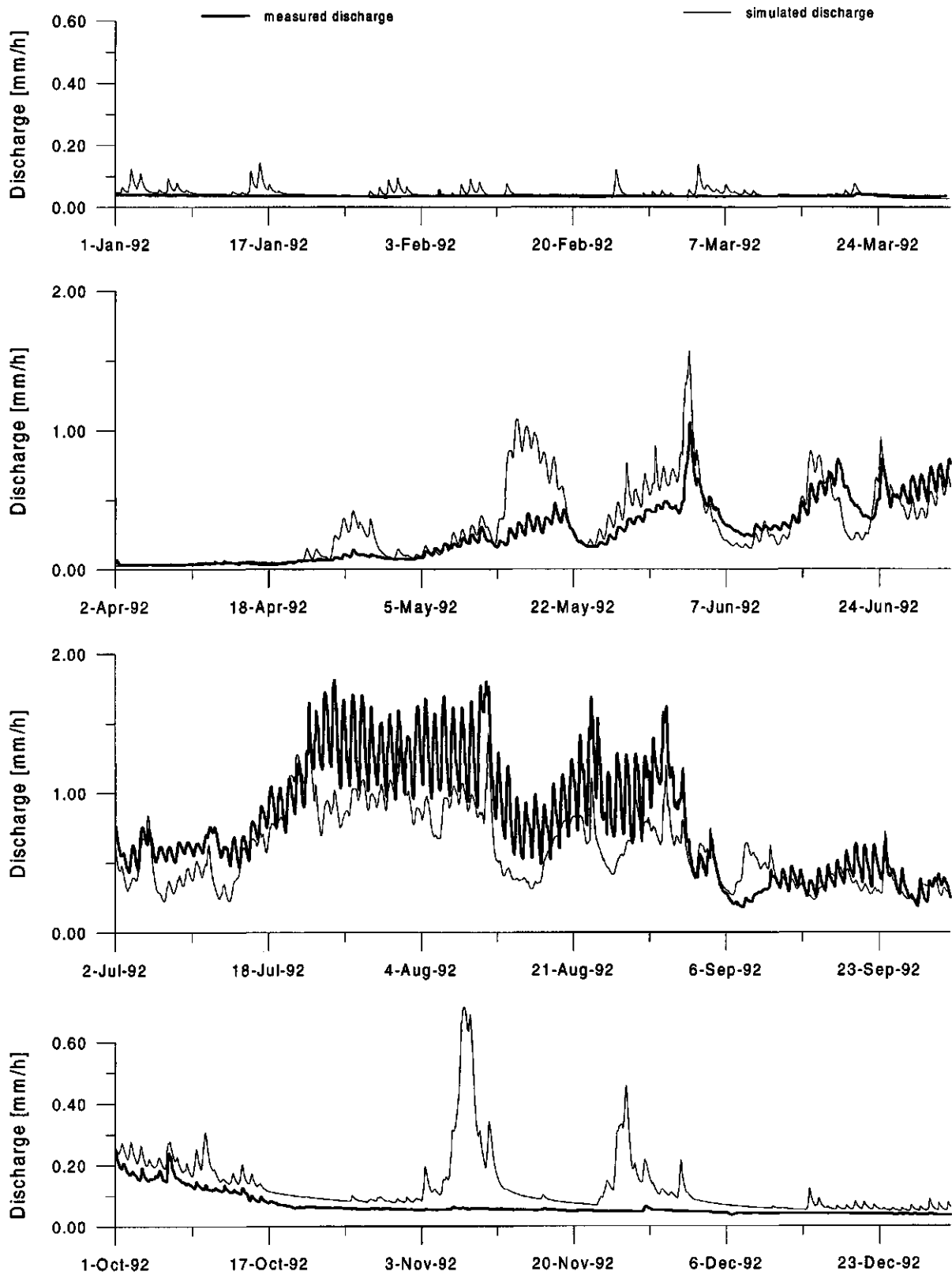


**Figure 6-1: Simulated and measured discharge of Gletsch using WaSiM-ETH without glacier model.**

### 6.2.2 The glacier model included

To calibrate the model, using the new glacier model, the year 1992 was also used. To obtain initial values the same method was applied as for the run without the glacier model. Initial values of the run with the glacier model differ from the initial values of the run without the glacier model. This difference is due to the difference between the calculation methods for 1990 and 1991.

When calibrating the model, the baseflow turned out to be a particularly difficult part of the water balance. The more or less constant discharge in autumn, which lasts until early spring, is very hard to model with a linear reservoir approach. When a time related linear reservoir approach is chosen, a value of 3500 hours would have been necessary. However, the algorithm used for the modelling of the baseflow is related to the depth of the groundwater level (Equation 3-17). Therefore it is of no use to determine the storage constant from the observed discharges.

This particular runoff regime is probably a consequence of the special geological deposits in the valley in front of Gletsch (see Section 4.2).

The calibration is entirely based on results found in the sensitivity analysis in the present study and earlier studies. The  $R^2(\text{lin})$  and  $R^2(\text{log})$  values were used to determine the optimal fit. In this way an objective comparison between the different runs can be made. Results for individual periods could be improved when only these periods are concerned. Hock (1998), for instance, only calibrated for the three summer months. Therefore, results are not completely comparable.

The results for 1992 are shown in the Figure 6-2. For this run the  $R^2(\text{lin})$  is 0.931 and the  $R^2(\text{log})$  is 0.808. In particular the results in summer show that the performance of the model has improved considerably. Simulated discharge reflect daily, as well as seasonal fluctuations very well. The amplitude of the diurnal fluctuations in mid summer, however, appear a little bit too low. It might be improved by changing the values for  $a_{\text{ice}}$ ,  $a_{\text{snow}}$ ,  $k_{\text{snow}}$  and  $k_{\text{ice}}$  (Sections 5.2.3 and 5.2.4). This, however, would affect the good results for spring time.

Besides some minor deviations, two distinct differences between simulated and measured discharges can be noticed. Firstly, the baseflow in spring appears too small, probably as a consequence of processes in the valley near Gletsch which are not reflected by the model. Secondly runoff peaks are simulated in autumn, but these have not been observed. Peaks can be smoothed by increasing the storage constants of the reservoirs for snow and ice. However they will not disappear. Another explanation can be found when the meteorological data is studied. The melt peak corresponds with a period of higher temperatures and less precipitation (see Appendix 1), implying that simulated melt is responsible for the simulated discharge. In practise this melt does not occur.

Figure 6-3 shows the relationship between vapour pressure and simulated discharge. The runoff peak does not only correspond with a period of higher temperatures but also with low vapour pressure.

In practise this low vapour pressure probably results in an increased evapotranspiration. This evapotranspiration decreases the amount of energy available for the melting process. As melt is not simulated by an algorithm based on the energy balance, this process can not be simulated correctly. Another explanation, also based on the concept of the energy balance, is that the area covered by fresh snow. The albedo of fresh snow is larger than the albedo of old snow. Therefore, the melt rate from surfaces covered by old snow is considerably higher than from surfaces covered by fresh snow.

## 6 Results of simulations

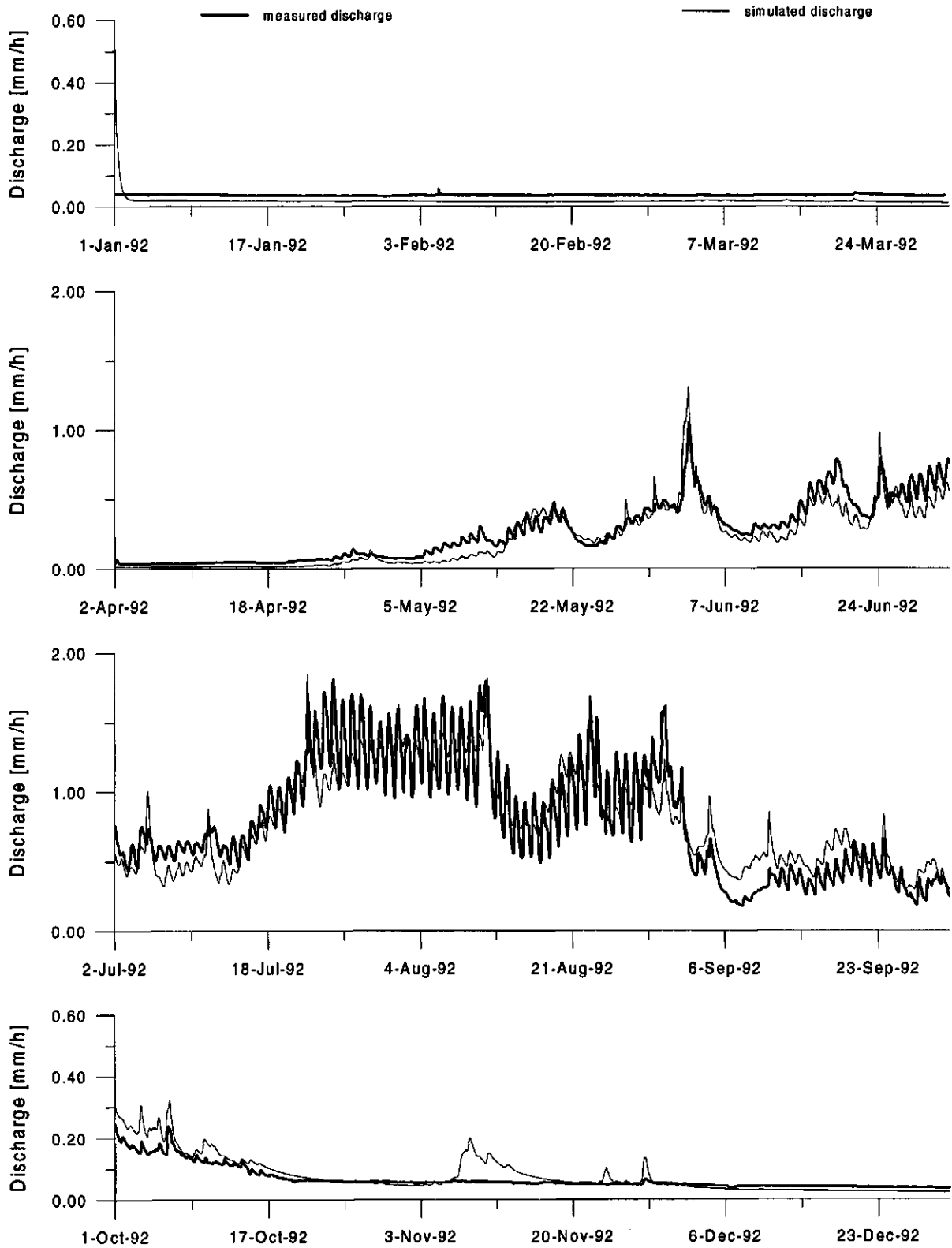


**Figure 6-2: Simulated and measured discharge for Gletsch for the calibration year 1992, using WaSiM-ETH including the glacier model.**

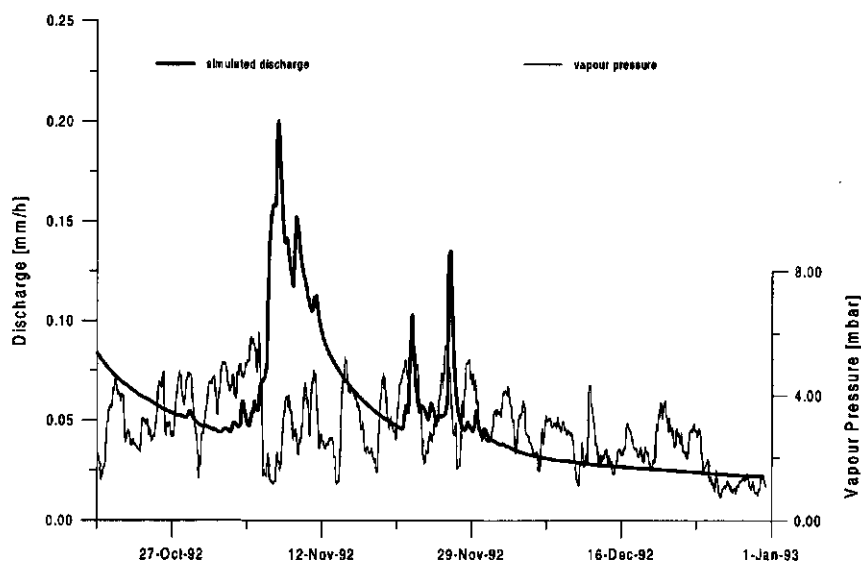


**Figure 6-3: Vapour pressure and simulated discharge of Gletsch (1992).**

The model results can also be investigated by plotting simulated and measured values against each other. Such a plot is shown in Figure 6-4. These plots can be used to determine whether there is a systematical deviation or not.

When looking at this figure it can be concluded that, simulated values vary randomly in a range which is comparable to that of the observed discharges. Discharges are not consistently simulated too high or too low. Only simulated discharges that exceed 1.5 mm per hour are slightly too low. This corresponds with daily amplitudes which are slightly too low due to the mean values for  $a_{ice}$ ,  $a_{snow}$ ,  $k_{snow}$  and  $k_{ice}$ . On the left side of the plot the errors in the initial assessment value from the beginning of the model run can be found.

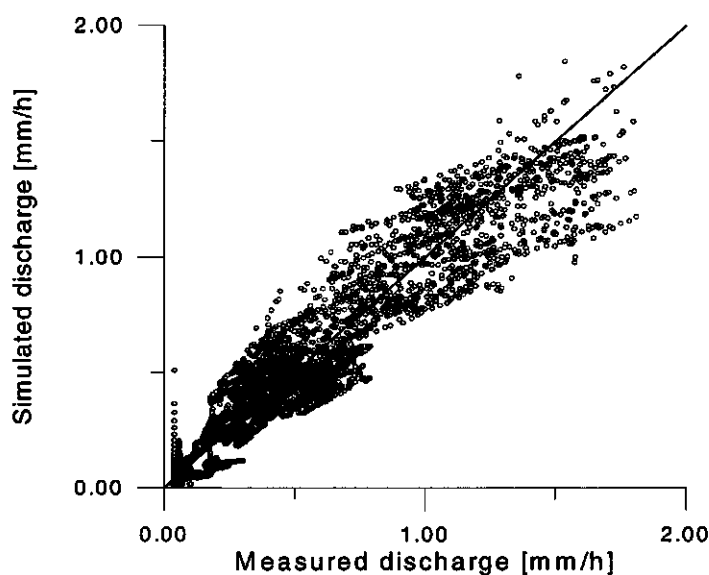


**Figure 6-4: Measured versus simulated hourly discharges of 1992 using WaSiM-ETH including the glacier model.**

In order to obtain a better understanding of the hydrological processes, the water balance for 1992 is given in Table 6-1. Differences between the total simulated runoff and measured runoff are relatively modest. Simulated total runoff is 97 mm lower than measured values, equaling 3.8 percent.

Values found for surface runoff, interflow and baseflow as well as changes in groundwater storage can not be verified, because no data were available.

The overall balance for 1992 clearly is negative. The input of water is lower than the output from runoff and evapotranspiration. This can only be accomplished if the volumes of water stored in the ice, firn and snow reservoir have diminished. This means that the volume of the glacier has decreased. Studying the changes in volume is only possible for the snow reservoir, because the volumes of the ice and firn area are not calculated. The simulated change in groundwater storage can be neglected. At the end of the year the groundwater level, as an average of the whole area, has changed about 2 cm from the groundwater level at the beginning of the year. When the effective porosity is taken into account this 2 cm, or 20 mm, corresponds to 5 mm water.

The water balance for 1993 and 1994 is also negative, but during the years 1995 and 1996 water is stored. The storage change of the water balance for the period 1992 – 1996 is negative: 468 mm.

**Table 6-1: Water balance for Gletsch catchment of 1992 (mm/year).**

<b>Water balance 1992</b>	
<b>Measured runoff</b>	<b>2558</b>
<b>Simulated runoff</b>	<b>2461</b>
<b>Glacier runoff</b>	<b>1558</b>
<i>ice melt</i>	494
<i>firn melt</i>	534
<i>snow melt</i>	530
<b>Surface runoff</b>	<b>615</b>
<b>Interflow</b>	<b>75</b>
<b>Baseflow</b>	<b>213</b>
<b>Precipitation</b>	<b>2206</b>
<b>Evapotranspiration</b>	<b>125</b>
<b>Storage change</b>	<b>unknown</b>
groundwater storage	-
snow storage	173
firn storage	unknown
ice storage	unknown

### **6.3 Validation results of WaSiM-ETH**

When the model is calibrated for one period of time, i.e. the parameters are adjusted for that period, the model should be validated for other years. For these runs, the same parameter values are used. The model is validated for the years 1993 - 1996. The results for 1994 are shown in Figure 6-5. Plots of simulated discharges in regard with observed discharges for 1995 and 1996 can be found in Appendix 8. At the end of each year output data is saved and used as input data for the following year.



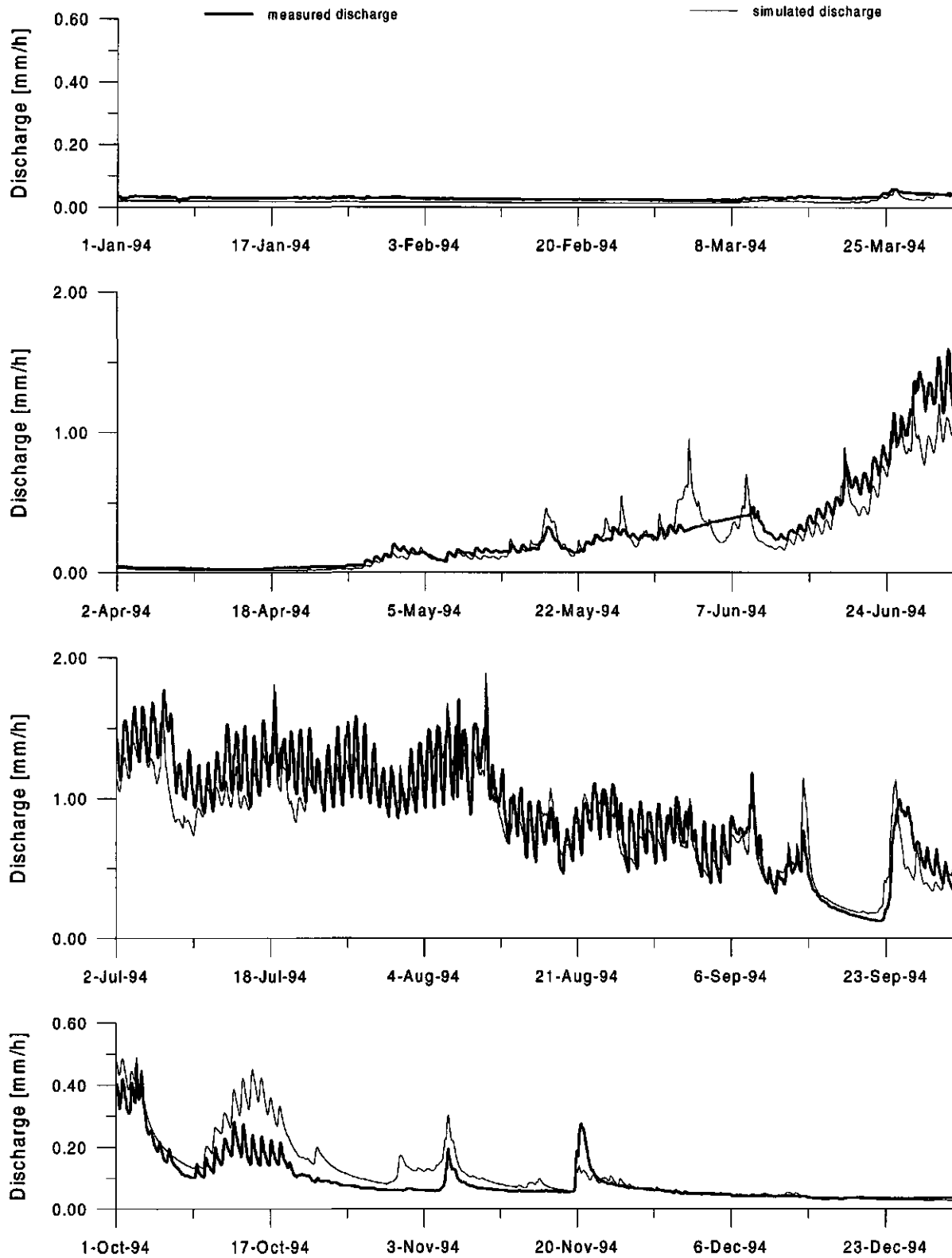


Figure 6-5: Simulated and measured discharge for Gletsch for the validation year 1994.

The comparison of the simulated hydrographs with the corresponding observed hydrographs shown in Figure 6-5 and in Appendix 8 shows that the model does not only produce good results for 1992, but also for the other years. On the basis of these results it is concluded that the calibrated set of parameters and coefficients is not only valid for 1992 but can be used in other years as well.

The results for the efficiency criteria  $R^2(\text{lin})$  and  $R^2(\text{log})$  for the different years are shown in Table 6-2.

In comparison with 1992, the baseflow for the year 1994 is much better simulated. In spring and late autumn the fit is almost completely perfect. This good fit is reflected in the value for  $R^2(\text{log})$  which is 0.926 for 1994. Another remarkable attribute in the figure is the interpolated (measured) data around the 7<sup>th</sup> of June. Data was lost and therefore interpolated by the 'Landeshydrologie'.

Except from some small deviations, simulations in summer are, as for 1992, very good. The simulated discharge is only too high during the week of the 17<sup>th</sup> of October. This deviation negatively affects simulated values for over more than two weeks. The deviation is probably due to the same three reasons that were given in the discussion about the simulated discharge in autumn 1992 (Section 6.2.2).

**Table 6-2: Results of discharge simulations of Gletsch for the calibration year (1992) and the validated years (1993-1996).**

	1992	1993	1994	1995	1996
$R^2(\text{lin})$	0.931	0.916	0.941	0.908	0.914
$R^2(\text{log})$	0.808	0.857	0.926	0.859	0.885

#### **6.4 Comparison of two temperature index methods**

Two methods to calculate the melt rate of the glacier are inserted into WaSiM-ETH. Since Hock (1998) found better results when radiation was included, this method has been used until now to simulate the runoff of the Gletsch catchment. To compare Hock's radiation method with the classical degree day approach, both methods were used to simulate the discharge of 1992.

The discharge simulation using the radiation factor is equal to the calibration run, described in Section 6.2.2. The same parameter values were used for the run using the classical degree day method, except the degree day factors were different. After calibration, an optimal degree day factor of 6.5 was found for snow and firn melt, and 7.5 for ice melt. The simulated discharge hydrographs for the main melt period are given in Figure 6-6.

The  $R^2$ -efficiency criteria for the simulations with the classical degree day method are 0.90 for  $R^2(\text{lin})$  and 0.83 for  $R^2(\text{log})$ , while  $R^2(\text{lin})$  is 0.93 and  $R^2(\text{log})$  is 0.81 for the simulations with Hock's radiation method. The simulated total discharge volume of 1992 for the classical degree day method is 2599 mm while it is 2461 mm for the method with a radiation factor. The observed discharge volume of 1992 is 2558 mm. This means that the total discharge volume is slightly overestimated by the classical degree day method and underestimated by the radiation factor method, at least for 1992.

The two methods show approximately the same seasonal variation in discharge. Differences in discharge simulations are mainly observed in the diurnal discharge fluctuations. Both models produce variations in daily discharge, but the amplitude of the daily discharge is simulated better by Hock's radiation method. The insufficient simulation of the diurnal discharge variation by the classical degree day method is reflected in the linear  $R^2$ -efficiency criteria. This improvement of daily discharge simulations by using a degree day method including a radiation factor was also observed by Hock (1998). It is a consequence of daily

cycles of melt rate and solar radiation and the large spatial variability of radiation. The daily cycle of air temperature is relatively much smaller, than the daily variation in incoming solar radiation.

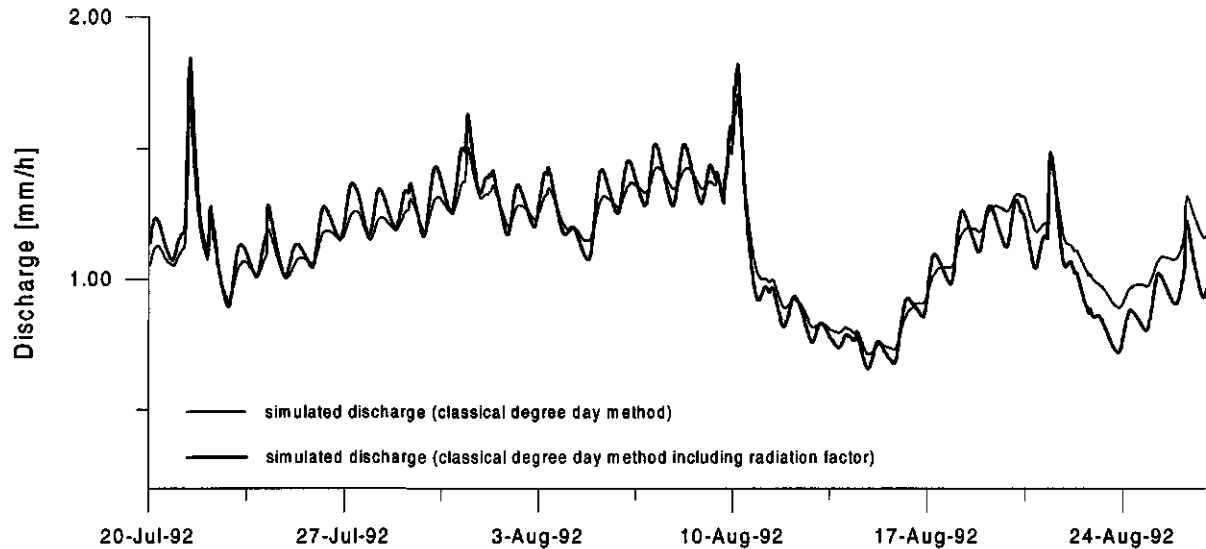


Figure 6-6: Simulated discharges of Gletsch using two temperature index methods.

### 6.5 Application on the Aletsch catchment

To test the consistency of WaSiM-ETH in which the glacier model is included, a test run is completed for the Aletsch catchment. The main aim of this run was to provide a first guess of WaSiM-ETH applied on another catchment area. The Aletsch catchment is five times larger than the Gletsch catchment and has a higher percentage glacierized area. Section 6.5.1 begins with a short description of the Aletsch catchment. The second section describes the simulation results for the Aletsch catchment.

#### 6.5.1 Description of the Aletsch catchment

The Aletsch catchment is, like the Gletsch catchment, a subcatchment of the Rhone basin and is also situated in Central-Switzerland. The catchment area is 195 km<sup>2</sup> and its discharge is measured near the snout of the Aletsch glacier in 'Blatten bei Naters' at a height of 1446 m. The discharge of the catchment area is transported by the river 'Massa'. The average height of the Aletsch catchment is 2945 m. The Aletsch glacier covers 65.9% of the Aletsch catchment (Landeshydrologie und -geologie, 1997).

The Aletsch glacier contains several glacierized areas which are situated at the south slope of the Jungfrau mountain range. As for the Rhone glacier, the Aletsch glacier has retreated during the last centuries and is divided into three glaciers. The glacierized area in 1973 was 128 km<sup>2</sup>, while it was 163 km<sup>2</sup> in 1856. The largest glacier, the 'Grosser Aletschgletsjer', is 87 km<sup>2</sup> and has a length of 24 km. The depth of this glacier is approximately 900 m. The two other glaciers are the 'Mittel Aletschgletsjer' (8.5 km<sup>2</sup>) and the 'Ober Aletschgletsjer' (22 km<sup>2</sup>) (Schweizer Lexikon, 1993).

## 6 Results of simulations

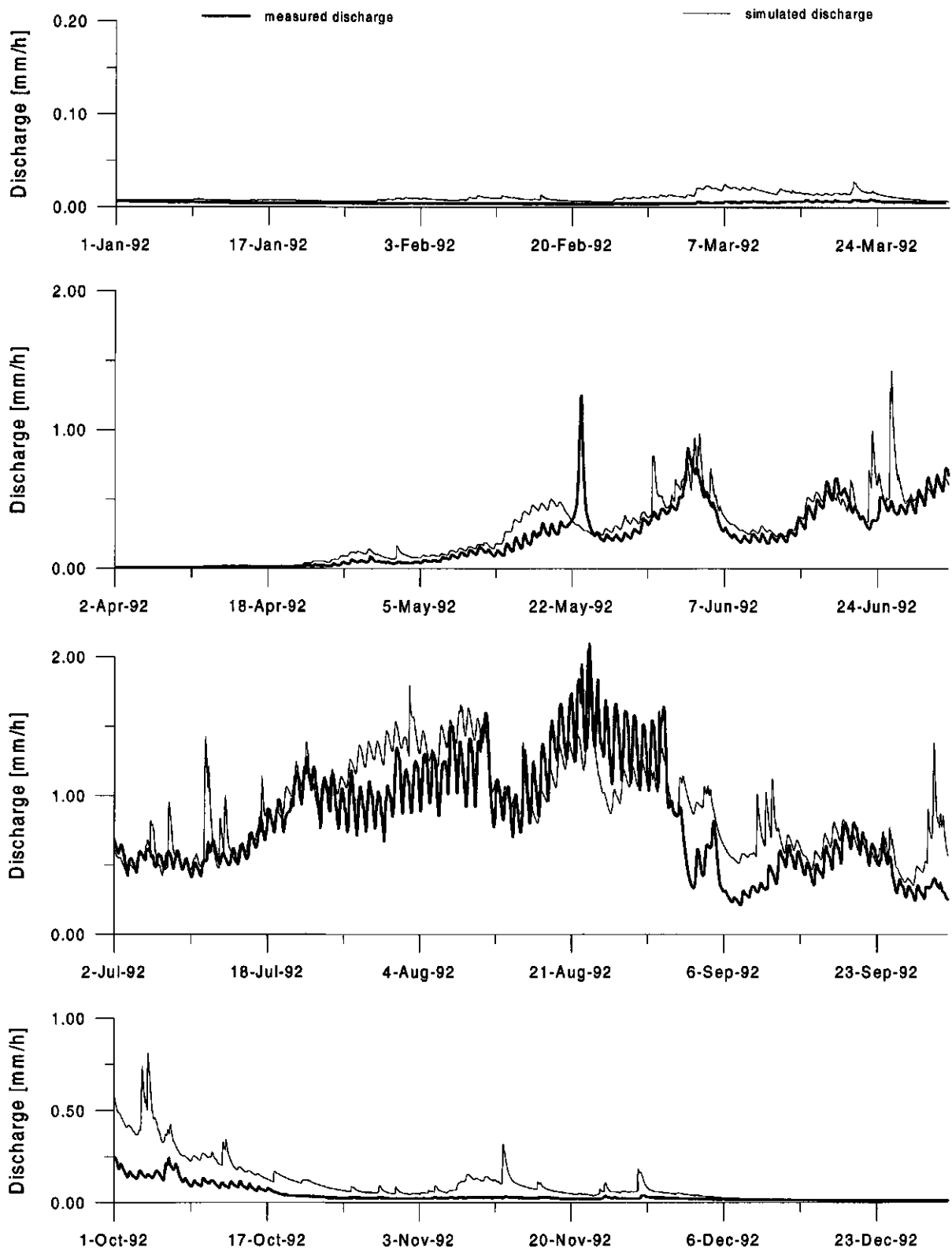


**Figure 6-7: Simulated and measured discharge of the Aletsch catchment (1992) using parameter values of Gletsch.**

The geological deposits of the Aletsch catchment differ from the Gletsch catchment. The Aletsch catchment does not cover a valley filled by fluvio-glacial sediments, but contains mainly stone, rock and ice. The discharge hydrograph (see Figure 6-7) therefore shows a distinct annual variation and a very low baseflow during the winter, while the discharge hydrograph of the Gletsch catchment shows a higher baseflow during winter. It shows that the discharge of the Aletsch catchment is to a greater extent determined by melt water from the glacier than the Gletsch catchment.

### 6.5.2 Results of the Aletsch catchment

To apply WaSiM-ETH on the Aletsch catchment, input data must be prepared, similarly to that for the Gletsch catchment. Discharge measurements at 'Blatten bei Naters' are completed by the 'Landeshydrologie und Geologie' of Bern for the period 1981-1997. The meteorological input data of the corresponding period were gained from five automatic meteorological stations, two conventional stations and five rain gauges. The digital elevation model and information about land use and soil type were also available. From the digital elevation model, grids with flow times, slope, exposure, and the catchment boundary were extracted. Further, a grid in which the glacier area and the equilibrium line are defined was built. The equilibrium line was estimated to be at a height of 2950 m. The parameter values were the same as for the Gletsch catchment, except the parameter values for the transformation of the glacier discharge to the outlet of the catchment area.

The years 1990 and 1991 were used to calculate starting values for the year of 1992. The simulated and observed discharge hydrograph for 1992 is given in Figure 6-7. The efficiency criterion  $R^2(\text{lin})$  is 0.86 and  $R^2(\text{log})$  is 0.90. The total simulated discharge volume for 1992 is 2856 mm, while the total observed discharge volume is 2388 mm. The discharge is overestimated, especially during autumn when a long period of melt water discharge was calculated. This result can be improved by calibrating this period and changing the melt factors, the storage constants of firn, snow and ice, or the parameter values of the soil model. However, the daily variation in discharge during the summer, and the time when the melt period begins, are simulated accurately. The calculated peaks around the 24<sup>th</sup> of June are probably caused by precipitation that is transported too quickly to the outlet of the catchment area, while, in reality, it is retained by the snow or glacier. The observed discharge peak on the 22<sup>nd</sup> of May is not simulated. On that day, no high temperatures, precipitation rates or radiation values were measured. This observed peak is apparently a result of a release of a water pocket within the glacier or an outburst of stored water from an ice-dammed lake, which is not simulated by WaSiM-ETH.

## 6 Results of simulations

## 7 Discussion of the results

Modelling the Gletsch catchment with WaSiM-ETH, in this study extended with the glacier model, yielded a good agreement between simulated and measured discharges. The model simulated the seasonal variation in discharge, the diurnal discharge fluctuations and the time at which the melt period starts and terminates remarkably well. The model performs considerably better for the Gletsch catchment area than using this model without the glacier melt procedure.

WaSiM-ETH is the first hydrological model that includes the calculation of glacier melt. Therefore a comparison with results of another model with glacier melt runoff can not be carried out. The results of the study with a similar model, PREVAH (Badoux, 1999), were not available.

However, the results of this study can be compared to the results of WaSiM-ETH without the glacier model for the Thur and Wernersbach catchments (Schulla, 1997). The efficiency criterium of the calibration period for the Thur basin (spatial resolution: 500 m, temporal resolution: 1 h) was  $R^2 = 0.92$  and for the Wernersbach catchment (spatial resolution: 50 m, temporal resolution: 1 h)  $R^2 = 0.86$ , while the efficiency criterium for the calibration of 1992 data of the Gletsch catchment (spatial resolution: 100 m, temporal resolution: 1 h) is  $R^2 = 0.93$ .

The results of Gletsch are in accordance with the results of Schulla and emphasize that the glacier model is successfully incorporated into WaSiM-ETH. WaSiM-ETH with the glacier melt is now suitable to simulate discharges of partly glacierized catchment areas. However, in winter the baseflow tends to be underestimated, as is the discharge at the beginning of the melt period. In autumn, discharge volumes and runoff peaks are sometimes overestimated.

A part of the deviations is attributed to the inappropriate assumption of a linear reservoir approach for firn, snow and ice runoff. A linear reservoir implies that discharge from a reservoir is proportional to its volume. However, during winter the crevasses and passageways within the glacier close, resulting in a lower transport of melt water. As the melt season progresses, the glacier drainage system evolves and more passageways develop. The runoff of each reservoir depends on this temporal and spatial variability of the glacial drainage system, implying the non-linearity of these reservoirs. To account for the seasonal changes of the glacial drainage system, an algorithm with variable outflow parameters for the reservoirs should be used.

Further, deviations can be attributed to equal parameter and constant values for the Rhone and the Mutt glacier. Equal storage constants for both glaciers were taken since the discharges of both glaciers are not observed and therefore estimating storage constants is too difficult. In reality, the storage constants are different for each glacier, because storage constants depend on the volume of the glacier. It was assumed identical storage constants for both glaciers would not have much effect on the simulated discharge since the Rhone glacier is at least thirty times larger than the Mutt glacier.

For the same reason, equal values of the parameters and constants for transferring the discharge of the Mutt glacier to the outlet of the catchment basin were taken as for the Rhone glacier. In fact, the Muttbach and the Rhone have a different width and slope, and the distance between the snout of the Rhone glacier and Gletsch is shorter than the distance between the Mutt glacier and Gletsch. The time needed for the glacier discharge to flow to the outlet of the catchment basin is therefore different for both glaciers.

The underestimated baseflow during winter can either be due to the simulated glacier discharge or the runoff from the unglacierized part of the catchment area which are both too low.

Although glacier runoff has a small contribution to the winter discharge, a low glacier runoff could induce this underestimation. An increase in winter discharge occurs when the storage constant of, for example, the firm reservoir is increased. The firm reservoir is the reservoir with the largest recession time compared to ice and snow. However, increasing the storage constant for firm also results in a decrease of the discharge from the firm reservoir during the melt season, as well as a decrease in daily discharge fluctuations. The decrease in discharge fluctuations can be compensated by increasing the melt factors. However, increasing the storage constant for firm is not based on the physical aspects of the runoff processes, but is rather used to approach the observed discharges. Using a high value for the storage constant of firm would result in an overestimation of baseflow for the Aletsch catchment. Therefore, the underestimated baseflow at Gletsch is probably affected by another factor.

Looking at the observed runoff hydrograph of Gletsch, the winter discharge seems to be produced by a large reservoir, because the discharge is almost constant during the winter months. This large reservoir could be the valley of the Gletsch catchment. During the melting season, melt water from the glacier and rainwater infiltrate into the soil. Near Gletsch, the valley is blocked by a natural dam of rock, which prevents groundwater from flowing out of the catchment area. It is assumed that during winter the reservoir is emptied. These processes are not taken into account by WaSiM-ETH. WaSiM-ETH probably does not correctly simulate the infiltration of rain and melt water from the glacier into the soil of the valley and the generation of baseflow. Or the re-infiltration of water from the river into the soil and the infiltration of the infiltration of surface runoff into the soil of neighbour cells are underestimated.

In any case, the Gletsch catchment is unique due to the geological settings near Gletsch, which are difficult to interpret and simulate. The Aletsch catchment does not cover a valley and the baseflow of the Aletsch catchment is not underestimated during winter.

Simulated discharges which are too high during autumn are either due to the storage constants of the three reservoirs, which are too low, or to a simulated melt rate which is too large. Although the temperature index method used is extended by a radiation factor and measured global radiation, it is not capable to account for all processes which influence the energy balance of a glacier. Therefore, some incorrect melt peaks may be simulated, which are not observed. For example, during days with a low water vapour pressure, much of the net radiation is used for evaporation, and less energy is available for glacier melt. Besides the water vapour pressure, the melt rate is not adjusted to differences in the albedo values of snow.

An energy balance method takes into account the differences in melt rate under varying albedo value, water vapour pressure or wind speed, and will therefore yield improved melt rate simulations. However, an energy balance method is more complex, because it requires more meteorological input data. Further, an energy balance method can not be used outside the main melt period if the heat content of the snow pack or the glacier is not taken into account. Regardless of this, temperature index methods are widely used and, for the Gletsch catchment, the degree day method including a radiation factor accomplished good simulation results.

The simulation results of the classical degree day method proved that diurnal discharge fluctuations are poorly simulated when measured global radiation is not taken into account. Hock (1998) concluded a similar result from the simulation results of Storglaciären. However, these simulation results of the classical degree day method showed worse daily discharge fluctuations than the results of the Gletsch catchment. The difference is explained by the temperature correction of WaSiM-ETH. The glacier melt model of Hock (1998) does



not modify the temperature according to exposition and topographic shading, which determine, to a large extent, the spatial variability of melt rates. Additionally, the amplitude of the diurnal temperature fluctuations is somewhat larger at Gletsch than at Storglaciären, resulting in higher diurnal variation in the melt rate at Gletsch.



## 8 Recommendations

After implementing the glacier model, WaSiM-ETH became a useful tool for simulating the processes of the hydrological system in partly glacierized catchment areas. This chapter will provide some recommendations about the use of WaSiM-ETH including the glacier model in partly glacierized areas. Additionally, some remarks are given on how to change the concept of the glacier model if the objective of the model is extended to simulating the effects of climate change.

The calibration and validation are the most important activities in the search for the best parameter fit. In this study, runoff data at Gletsch was the only data source that could be used to calibrate the model. The discharge of glacierized catchment areas, however, is influenced by many processes. Therefore, it is recommended to use as much data as possible for calibration. Runoff of the glacier alone clarifies the processes which take place on the glacierized areas. The time series of the groundwater level also provide useful information. When, for instance, no data is available about groundwater levels, it is difficult to determine whether the simulated baseflow is correct.

When modelling with WaSiM-ETH including the glacier model, special consideration should be given to the melt and radiation factors. In particular, the interdependency between these factors causes difficulties to find an optimal fit. Efficiency criteria should be used to determine the best combination, because the use of efficiency criteria is an objective method to calibrate the model.

WaSiM-ETH with the new glacier model included can now be used for short term forecasts. When the model is calibrated, weather forecasts can be used as input data to estimate the discharge from the catchment areas a few days in advance. The reliability of the results is, of course, mainly dependent on the reliability of the weather predictions. Besides short term predictions, the model can now be used for simulating the entire Swiss territory.

The present model can not be used to study the impacts of climate change on glaciers and the catchment areas they belong to, because processes such as glacier retreat and progress are not simulated. The glacierized area is now assumed to be constant in time and is defined by an input grid. In order to simulate the progress or retreat of the glacier, the mass balance of the glacier should be calculated, implying processes such as the transformation of snow into firn, and firn into ice as well as the glacier movement from the accumulation area to the ablation area. Further, the equilibrium line, which is now defined by an input grid, changes in time and should be re-calculated every year.

If the water balance of the glacier is known, the water balance of the total catchment area can be determined, which is now impossible. As was mentioned before, observed glacier discharge is useful concerning the calibration procedure of the glacier model. Measurements such as the equilibrium line, the position of the glacier snout, and the depth of snow, firn and ice are needed to calibrate and validate WaSiM-ETH when it is adjusted to simulate the processes of the glacier water balance.

WaSiM-ETH can be adjusted for simulations of climate change in the following way. Firstly, the ice and firn areas should be described as reservoirs for which separate balances are calculated. Snow that falls on the accumulation zone should be transformed into firn and ice with a certain delay. Secondly, the transport from the accumulation towards the ablation area should be simulated. Such an adjustment can only be successful if enough data about the glacier movement is available, otherwise many new calibration parameters must be introduced.

## 8 Recommendations

## References

- Anderson, E.A., 1973: National weather service river forecast system / snow accumulation and ablation model. NOAA Technical Memorandum NWS HYDRO-17 (U.S. Dept. Of Commerce, Silver Spring, Md.), 217 pp.
- Badoux, A., 1997: Untersuchungen zur Modellierung von Schneeschmelze und Abfluss im Dischma-Gebiet, Semesterarbeit in Hydrologie. Abteilung für Erdwissenschaften, Geographisches Institut, ETH Zürich, 26 pp.
- Badoux, A., 1999: Untersuchungen zur flächendifferenzierten Modellierung von Abfluss und Schmelze in vergletscherten Einzugsgebieten. Geographisches Institut, ETH Zürich.
- Baker, D., Escher-Vetter, H., Moser, H., Oerter, H. and Reinwarth, O., 1982: A glacier discharge model based on results from field studies of energy balance, water storage and flow. In: Glen, J.W. (Ed): Hydrological aspects of alpine and high-mountain areas. Proceedings of the Exeter Symposium 1982: IAHS Publ. No. 138, 103-112.
- Bernath, A., 1991: Zum Wasserhaushalt im Einzugsgebiet der Rhone bis Gletsch, Züricher geographischen Schriften 43, Department of Geography, ETH Zürich. 383 pp.
- Beven, K.J. and Kirkby, M.J., 1979: A physically based variable contributing area model of basin hydrology. Hydrol. Sci. Bull., 24 (1) 43-69.
- Blöschl, G., 1996: Scale and Scaling in Hydrology, Wiener Mitteilungen band 132, Institut für Hydraulik, Gewässerkunde und Wasserwirtschaft, Technisch Universität Wien, 346 pp.
- Braun, L.N., 1985: Simulation of snowmelt-runoff in lowland and lower Alpine regions of Switzerland. Zürcher geographischen Schriften 21, Department of Geography, ETH Zürich, 160 pp.
- Braun, L.N., 1988: Parameterization of Snow- and Glaciersmelt. Berichte und Skripten Nr. 34, Geographisches Institut ETH Zürich, 72 pp.
- Bundesamt für Landestopographie - BFL, 1991: Digitales Höhenmodell RIMINI. Wabern.
- Bundesamt für Landestopographie - BFL, 1980: Landeskarte der Schweiz 1 : 50000; Sustenpas.
- Bundesamt für Statistik - BFS, 1993: Die Bodennutzung der Schweiz , Arealstatistik 1979/85, resultate nach Bezirke und Kantone, Bern.
- Bundeasamt für Statistik - BFS, 1995: Digitale Bodeneignungskarte 1:200'000, Bern.
- Douglas, J.R., 1974: Conceptual Modelling in Hydrology, report no 24. Institute of Hydrology, Howbery Park.
- Dyck, S. and Peschke, G., 1989: Grundlagen der Hydrologie. 2. Aufl., Verlag für Bauwesen, Berlin, 480 pp.

## References

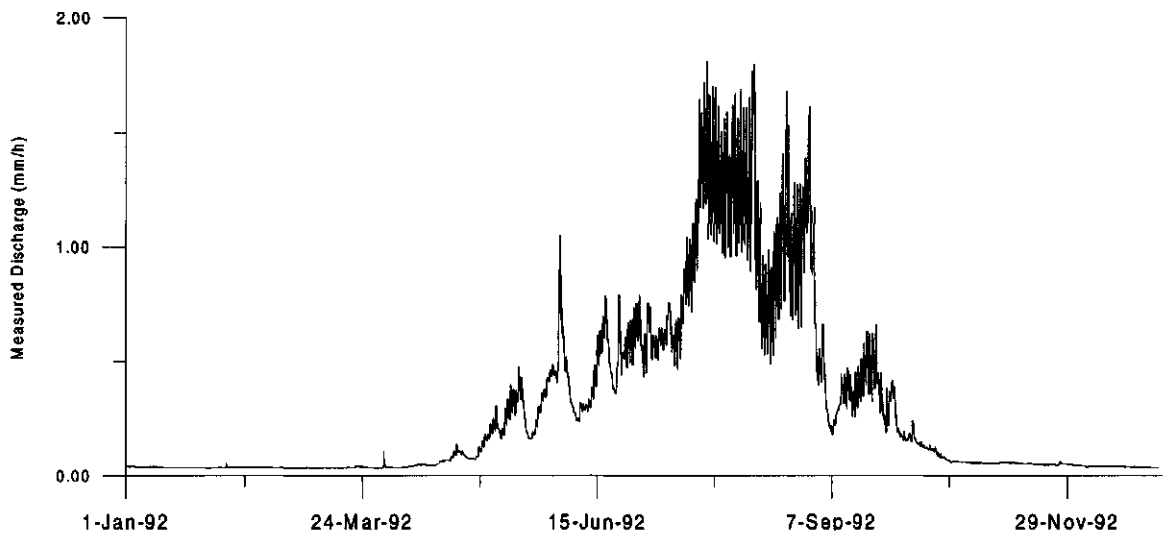
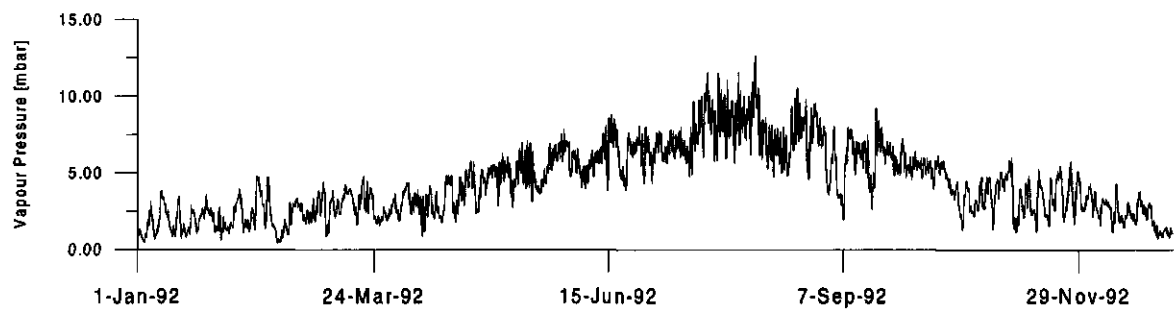
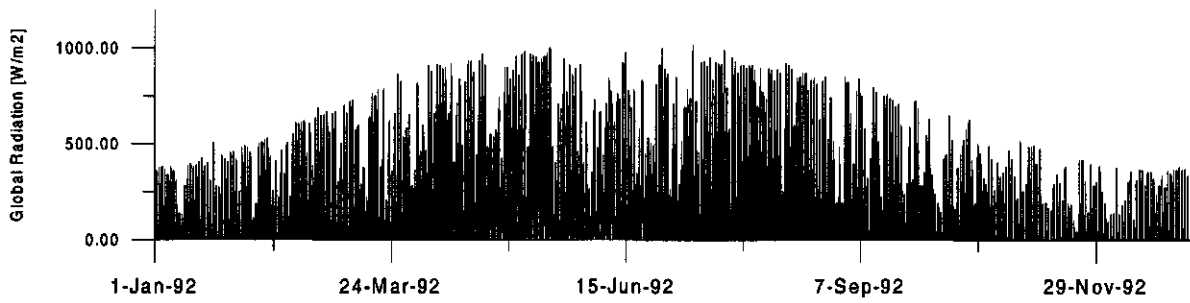
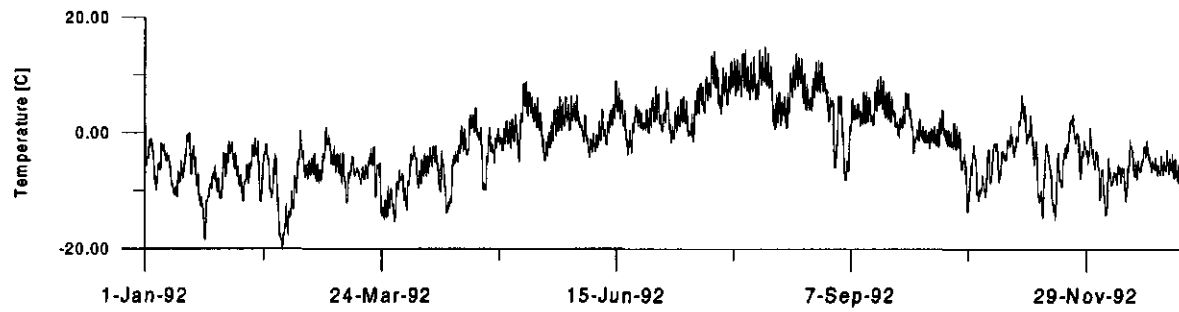
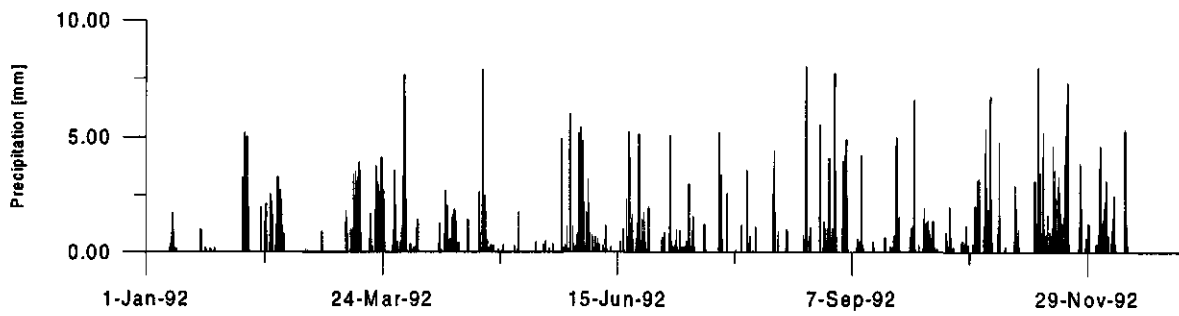
- Federer, C.A., and Lash., D., 1983: BROOK - A hydrologic simulation model for eastern forests. Water Resources Research Centre, University of New Hampshire.
- Finsterwalder, S. and Schunk, H., 1887: Der Suldenferner. Zeitschrift des Deutschen und Oesterreichischen Alpenvereins 18, 72-89.
- Grabs, W. (Ed.), 1997: Impact of climate change on hydrological regimes and water resources management in the Rhine basin. International Commission for the Hydrology of the Rhine Basin (CHR), CHR-Report no. I-16, Lelystad, 172 pp.
- Guisan, A., Holten, J.I. and Spichiger, R., 1995: Potential ecological impacts of climate change in the Alps and Fennoscandian mountains : an annex to the Intergovernmental Panel of Climate Change (IPCC) second assessment report , Working Group 2-C (Impacts of climate change on mountain regions). Ville de Geneve, Geneve, 194 pp.
- Hock, R., 1998: Modelling of glacier melt and discharge. Zürcher geographischen Schriften 70, Department of Geography, ETH Zürich, 126 pp.
- Kümmerly and Frey Geographischer Verlag Bern, 1980: Die Schweiz und Ihre Gletscher; von der Eiszeit bis zur Gegenwart. Schweizerische Verkehrszentrale Zürich, Zürich.
- Landeshydrologie und -geologie, 1997: Hydrologisches Jahrbuch der Schweiz. Bundesamt für Umweltschutz, Bern.
- Lang, H., 1986: Forecasting melt water runoff from snow-covered areas and from glacier basins. In: Kraijenhoff, D. A. and Moll, J. R. (Eds): River flow modelling and forecasting. Water Science and Technology Library, D. Reidel Publishing Company, Holland, 99-127.
- Lang, H. and L. Braun, 1990: On the information content of air temperature in the context of snow melt estimation. In L. Molnar (Ed), Hydrology of mountainous areas. Proceedings of the Strbske Pleso Symposium 1992: IAHS Publ. No. 190, 347-354.
- Menzies, J., 1995: Hydrology of glaciers. In: Menzies, J. (Ed): Modern Glacial Environments; Processes, Dynamics and Sediments. Glacial Environments: Vol. 1. Butterworth-Heinemann, Oxford, 197-259.
- Monteith, J.L., 1975: Vegetation and the atmosphere, vol. 1: Principles. Academic Press, London.
- Müller, H., 1985: Review paper: On the radiation budget in the Alps. J. Climatol. 5, 445-462.
- Noetzli, C., 1996: Die Simulation des Abflusses am Storglaciären, Nordschweden mit einem Linearspeichermodell. Master's thesis, Department of Geography, ETH Zürich, 108 pp.
- Paterson, W.S.B., 1981: The physics of glaciers (2<sup>nd</sup> Edition). Oxford, Pergamon Press, 380 pp.
- Röthlisberger, H. and Lang, H., 1987: Glacial Hydrology. In: Gurnell, A.M. and Clark, M.J. (Eds.): Glacio-fluvial sediment transfer. John Wiley and Sons, New York, 207-284.
- Sharp, R. P., 1960: Glaciers. University of Oregon Press, Eugene, Oregon, U.S.A., 78 pp.

- Schulla, J., 1997: Hydrologische Modellierung von Flussgebieten zur Abschätzung der Folgen von Klimaänderungen. Zürcher geographischen Schriften 69, Department of Geograpy, ETH Zürich, 187 pp.
- Schulla, J. and K. Jasper, 1998: Modellbeschreibung WaSiM-ETH, Institut für Hydromechanik und Wasserwirtschaft, ETH Zurich, *unpublished*, 144 pp.
- Schulla, J. and K. Jasper, 1999: Modellbeschreibung WaSiM-ETH, Institut für Hydromechanik und Wasserwirtschaft, ETH Zurich, *unpublished*, 155 pp.
- Schweizer Lexikon, 1993: Gletscher und Eis, Das Lexikon zu Glaziologie, Schnee- und Lawinenforschung der Schweiz. Herausgegeben von der Redaktion Schweizer Lexikon und der Gletscherkommission der Schweizerischen Akademie der Naturwissenschaften, Verlag Schweizer Lexikon Mengis & Ziehr, Luzern.
- Sevruk B. et al. (1985): Der Niederschlag in der Schweiz. In: Beitrage zur Geologie der Schweiz - Hydrologie, Nr. 31, Bericht der Arbeitsgruppe "Niederschlag". Schweizer Geotechnische Kommission und Hydrologische Kommission der Schweizerischen Naturforschenden Gesellschaft.
- Stuyt, L.C.P.M. 1978: A Deterministic Model for Streamflow Prediction, intern rapport, Institute of Hydrology Wageningen, Department of Hydraulics and Catchment Hydrology.
- Verlag Schweizer Lexikon Mengis + Ziehr, 1993: Gletscher, Schnee und Eis; das Lexikon zu Glaziologie Schnee- und Lawinenforschung in der Schweiz, Redaktion Schweizer Lexikon und der Gletscherkommission der Schweizerischen Akademie der Naturwissenschaften.
- Warren, S.G., 1982: Optical properties of snow. Rev. Geophys. And Space Phys. 20(1). 67-89.
- Weilenman, U., 1979: Der Rhonegletscher und sein Vorfeld; ein geographische Grundlagenbeschaffung, Dilpomarbeit am Geographischen Institut ETH, Zurich, 156 pp.
- Wendling, U., 1975: Zur Messung und Schätzung der potentiellen Verdunstung. Zeitschrift für Meteorologie, 25 (2), 103-111.

## Appendix 1

### Meteorological data and discharge for the Gletsch catchment for 1992





## Appendix 2

Control-file for WaSiM-ETH including glacier model

```

$set $year = 92
#
# comment lines are indicated by an "#". They are allowed after the entries or at the beginning of the lines
#
# paragraphs of the control file:
# [output_interval] (geogr. coordinates)
# [coordinates] (name of the elevation model)
# [elevation_model] (name of the zone grid)
# [zonengrid] (name of other static grids like slope angle, slope aspect, topogr. factor)
# [standardgrids] (names of albedo and soil storage - used by more than one modules)
# [variable_grids] (start end end-dates of model time)
# [model_time] (number of mete data to interpolate)
# [meteo_data_count] (names of mete data to interpolate)
# [meteo_names] (names of mete data to interpolate)
# [precipitation_correction] (paragraph for parameters of the prec.-correction)
# [radiation_correction] (paragraph with parameters for radiation correction)
# [evapotranspiration] (paragraph with parameters for evapotranspiration)
# [snow_model] (paragraph with parameters for the snow model)
# [interzeption_model] (paragraph with parameters for the interzeption model)
# [infiltration_model] (paragraph with parameters for the infiltration model)
# [soil_model] (paragraph with parameters for the soilmodel)
# [unsatzone_model] (paragraph with parameters for the unsaturated zone model)
# [routing_model] (paragraph with Parameter for discharge routing)
# [landuse_table] (paragraph with land use (vegetation) parameters)
# [soil_table] (paragraph with soil properties)
#
#
# symbol definitions begin with the set command:
# max. 200 symbols can be defined

$set $outpath = /net/ezges53c/scratch/WASIM/output/
$set $inpath = /net/ezges53c/scratch/WASIM/input/
$set $time = 60.0

$set $grid = g100
$set $stack = r100
$set $suffix = grid
$set $code = s

# variables for standardgrids
# first section: grids, which differ for different subdivisions of the basin
$set $zone_grid = // $grid//zn2
$set $subcatchments = // $grid//zn2
$set $flow_time_grid = // $grid//tzn
$set $river_links_grid = // $grid//lnk

#second section: grids, which doesn't depend on subdivision (only pixel-values are of interest)
$set $elevation_model = // $grid//dhn

```

```

$set $slope_grid = // $grid//slp
$set $aspect_grid = // $grid//exp
$set $land_use_grid = // $grid//use
$set $ice_firn_grid = // $grid//ice
$set $field_capacity_grid = // $grid//mfk
$set $ATBgrid = // $grid//atb
$set $hydr_cond_grid = // $grid//k
$set $soil_types = // $grid//art
$set $sky_view_factor_grid = // $grid//hor
$set $rain_depth_grid = // $grid//drm
$set $rain_distance_grid = // $grid//dis
$set $irrigationcodes = // $grid//irr
$set $max_pond_grid = // $grid//pnd
$set $clay_depth_grid = // $grid//cly
$set $river_depth_grid = // $grid//dep
$set $river_width_grid = // $grid//wit
$set $tracer_1 = // $grid//c1
$set $tracer_2 = // $grid//c2
$set $tracer_3 = // $grid//c3
$set $tracer_4 = // $grid//c4
$set $tracer_5 = // $grid//c5
$set $tracer_6 = // $grid//c6
$set $tracer_7 = // $grid//c7
$set $tracer_8 = // $grid//c8
$set $tracer_9 = // $grid//c9
$set $kolmatingsrid = // $grid//kol
$set $gw_kx_1_grid = // $grid//kx1
$set $gw_kx_2_grid = // $grid//kx2
$set $gw_kx_3_grid = // $grid//kx3
$set $gw_ky_1_grid = // $grid//ky1
$set $gw_ky_2_grid = // $grid//ky2
$set $gw_ky_3_grid = // $grid//ky3
$set $gw_bound_h_1_grid = // $grid//bh1
$set $gw_bound_h_2_grid = // $grid//bh2
$set $gw_bound_h_3_grid = // $grid//bh3
$set $gw_bound_q_1_grid = // $grid//bq1
$set $gw_bound_q_2_grid = // $grid//bq2
$set $gw_bound_q_3_grid = // $grid//bq3
$set $aquiferthick1 = // $grid//aq1
$set $aquiferthick2 = // $grid//aq2
$set $aquiferthick3 = // $grid//aq3
$set $gw_storage_coeff_1 = // $grid//s01
$set $gw_storage_coeff_2 = // $grid//s02
$set $gw_storage_coeff_3 = // $grid//s03
$set $gw_kolmat_1 = // $grid//gk1
$set $gw_kolmat_2 = // $grid//gk2
$set $gw_kolmat_3 = // $grid//gk3

```

# grids for surface hydrology modules

```

$set $aibedo_grid = albe/$grid//.$suffix
$set $solstoragegrid = sb_/$grid//.$suffix
$set $roughfall = ql_/$grid//.$suffix
$set $snowcover_outflow = qsnoc/$grid//.$suffix
$set $tim_melt = qfir/$grid//.$suffix
$set $ice_melt = qice/$grid//.$suffix
$set $preci_grid = prec/$grid//.$suffix
$set $irrig_grid = iri/$grid//.$suffix
$set $tempgrid = temp/$grid//.$suffix
$set $windgrid = wind/$grid//.$suffix
$set $sunshinegrid = ssd_/$grid//.$suffix
$set $radiationgrid = rad_/$grid//.$suffix
$set $humiditygrid = humi/$grid//.$suffix
$set $vaporgrid = vapo/$grid//.$suffix
$set $ETPgrid = etp_/$grid//.$suffix
$set $ETRgrid = eir_/$grid//.$suffix
$set $$SSNOgrid = ssno/$grid//.$suffix
$set $SLUQgrid = slq/$grid//.$suffix
$set $sat_def_grid = sd_/$grid//.$suffix
$set $SUZgrid = suz_/$grid//.$suffix
$set $SIFgrid = sif_/$grid//.$suffix
$set $Elgrid = ei_/$grid//.$suffix
$set $$Sgrid = si_/$grid//.$suffix
$set $ExpoCorrgrid = exco/$grid//.$suffix
$set $Tcorrgrid = tcor/$grid//.$suffix
$set $Shapegrid = shap/$grid//.$suffix
$set $INFEXgrid = infx/$grid//.$suffix
$set $SATTgrid = sat/$grid//.$suffix
$set $Nagrid = na_/$grid//.$suffix
$set $SSPgrid = ssp_/$grid//.$suffix
$set $Peakgrid = peak/$grid//.$suffix
$set $SBIagrid = sbia/$grid//.$suffix
$set $cia_grid = nfxi/$grid//.$suffix

```

# now variables for unsaturated zone model

```

$set $QDgrid = qd_/$grid//.$suffix
$set $Qlgrid = qil/$grid//.$suffix
$set $GWdepthgrid = gwst/$grid//.$suffix
$set $GWthetagrid = gwth/$grid//.$suffix
$set $GWNgrid = gwn_/$grid//.$suffix
$set $GWLLEVELgrid = gwlv/$grid//.$suffix
$set $QDRAINgrid = qdri/$grid//.$suffix
$set $QBgrid = qb_/$grid//.$suffix
$set $GWINgrid = gwri/$grid//.$suffix
$set $GWEXgrid = gwex/$grid//.$suffix
$set $act_pond_grid = pond/$grid//.$suffix

```

# variables for groundwater modeling

```

$set $flowx1grid = gwx1/$grid//.$suffix

```

```

$set $flowx2grid = gwx2/$grid//.$suffix
$set $flowx3grid = gwx3/$grid//.$suffix
$set $flowy1grid = gwy1/$grid//.$suffix
$set $flowy2grid = gwy2/$grid//.$suffix
$set $flowy3grid = gwy3/$grid//.$suffix
$set $head1grid = gwh1/$grid//.$suffix
$set $head2grid = gwh2/$grid//.$suffix
$set $head3grid = gwh3/$grid//.$suffix

```

# Ergebnis-stacks for Unseazonmodel

```

$set $Thetastack = teth/$stack//.$suffix
$set $hydraulic_heads_stack = hhyd/$stack//.$suffix
$set $geodetic_altitude_stack = hgeo/$stack//.$suffix
$set $flowstack = qu_/$stack//.$suffix
$set $concstack = conc/$stack//.$suffix

```

# parameters for interpolation of meteorological input data

```

$set $SzenUse = 0
$set $IDWmaxdist = 20000
$set $IDWweight = 2
$set $Anisotrope = 35.0
$set $Anisotropie = 0.65

```

# explanation of writgrid and outputcode some lines below

```

$set $Writgrid = 0
$set $Writestack = 3
$set $outputcode = 1001
$set $output_meteo = 1001
$set $day_sum = 3024
$set $day_mean = 1024
$set $hour_mean = 2001
$set $routing_code = 4001

```

# readgrids : 1 = read storage grids from hard disk, 0=generate and initialize with 0

```

$set $readgrids = 1

```

# Writgrid : max. 3 digits (nnn)

# only if writgrid >= 100: 1. digit (1nn, or 2nn or 3nn)

# 0 = no minimum or maximum grid is written

# 1 = minimum grid is written (minimum value for each of the grid cells over the entire model period)

# 2 = maximum grid is written (maximum value for each of the grid cells over the entire model period)

# 1 = both grids are written (minimum and maximum value over the entire model period)

# only if Writgrid >= 10: 2nd digit: sums or means (n1n ... n8n)

# 0 = no sum grid will be written

# 1 = one sum grid will be written at the end of the model run

# 2 = one sum grid per model year

# 3 = one sum grid per model month

# 4 = one sum grid per day (only, if timestep < 1 day)

# 5 = one mean value grid at the end of the model run

```

# 6 = one mean value grid per model year
# 7 = one mean value grid per month
# 8 = one mean value grid per day
# last digit (nn1 .. nn5) (for actual values, not for Sums or means)
# 1 = (over)write each timestep into the same grid (for security in case of model crashes)
# 2 = write grids each timestep to new files, the name is build from the first 4 letters
# of the regular grid name and then from the number of month, day and hour
# 3 = only the last grid of the model run will be stored
# 4 = the grid from the last hour of each day (24:00) will be stored
# 5 = like 4, but each day a new grid file is created (like for code 2)
# outputcode (for statistic files for zones or subcatchments)
# the Codes behind the names of the statistic files have the meaning of:
# <1000 : no output
# 1<-<nnn> : spatial mean values for the entire basin, averaged in time over <nnn> intervals (timesteps)
# 2<-<nnn> : spatial mean values for all zones (subbasin) and for the entire basin, averaged in time over
<nnn> intervals (timesteps)
# 3<-<nnn> : spatial means for the entire basin, added up in time over <nnn> intervals (timesteps)
# 4<-<nnn> : spatial means for all zones (subbasin) and for the entire basin, added up in time over <nnn>
intervals (timesteps)
# 5<-<nnn> : spatial means for the entire basin and for those subbasins which are specified in the output-list,
averaged in time over <nnn> intervals
# 6<-<nnn> : spatial means for the entire basin and for those subbasins which are specified in the output-list,
added up in time over <nnn> intervals
# example:
# 2001 = per timestep for all subcatchments (and for the entire basin) one (spatially averaged) value,
# 4024 = Sums of the mean subcatchment/entire basin values of the timesteps over 24 timesteps
# 3120 = averaged values (over 120 time steps) only for the entire basin (spatially averaged)

[output_list]
1 # number of subbasins which are scheduled for output
2 1 # codes for the subbasins

[output_interval]
49 # increment of time steps until an output to the screen is done
1 # warning level for interpolation (no station within search radius)
0 # unit of routed discharge (0=mm/timestep, 1=m3/s)

[coordinates]
46.6 # geogr. latitude (center of the basin -> for radiation calculations)
8.4 # geogr. longitude (center of the basin)
15.0 # meridian according to the official time (middle europe: 15)
1 # time shift of Meteo-data-time with respect to the true local time (mean sun time)
# e.g.: if meteo-data are stored in UTC-time and the time meridian is 15 east (central europe),
# than the local time is 1 hour later than the time in the meteo-data-file, so 1 hour has to be added to the
# time from this file. this is important for calculation of sunshine duration and radiation

[elevation_model]
$inpath/$elevation_model # grid with the digital elevation data

```

```

[zone_grid]
$inpath/$zone_grid # grid with Zone codes

[standard_grids]
7 # number of standard grids
$inpath/$land_use_grid landuse 1 # grid with land use data
$inpath/$ice_firn_grid ice_firn 0 # grid with firn or ice cells (code 0: nodata values should
not be replaced by nearest neighbour)
$inpath/$slope_grid slope_angle 1 # grid with slope angle data
$inpath/$aspect_grid slope_aspect 1 # grid with slope aspect data
#$inpath/$ATBgrid topographic_faktor 1 # soil-topographic-factor ln(A/(T*lanb))
$inpath/$subcatchments zonegrid_solmodel 1 # zone grid for the runoff generation model
$inpath/$soil_types soil_types 1 # soil types as codes for the soil table
#$inpath/$sky_view_factor_grid sky_view_factor 1 # grid with Sky-View-Factor
$inpath/$flow_time_grid flow_times 1 # grid with flow times for surface runoff to the outlet
#$inpath/$hydr_cond_grid hydraulic_conductivity 1 # grid with hydraulic conductivity of the soil
$inpath/$field_capacity_grid available_soil_moisture 1 # grid with available soil moisture at field
capacity (mm) -> old soil model in seconds
$inpath/$tracer_1 conflux_tracer_1_input 1
$inpath/$tracer_2 conflux_tracer_2_input 1
$inpath/$tracer_3 conflux_tracer_3_input 1
$inpath/$river_depth_grid river_depth 0
$inpath/$river_width_grid river_width 0
$inpath/$river_links_grid river_links 0
$inpath/$kolmationsgrid kolmation 0
$inpath/$drain_depth_grid drainage_depth 1
$inpath/$drain_distance_grid drainage_distance 1
$inpath/$clay_depth_grid clay_depth 1
$inpath/$max_pond_grid max_ponding_storage 1
$inpath/$irrigationcodes irrigation_codes 1 # grid with codes according to the irrigation table
$inpath/$aquiferthick1 aquifer_thickness_1 1 # grid with thickness of first aquifer
$inpath/$gw_storage_coeff_1 gw_storage_coeff_1 1 # storage coefficients for 1. aquifer
$inpath/$gw_bound_h_1_grid gw_boundary_fix_h_1 0 # boundary conditions 1 constant head for layer 1
$inpath/$gw_bound_q_1_grid gw_boundary_fix_q_1 0 # boundary conditions 2 for layer 1
$inpath/$gw_kx_1_grid gw_k_x_1 1 # lateral hydraulic conductivities for the 1. aquifer in x direction
$inpath/$gw_ky_1_grid gw_k_y_1 1 # lateral hydraulic conductivities for the 1. aquifer in y direction
$inpath/$gw_kolmation_1 gw_kolmation_1 1 # kolmation (leakage factor) between 1st and 2nd aquifer
$inpath/$aquiferthick2 aquifer_thickness_2 1 # grid with thickness of first aquifer
$inpath/$gw_storage_coeff_2 gw_storage_coeff_2 1 # storage coefficients for 1. aquifer
$inpath/$gw_bound_h_2_grid gw_boundary_fix_h_2 # boundary conditions 1 constant head for layer 1
$inpath/$gw_bound_q_2_grid gw_boundary_fix_q_2 0 # boundary conditions 2 for layer 1
$inpath/$gw_kx_2_grid gw_k_x_2 1 # lateral hydraulic conductivities for the 1. aquifer in x direction
$inpath/$gw_ky_2_grid gw_k_y_2 1 # lateral hydraulic conductivities for the 1. aquifer in y direction
$inpath/$gw_kolmation_2 gw_kolmation_2 1 # kolmation (leakage factor) between 2nd and 3rd aquifer

# variable grids are used by more than one module or can be changed (like albedo and soil storage)
[variable_grids]

```

```

2      # Number of variable grids to read
$outpath/$albedo_grid  albedo 1 # albedo; for time without snow derived from land use data
$Wwritegrid # Writegrid for albedo_grid
$readgrids # 0, if albedo is derived from land use at model start time, 1, if albedo is read from file
$outpath/$soilstoragegrid soil_storage 1 # soil water storage
$Wwritegrid # Writegrid for this grid
$readgrids # 0, if soil_storage should be derived from soil types, 1, if it should be read from file

[model_time]
1 # start hour
1 # start day
1 # start month
19/$year # start year
24 # end hour
31 # end day
12 # end month
19/$year # end year

[meteo_data_count]
6

[meteo_names]
precipitation
temperature
vapor_pressure
global_radiation
wind_speed
sunshine_duration
#air_humidity

[temperature]
2 # Methode 1=idw, 2=regress, 3=idw+regress, 4=Thiessen
$outpath/temp/$year/.inp # file name with station data (if method = 1, 3 or 4, else ignored)
$outpath/temp/$year/.reg # file name with regression data (if method = 2 or 3)
5/$Wwritegrid # name of the output grid
0.1 # 0, if no grid-output is needed, else one of the codes described above
# correction factor for results
$outpath/temp/$grid/.$code/$year $hour_mean # file name for the statistic output
998 # error value: all data in the input file greater than this values or lesser the negative
value are nodata
$IDWweight # weighting of the reciprocal distance for IDW
0.75 # for interpolation method 3: relative weight of IDW-interpolation in the result
$IDWmaxdist # max. distance of stations to the actual interpolation cell
$Anisoslope # slope of the mean axis of the anisotropy-ellips
$Anisotropie # ratio of the short to the long axis of the anisotropy-ellips
-40 # lower limit of interpolation results
-40 # replace value for results below the lower limit
40 # upper limit for interpolation results
40 # replace value for results with larger values than the upper limit

$SzenUse # 1=use scenario data for correction, 0=dont use scenarios
1 # 1=add scenarios, 2=multiply scenarios, 3=percentual change
4 # number of scenario cells

[wind_speed]
2 # method: 1=idw 2=regress 3=idw+regress 4=thiessen
$outpath/wind/$year/.inp # file name with station data (if method = 1, 3 or 4, else ignored)
$outpath/wind/$year/.reg # file name with regression data (if method = 2 or 3)
5/$Wwritegrid # name of the output grid
0.1 # 0, if no grid-output is needed, else one of the codes described above
# correction faktor for results
$outpath/wind/$grid/.$code/$year $hour_mean # file name for the statistic output
998 # error value: all data in the input file greater than this values or lesser the negative
value are nodata
$IDWweight # weighting of the reciprocal distance for IDW
0.3 # for interpolation method 3: relative weight of IDW-interpolation in the result
$IDWmaxdist # max. distance of stations to the actual interpolation cell
$Anisoslope # slope of the mean axis of the anisotropy-ellips
$Anisotropie # ratio of the short to the long axis of the anisotropy-ellips
0 # lower limit of interpolation results
0 # replace value for results below the lower limit
90 # upper limit for interpolation results
90 # replace value for results with larger values than the upper limit
$SzenUse # 1=use scenario data for correction, 0=dont use scenarios
3 # 1=add scenarios, 2=multiply scenarios, 3=percentual change
4 # number of scenario cells

[precipitation]
3 # method: 1=idw 2=regress 3=idw+regress 4=thiessen
$outpath/regen/$year/.inp # file name with station data (if method = 1, 3 or 4, else ignored)
$outpath/regen/$year/.reg # file name with regression data (if method = 2 or 3)
5/$Wwritegrid # name of the output grid
0.1 # 0, if no grid-output is needed, else one of the codes described above
# correction faktor for results
$outpath/regen/$grid/.$code/$year $hour_mean # file name for the statistic output
998 # error value: all data in the input file greater than this values or lesser the negative
value are nodata
$IDWweight # weighting of the reciprocal distance for IDW
0.75 # for interpolation method 3: relative weight of IDW-interpolation in the result
$IDWmaxdist # max. distance of stations to the actual interpolation cell
$Anisoslope # slope of the mean axis of the anisotropy-ellips
$Anisotropie # ratio of the short to the long axis of the anisotropy-ellips
0.1 # lower limit of interpolation results
0 # replace value for results below the lower limit
900 # upper limit for interpolation results
900 # replace value for results with larger values than the upper limit
$SzenUse # 1=use scenario data for correction, 0=dont use scenarios
2 # 3 # 1=add scenarios, 2=multiply scenarios, 3=percentual change
1 # 4 # number of scenario cells

```

```

699000 235000 0.5 0.5 0.5 0.5 0.5 0.5 0.5 0.5 0.5 0.5 0.5 # coordinates of the cells, then one value
for each month of a year

[sunshine_duration]
1 # method: 1=idw 2=regress 3=idw+regress 4=thiessen
$inpath/soni/$year/.inp # file name with station data (if method = 1, 3 or 4, else ignored)
$inpath/soni/$year/.reg # file name with regression data (if method = 2 or 3)
$outpath/$sunshinegrid # name of the output grid
5/$Writegrid # 0, if no grid-output is needed, else one of the codes described above
1.0 # correction faktor for results
$outpath/sonni/$grid/.$code/$year $hour_mean # file name for the statistic output
998 # error value
$IDWweight # weighting of the reciprocal distance for IDW
0.5 # for interpolation method 3: relative weight of IDW-interpolation in the result
$IDWmaxdist # max. distance of stations to the actual interpolation cell
$Anisotlope # slope of the mean axis of the anisotropy-ellipsis
$Anisotropie # ratio of the short to the long axis of the anisotropy-ellipsis
0 # lower limit of interpolation results
0 # replace value for results below the lower limit
1.0 # upper limit for interpolation results
1.0 # replace value for results with larger values than the upper limit
$SzenUse # 1=use scenario data for correction, 0=dont use scenarios
3 # 1=add scenarios, 2=multply scenarios, 3=percentual change
1 # number of scenario cells

[global_radiation]
2 # method: 1=idw 2=regress 3=idw+regress 4=thiessen
$inpath/glob/$year/.inp # file name with station data (if method = 1, 3 or 4, else ignored)
$inpath/glob/$year/.reg # file name with regression data (if method = 2 or 3)
$outpath/$radiationgrid # name of the output grid
1/$Writegrid # 0, if no grid-output is needed, else one of the codes described above
1.0 # correction faktor for results
$outpath/glob/$grid/.$code/$year $hour_mean # file name for the statistic output
998 # error value
$IDWweight # weighting of the reciprocal distance for IDW
0.5 # for interpolation method 3: relative weight of IDW-interpolation in the result
$IDWmaxdist # max. distance of stations to the actual interpolation cell
$Anisotlope # slope of the mean axis of the anisotropy-ellipsis
$Anisotropie # ratio of the short to the long axis of the anisotropy-ellipsis
0 # lower limit of interpolation results
0 # replace value for results below the lower limit
1367 # upper limit for interpolation results
1367 # replace value for results with larger values than the upper limit
$SzenUse # 1=use scenario data for correction, 0=dont use scenarios
1 # 1=add scenarios, 2=multply scenarios, 3=percentual change
4 # number of scenario cells

[air_humidity]
1 # method: 1=idw 2=regress 3=idw+regress 4=thiessen

```

```

$inpath/feuch/$year/.a.dat # file name with station data (if method = 1, 3 or 4, else ignored)
$inpath/feuch/$year/.out # file name with regression data (if method = 2 or 3)
5/$Writegrid # name of the output grid
0.001 # 0, if no grid-output is needed, else one of the codes described above
# correction faktor for results
$outpath/humi/$grid/.$code/$year $hour_mean # file name for the statistic output
998 # error value
$IDWweight # weighting of the reciprocal distance for IDW
0.5 # for interpolation method 3: relative weight of IDW-interpolation in the result
$IDWmaxdist # max. distance of stations to the actual interpolation cell
$Anisotlope # slope of the mean axis of the anisotropy-ellipsis
$Anisotropie # ratio of the short to the long axis of the anisotropy-ellipsis
0.01 # lower limit of interpolation results
0.01 # replace value for results below the lower limit
1.0 # upper limit for interpolation results
1.0 # replace value for results with larger values than the upper limit
$SzenUse # 1=use scenarios, 2=multply scenarios, 3=percentual change
3 # 1=add scenarios, 2=multply scenarios, 3=percentual change
1 # number of scenario cells
699000 235000 0.0 0.0 0.0 0.0 0.0 0.0 0.0 0.0 0.0 0.0 0.0

[vapour_pressure]
2 # method: 1=idw 2=regress 3=idw+regress 4=thiessen
$inpath/dampf/$year/.inp # file name with station data (if method = 1, 3 or 4, else ignored)
$inpath/dampf/$year/.reg # file name with regression data (if method = 2 or 3)
$outpath/$vaporgrid # name of the output grid
5/$Writegrid # 0, if no grid-output is needed, else one of the codes described above
0.1 # correction faktor for results
$outpath/dampf/$grid/.$code/$year $hour_mean # file name for the statistic output
998 # error value
$IDWweight # weighting of the reciprocal distance for IDW
0.5 # for interpolation method 3: relative weight of IDW-interpolation in the result
$IDWmaxdist # max. distance of stations to the actual interpolation cell
$Anisotlope # slope of the mean axis of the anisotropy-ellipsis
$Anisotropie # ratio of the short to the long axis of the anisotropy-ellipsis
0 # lower limit of interpolation results
0 # replace value for results below the lower limit
90 # upper limit for interpolation results
90 # replace value for results with larger values than the upper limit
$SzenUse # 1=use scenario data for correction, 0=dont use scenarios
1 # 1=add scenarios, 2=multply scenarios, 3=percentual change
4 # number of scenario cells
699000 235000 0.994 1.187 1.021 1.035 1.201 1.021 .635 .566 .538 1.021 .800 1.007

#irrigation_interpol]
1 # method: 1=idw 2=regress 3=idw+regress 4=thiessen
$inpath/irrig/$year/.dat # file name with station data (if method = 1, 3 or 4, else ignored)
$inpath/irrig/$year/.out # file name with regression data (if method = 2 or 3)
$outpath/irrig_grid # name of the output grid

```

```

1/Writegrid # 0, if no grid-output is needed, else one of the codes described above
1.0 # correction factor for results
$OutputPath/irri/$Grid//Year $hour $mean # file name for the statistic output
998 # error value
2 # weighting of the reciprocal distance for IDW
0.75 # for interpolation method 3: relative weight of IDW-interpolation in the result
5000 # max. distance of stations to the actual interpolation cell
0 # slope of the mean axis of the anisotropy-ellipse
1 # ratio of the short to the long axis of the anisotropy-ellipse
0.1 # lower limit of interpolation results
0 # replace value for results below the lower limit
900 # upper limit for interpolation results
900 # replace value for results with larger values than the upper limit
0 $zenUse # 1=use scenario data for correction, 0=dont use scenarios
2 # 3 # 1=add scenarios, 2=multiply scenarios, 3=percentual change
1 # 4 # number of scenario cells
699000 235000 0.5 0.5 0.5 0.5 0.5 0.5 0.5 0.5 0.5 # coordinates of the cells, then one value
for each month of a year
# ----- parameter for model components -----
# for precipitation correction the paragraphs "precipitation" "temperature" and
# "wind_speed" are searched in the memory. If they are not there (no definition in the control file
# for precipitation, wind or temperature), the prec. corr. will not be calculated

[precipitation_correction]
1 # 0=ignore this module, 1 = run the module
0.5 # Snow-rain-temperature
1.01 # liquid: b in: y = p(ax + b)
0.01 # liquid: a in: y = p(ax + b) = 1% more per m/s + 0.5% constant
1.10 # Snow: b in: y = p(ax + b)
0.13 # Snow: a in: y = p(ax + b) = 15% more per m/s + 45% constant

# correction factors for direct radiation are calculated
# if the cell is in the shadow of another cell, or if a cell is not in the sun (slope angle)
# then the factor is 0.
# control_parameter: 1 = radiation correction WITH shadow WITHOUT temperature correction
# 2 = radiation correction WITH shadow WITH temperature correction
# 3 = radiation correction WITHOUT shadow WITHOUT temperature correction,
# 4 = radiation correction WITHOUT shadow WITH Temperature

[radiation_correction]
1 # 0=ignore this module, 1 = run the module
$Time # duration of a time step in minutes
2 # control parameter for radiation correction (see above)
$OutputPath/$TcorrGrid # name of the grids with the corrected temperatures
5/$Writegrid # Writegrid for corrected temperatures
5 # factor x for temperature correction x * (-1.6 ..... +1.6)
$OutputPath/$ExpoCorrGrid # name of the grids with the correction factors for the direct radiation
$Writegrid # Writegrid

```

```

$OutputPath/$Shapegrid # name of the grids for codes 1 for theor. shadow, 0 for theor. no shadow
$Writegrid # Writegrid
1 # interval counter, after reaching this value, a new correction is calculated
1 # Spitting of the interval, usefull for time step=24 hours

[evapotranspiration]
1 # 0=ignore this module, 1 = run the module
$Time # duration of a time step in minutes
1 # Method: 1=Penman-Monteith, 2=Hamon (only daily), 3=Wendling (only daily) 4=Haude
(daily timesteps only)
0.5 0.6 0.8 1.0 1.1 1.1 1.2 1.1 1.0 0.9 0.7 0.5 # PEC correction factor for HAMON-evapotranspiration
0.20 0.20 0.21 0.29 0.29 0.28 0.26 0.25 0.22 0.20 0.20 # fh (only for method 4: Haude) monthly values
0.5 # fh -> factor for Wendling-evapotranspiration (only for Method = 3)
$OutputPath/$ETPGrid # result grid for pot. evapotranspiration in mm/dt
1/$Writegrid # 0, if no grid-output is needed, else one of the codes described above
$OutputPath/etp_/$Grid//Year $hour $mean # statistic for Teilgebiete of pot. evapo-Transpiration
$OutputPath/$ETFRGrid # result grid for real evapotranspiration in mm/dt
1/$Writegrid # 0, if no grid-output is needed, else one of the codes described above
$OutputPath/etr_/$Grid//Year $hour $mean # statistic for subcatchments of real evapotranspiration
$OutputPath/rge/$Grid//Year $hour $mean # statistic for subcatchments of the corrected radiation
+0.23 +1.77 -2.28 +1.28 # coefficients c for Polynom of order 3 RG = c1 + c2*SSD + c3*SSD^2 +
c4*SSD^3
+0.072 -0.808 +2.112 -0.239 # coefficients x for Polynom of order 3 SSD = x1 + x2*RG + x3*RG^2 +
x4*RG^3
0.88 0.05 # Extinktion coefficient for RG-modelin (summer phi = phi-dphi, winter phi=phi+dphi)
1654.0 # recession constant (e-lunction for recession of the daily temperature amplitude with altitude [m]
3.3 4.4 6.1 7.9 9.4 10.0 9.9 9.0 7.8 6.0 4.2 3.2 # monthly values of the max. daily T-amplitudes
3.4 0.62 0.1 # part of the temperature amplitude (dt), that is added to the mean day-temperature
# followed by the range of changing within a year ddt) to get the mean temperature of light day
# in the night: mean night temperature is mean day temperature minus (1-dt)*(temp. amplitude)

[snow_model]
1 # 0=ignore this module, 1 = run the module
$Time # duration of a time step in minutes
1 # method 1=T-index, 2=t-u-index, 3=Anderson comb., 4=extended com.
1.0 # transient zone for rain-snow (TOR +- this range)
0.6 # TOR temperature limit for rain (Grad Celsius)
0.0 # T0 temperature limit snow melt
0.05 # CWH storage capacity of the snow for water (relative part)
1.0 # CRFR coefficient for refreezing
2.2 # C0 degree-day-factor mm/d/C
1.0 # C1 degree-day-factor without wind consideration mm/(d*C)
0.8 # C2 degree-day-factor considering wind mm/(d*C*m/s)
0.07 # z0 roughness length cm for energy balance methods (not used)
1.5 # RMFMIN minimum radiation melt factor mm/d/C comb. method
2.5 # RMFMAX maximum radiation melt factor mm/d/C comb. method
0.85 # ALBSnow albedo for snow
#0.07 # SCA surface parameter for snow cover (not used)
$OutputPath/$snowcover_outflow # discharge from snow, input (precipitation) for following modules

```



```

$Writgrid # 0, if no grid-output is needed, else one of the codes described above
$oupath/qsch/$grid//.$code/$year $hour_mean # melt flow (or rain, if there is no snow cover) in mm/dt
$oupath/$SSNOgrid # name of the grids with the snow storage solid in mm
$Writgrid # 0, if no grid-output is needed, else one of the codes described above
$oupath/$SLIQgrid # name of the grids with the snow storage liquid in mm
$Writgrid # 0, if no grid-output is needed, else one of the codes described above
$oupath/$sso/$grid//.$code/$year $hour_mean # total snow storage, in mm, (liquid and solid fraction)
$readgrids # 1=read snow storage solid, liquid grids from disk, 0=generate new grids

[ice_firm]
2 # method for glacier melt: 1=classical t-index, 2=t-index with correction by radiation
5 # t-index factor for ice
4 # t-index factor for firm
3 # t-index factor for snow
1.8 # melt factor
0.0005 # radiation coefficient for ice (for method 2)
0.0004 # radiation coefficient for snow (for method 2)
40 # eis-konstante for ice
350 # eis-konstante for firm
120 # eis-konstante for snow
0.0006 # initial reservoir content for ice discharge (single linear storage approach)
0.0006 # initial reservoir content for firm discharge (single linear storage approach)
0.0006 # initial reservoir content for snow discharge (single linear storage approach)
$oupath/$firm_melt # melt from firm
$Writgrid # 0, if no grid-output is needed, else one of the codes described above
$oupath/qfir/$grid//.$code/$year $hour_mean # melt from firm as statistic file
$oupath/$ice_melt # melt from ice
$Writgrid # 0, if no grid-output is needed, else one of the codes described above
$oupath/qice/$grid//.$code/$year $hour_mean # melt from ice as statistic file
$oupath/qgic/$grid//.$code/$year $hour_mean # discharge from snow, ice and firm as statistic file

[interception_model]
1 # 0=ignore this module, 1 = run the module
$time # duration of a time step in minutes
$oupath/$troughfall # result grid : = outflow from the interception storage
$Writgrid # 0, if no grid-output is needed, else one of the codes described above
$oupath/qj_/$grid//.$code/$year $hour_mean # statistic file interception storage outflow
$oupath/$Eigrd # Interception evaporation, grid
1/$Writgrid # 0, if no grid-output is needed, else one of the codes described above
$oupath/qe/$grid//.$code/$year $hour_mean # zonal statistic
$oupath/$Sigrd # storage content of the interception storage
$Writgrid # 0, if no grid-output is needed, else one of the codes described above
0.35 # layer thickness of the waters on the leaves (multiplied with LAI -> storage capacity)
$readgrids # 1=read grids from disk, else generate internal

[infiltration_model]
0 # 0=ignore this module, 1 = run the module
$time # duration of a time step in minutes
$oupath/$INFEXgrid # grid with infiltration excess in mm (surface runoff)

```

```

1/$Writgrid # Writgrid for surface discharge (fraction 1)
$oupath/infx/$grid//.$code/$year $hour_mean # statistic file for the infiltration excess
$oupath/$SATgrid # grid with code 1=saturation at interval start, 0=no saturation.
$Writgrid # Writgrid for saturation code grids
0.1 # fraction of reinfiltrating water (of the infiltration excess)

[unsatzon_model]
1 # 0=ignore this module, 1 = run the module
$time # duration of a time step in minutes
2 # method, 1=simple method, 2 = FDM-Method (strongly recommended)
1 # interaction with surface water: 0: no interaction, 1: exfiltration possible 2: in- and exfiltration possible
0 # controlling surface storage in ponds: 0 = no ponds, 1 = using ponds for surface storage
0 # controlling artificial drainage: 0 = no artificial drainage 1 = using drainage
0 # controlling clay layer: 0 = no clay layer, 1 = assuming a clay layer in a depth
5e-8 # permeability of the clay layer (is used for the clay layer only)
$oupath/qdra/$grid//.$code/$year $hour_mean # results drainage discharge in mm per zone
$oupath/gwst/$grid//.$code/$year $hour_mean # results groundwater depth
$oupath/gwn_/$grid//.$code/$year $hour_mean # results mean groundwater recharge per zone
$oupath/sb05/$grid//.$code/$year $hour_mean # results rel. soil moisture 0.05 m per zone
$oupath/sb1_/$grid//.$code/$year $hour_mean # results rel. soil moisture 0.1 m per zone
$oupath/infx/$grid//.$code/$year $hour_mean # results statistic of the infiltration excess
$oupath/pond/$grid//.$code/$year $hour_mean # results statistic of the ponding water storage content
$oupath/qdir/$grid//.$code/$year $hour_mean # results statistic of the direct discharge
$oupath/qdir/$grid//.$code/$year $hour_mean # results statistic of the interflow
$oupath/qbas/$grid//.$code/$year $hour_mean # results statistic of the baseflow
$oupath/qges/$grid//.$code/$year $hour_mean # results statistic of the total discharge
$oupath/gwin/$grid//.$code/$year $hour_mean # statistic of the infiltration from surface water into
groundwater (from rivers and lakes)
$oupath/gwex/$grid//.$code/$year $hour_mean # statistic of the exfiltration from groundwater into
surface water (into rivers and lakes)
$oupath/$Thetastack # stack, actual soil water content for all soil levels
$Writestack # Writecode for this stack
$oupath/$hydraulic_heads_stack # stack, containing hydraulic heads
$Writestack # Writecode for this stack
$oupath/$geodeic_altitude_stack # stack, containing geodaeitic altitudes of the soil levels
$Writestack # Writecode for this stack
$oupath/$flowstack # stack, containing the outflows from the soil levels
$Writestack # Writecode for this stack
$oupath/$GWdepthgrid # grid with groundwaterdepth
$Writgrid # writgrid for this grid
$oupath/$GWthetagrid # grid with theta in GWLEVEL
$Writgrid # writgrid for this grid
1/$Writgrid # grid with groundwater recharge
$oupath/$GWLEVELgrid # grid with level index of groundwater surface (Index der Schicht)
$Writgrid # writgrid for this grid
$oupath/$QDRAINgrid # grid with the drainage flows
$Writgrid # writgrid for this grid
$oupath/$SATgrid # grid with code 1=saturation at interval start, 0 no sat.

```

```

$Writegrid # writegrid for this grid
$outpath/$INFEXgrid # grid with infiltration excess in mm (surface discharge)
1/$Writegrid # writegrid for this grid
$outpath/$QDgrid # grid with direct discharge
1/$Writegrid # writegrid for this grid
$outpath/$QIgrid # grid with Interflow
1/$Writegrid # writegrid for this grid
$outpath/$QBgrid # grid with baseflow
1/$Writegrid # write code for baseflow
$outpath/$GWINgrid # grid with infiltration from rivers into the soil (groundwater)
1/$Writegrid # writegrid for re-infiltration
$outpath/$GWEgrid # grid with exfiltration (baseflow) from groundwater
1/$Writegrid # writegrid for exfiltration
$outpath/$act_pond_grid # grid with content of ponding storage
$Writegrid #
90 30 # coordinates of control plot, all theta and qu-values are written to files
$outpath/$qbotl/$grid//.$code/$year # name of a file containing the flows between the layers of the control
point:
$outpath/$theil/$grid//.$code/$year # name of a file containing the soil moisture as theta values of the
layers of the control point
$outpath/$hhyd/$grid//.$code/$year # name of a file containing the hydraulic head of the layers of the
control point
1 2 # codes of the subbasins (in the subbasin grid)
8.0 8.0 # recession parameters QD
8.0 8.0 # recession parameters QI
1.0 1.0 # flow density (for Interflow, channels per km)
0.8 0.8 # recession parameters k for Base discharge (in QB = Q0*exp(-k/z))
0.1 0.1 # correction of transmissivities Q0 for Baseflow in QB = Q0 * exp(-k/z)
0.2 0.2 # fraction of snow melt, which is direct flow (no infiltration)
$readgrids # 1=read grids from disk, else generate internal
[irrigation]
0 # 0=ignore this module, 1 = run the module
$time # duration of a time step in minutes
$outpath/$irgw/$grid//.$code/$year $hour_mean # statistic of the irrigation water from groundwater
$outpath/$irsw/$grid//.$code/$year $hour_mean # statistic of the irrigation water from surface water
[groundwater_flow]
0 # 0=ignore the module, 1 = run the module
$time # duration of a time step in minutes
1 # solving method: 1=Gauss-Seidel-iteration, 2=PCG (not yet implemented)
1000 # if iterative solving method (1): max.number of iterations
0.00005 # if iterative solving method (1): max. changes between two iterations
1.0 # Alpha for estimation of central differences 0.5 = Crank-Nicholson, 0 = fully explicite, 1 = fully implicite
-1.4 # factor for relaxing the iteration if using iterative method
$readgrids # 1=read grids for heads, 0= initialize with gw-level from unsaturated zone
1 # number of layers
$outpath/$head1grid # (new) grid for hydraulic heads for layer 1
$Writegrid # writecode for hydraulic heads for layer 1

```

```

$outpath/$flowx1grid # (new) grid for fluxes in x direction for layer 1
$Writegrid # writecode for flux-x-grid in layer 1
$outpath/$flowy1grid # (new) grid for fluxes in y direction for layer 1
$Writegrid # writecode for flux-y-grid in layer 1
$outpath/$head2grid # (new) grid for hydraulic heads for layer 2
$Writegrid # writecode for hydraulic heads for layer 2
$outpath/$flowx2grid # (new) grid for fluxes in x direction for layer 2
$Writegrid # writecode for flux-x-grid in layer 2
$outpath/$flowy2grid # (new) grid for fluxes in y direction for layer 2
$Writegrid # writecode for flux-y-grid in layer 2
$outpath/$head3grid # (new) grid for hydraulic heads for layer 3
$Writegrid # writecode for hydraulic heads for layer 3
$outpath/$flowx3grid # (new) grid for fluxes in x direction for layer 3
$Writegrid # writecode for flux-x-grid in layer 3
$outpath/$flowy3grid # (new) grid for fluxes in y direction for layer 3
$Writegrid # writecode for flux-y-grid in layer 3

```

# this paragraph is not needed for WaSiM-uzr but for the WaSiM-version with the variable saturated area approach (after Topmodel)

```

[soil_model]
0 # 0=ignore this module, 1 = run the module
$time # duration of a time step in minutes
1 # method, 1 = without slow baseflow, 2 = with slow baseflow (not recommended)
$outpath/$sat_def_grid # (new) saturation deficite-grid (in mm)
$Writegrid # writegrid for this grid
$outpath/$SUZgrid # (new) storage grid for unsat. zone
$Writegrid # writegrid for this grid
$outpath/$SIFgrid # (new) storage grid for interflow storage
$Writegrid # writegrid for this grid
$outpath/$SBIgrid # (new) grid for soil moisture in the inactive soil storage
$Writegrid # Writegrid for inactive soil moisture
$outpath/$Sclia_grid # (new) grid for plant available field capacity in the inactive soil storage
$Writegrid # writegrid for this grid
$outpath/$SSPgrid # (new) grid for the relative fraction of the soil storages, which is in contact with
ground water
$Writegrid # writegrid for this grid
$outpath/$QDgrid # (new) grid for surface runoff
1/$Writegrid # writegrid for this grid
$outpath/$QIgrid # (new) grid for Interflow
1/$Writegrid # writegrid for this grid
$outpath/$Peakgrid # (new) grid for Peakflow (maximum peakflow for the entire model time)
$outpath/$qir/$grid//.$code/$year $hour_mean # statistic of the surfeca discharge
$outpath/$qill/$grid//.$code/$year $hour_mean # statistic of the interflows
$outpath/$qbas/$grid//.$code/$year $hour_mean # statistic of the base flow
$outpath/$qbar/$grid//.$code/$year $hour_mean # statistic of the slow base flow
$outpath/$ages/$grid//.$code/$year $hour_mean # statistic of the total discharge
$outpath/$sb_/$grid//.$code/$year $hour_mean # soil storage in mm per zone
$outpath/$uz_/$grid//.$code/$year $hour_mean # drainage storage in mm per zone
$outpath/$sfil/$grid//.$code/$year $hour_mean # interflow storage in mm per zone

```

```

$oupath/$id_/$grid//$.code/$year $hour_mean # saturation deficit per zone in mm
1 # Codes der Teilgebiete im Zonengrid
0.025 # Rezessionsparameter m fuer Saetigungsflaechenmodell in Metern
1000 # Korrekturfaktor fuer Transmissivitaeten
1000 # Korrekturfaktor fuer K-Wert (vertikale Versickerung), Modell erwartet k in m/s
6.0 # Speicherrueckgangskonstante Direktabfluss ELS in h
0.0 # Speicherrueckgangskonstante Direktabfluss ELS in h
80.0 # Speicherrueckgangskonstante Interflow ELS in h
3600.0 # Rueckgangskonstante verzogelter Basisabfluss in h
0.03 # maximale Tiefenversickerungsrate bei Saetigung in mm/h
0.01 # Anfangswert QBB
0.0 # Anfangsuellung des SUZ-Speichers in n*nFK
0.0 # Anfangssaetigungsdefizit in n*nFK, beeinflusst den ersten Basisabfluss
10 # Anspringpunkt fuer Makroporenabfluss, alles darueber geht direkt in den Drainspeicher!
0 # Reduktionsfaktor fuer Aufuellung von Verdunstungsverlusten aus Grundwasser und Interflowspeicher
0.4 # Anteil effektiven Schneeschmelze, der bei geschlossener Schneedecke direkt abfließt und nicht in den Boden gelangen kann
$readgrds # 1=read grids from disk, else generate internal

[routing_model]
1 # 0=ignore this module, 1 = run the module, 2=run the module with observed inflows into routing channels
$lrme # duration of a time step in minutes
5 1200 90 24 # minimum/maximum specific discharge (l/s/km^2), number of log. fractions of the range, splitting of the timeintervall (24= 1 hour-intervalls are splitted into 24 Intervalls each of 2.5 min. duration)
$oupath/$gk/$grid//$.code/$year $routing_code # name of the statistic file with routed discharges
$inpath/$spende./$year # name of the file with observed discharges (l/s/km^2)
1 # number of following collumn descriptor
1 1 # if the first code would be a 7, then it would mean, that the modeled discharge of subbasin 1 (or lowest subbasin code) would communicate with the data column 7 in the specific discharge data file (date-columns are not counted!)
40 # timeoffset (for r-square calculation. intervals up to this parameter are not evaluated in r-square calculation,))
TG 1 (AE=39.68, AErel=1.0)
from OL 2 (kt=0.1, kv=0.4, Bh= 5.0, Bv= 20.0, Th= 1.5, Mh=25.0, Mv=10.0, I=0.0277, L=3107.1, AE=18.73)

[abstraction_rule_reservoir_1]
0
0 20.0
1e8 20.0

9 # number of points, reading now as x-y-values
1e4 1.0
1e5 1.0
1.0001e5 10.0
1e6 10.0
1.0001e6 50.0

```

```

1e7 50.0
1.0001e7 100.0
1e8 100.0
1.0001e8 500.0

[landuse_table]
13 # number of following land use codes, per row one use
#Co name of the albe- surface resistances rsc as monthly values julian day for LAI (eff.
veget. height) Veg.covering root depth [m] Param. root. theta-value for beginning
#de Landuse type do 1 2 3 4 5 6 7 8 9 10 11 12 the param.-sets 1 2 3 4 z01 2 3
4 1 2 3 4 1 2 3 4 distribution. etp-reduction
#-----
1 water 0.05 20 20 20 20 20 20 20 20 20 20 20 110 150 250 280 1 1 1 1 .01
.01 .1 .1 .1 0.01 0.01 0.01 0.01 -0.5 1.9
2 settl_dense 0.23 100 100 100 100 100 100 100 100 100 100 100 110 150 250 280 1 1 1 1
10 10 10 10 .5 .5 .5 .5 0.1 0.1 0.1 -0.5 1.9
3 settl_thin 0.2 100 100 100 100 100 100 100 100 100 100 100 110 150 250 280 1 1 1 1
10 10 10 10 .5 .5 .5 .5 0.15 0.15 0.15 -0.5 1.9
4 forest_thin 0.15 100 100 95 75 65 65 65 65 65 65 65 110 150 250 280 2 8 8
2 .3 10 10 .3 7 8 8 7 1.0 1.0 1.0 -0.5 1.9
5 forest_dense 0.1 90 90 85 70 52 57 52 57 60 80 90 110 150 250 280 8 12 12 8 10
10 10 10 .9 1.0 1.0 0.9 0.8 0.8 0.8 -0.5 1.9
6 agriculture 0.25 80 80 75 75 65 65 65 65 65 65 65 90 110 150 250 255 1 5 3 1 .05
.4 .05 .3 .8 .7 .3 0.1 0.4 0.3 0.1 -0.5 1.9
7 grass_low 0.25 90 70 75 65 55 55 55 60 70 90 90 110 150 250 280 1.5 3 3 1.5 .15
4 .3 .15 .95 .95 .95 0.3 0.4 0.4 0.3 -0.5 1.9
8 grass_high 0.25 90 90 75 65 55 55 55 55 60 70 90 110 150 250 280 2 4 2 4 .8
8 .4 .95 .95 .95 0.3 0.5 0.5 0.3 -0.5 1.9
9 bushes 0.20 80 80 70 70 50 50 55 55 55 70 80 110 150 250 280 3 5 3 1.5 2.5
2.5 1.5 .9 .95 .95 0.6 0.6 0.6 -0.5 1.9
10 fruit_garden 0.25 100 100 90 70 60 60 60 60 60 60 60 110 150 250 280 1 5 5 1 4
3 3 4 .75 .75 .75 0.8 0.8 0.8 -0.5 1.9
11 rock 0.12 250 250 250 250 250 250 250 250 250 250 250 110 150 250 280 1 1 1 1
.05 .05 .05 .8 .8 .8 0.01 0.01 0.01 -0.5 1.9
12 ice 0.37 150 150 150 150 150 150 150 150 150 150 150 110 150 250 280 1 1 1 1
.05 .05 .05 .8 .8 .8 0.1 0.1 0.1 -0.5 1.9
13 firm 0.65 100 100 100 100 100 100 100 100 100 100 100 110 150 250 280 1 1 1 1
.05 .05 .05 .8 .8 .8 0.1 0.1 0.1 -0.5 1.9

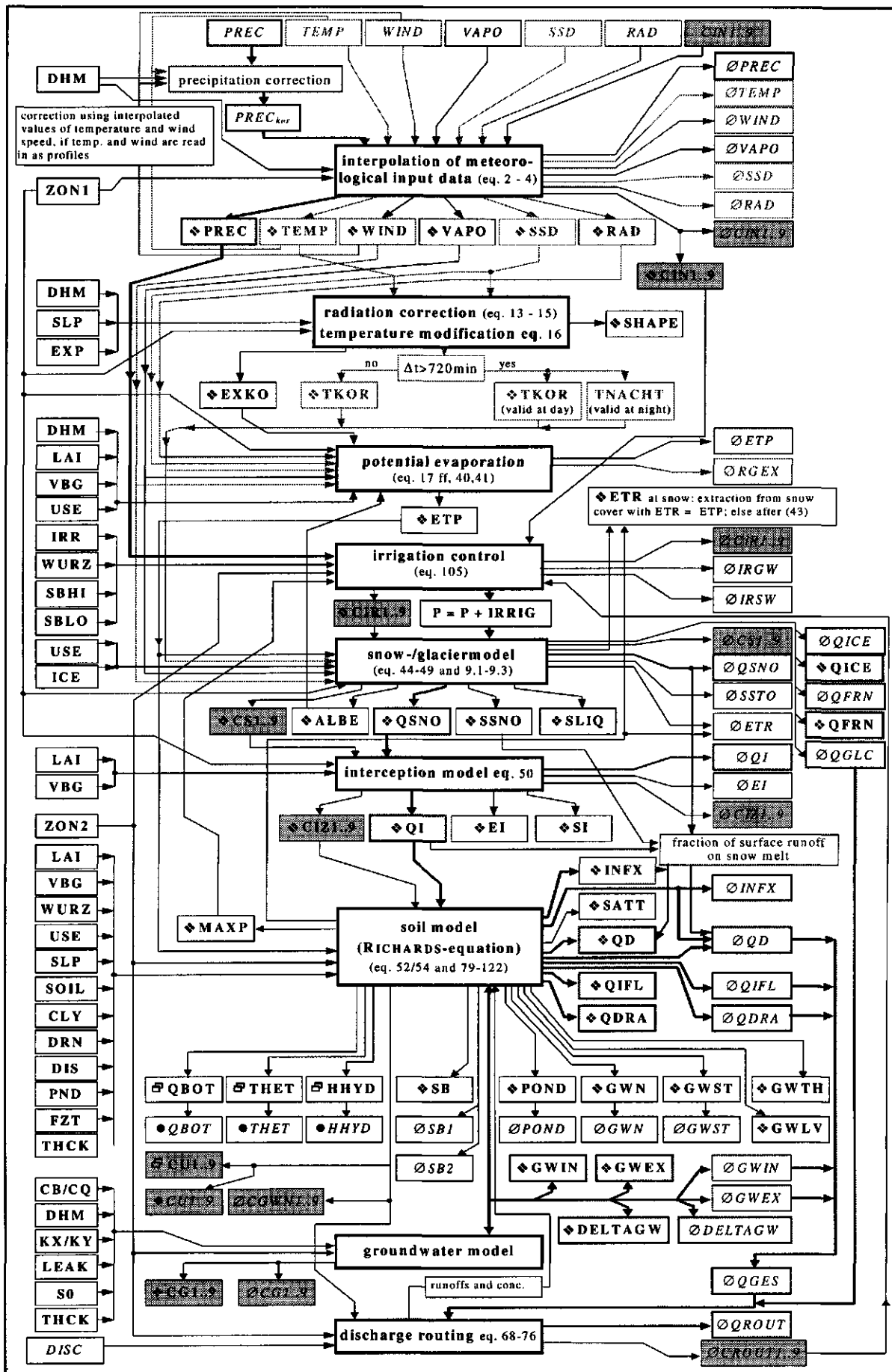
[soil_table]
16 # number of following entries
#Code name FC(Vol.%) mSB(Vol.%) ksat(m/s) suction. parameter Theta_sat Theta_res alpha n layer thick
maxratio k-recession
# [mm] 1=par 2=tab 1/1 1/1 1/m [m] ko_reli/ku_rel per m/ku/ko
#-----
1 Sand_(S) 6.21 38.5 8.25E-5 385 1 .43 .045 14.5 2.68 30 .3333 25 0.9
6 loamy_sand_(LS) 10.91 37.3 4.05E-5 373 1 .43 .057 12.4 2.28 30 .3333 25 0.9
5 sandy_loam_(SL) 12.28 34.5 1.23E-5 345 1 .41 .065 7.50 1.89 30 .3333 25 0.9
4 silty_loam_(SIL) 22.58 38.3 1.25E-6 383 1 .45 .067 2.00 1.41 30 .3333 25 0.9

```

3 loam_(L)	12.9	35.2	2.89E-6	352	1	.43	.078	3.60	1.56	30	.3333	25	0.9
2 sandy_clay_(SC)	19.49	28.0	3.33E-7	280	1	.38	.100	2.70	1.23	30	.3333	25	0.9
7 silty_clay_(SIC)	27.65	29.0	5.56E-8	290	1	.36	.070	0.50	1.09	30	.3333	25	0.9
8 clay_(C)	29.12	31.2	5.56E-7	312	1	.38	.068	0.80	1.09	30	.3333	25	0.9
9 moor_(M)	47.31	75.0	8.25E-5	750	1	.80	.200	4.00	1.23	30	.3333	25	0.9
10 settlements_rock_(R)	14.00	15.0	1.00E-9	50	1	.20	.040	6.00	1.80	30	.3333	25	0.9
11 clay_loam_(CL)	21.24	31.5	7.22E-7	315	1	.41	.095	1.90	1.31	30	.3333	25	0.9
12 silt_(SI)	26.17	42.6	6.94E-7	426	1	.46	.034	1.60	1.37	30	.3333	25	0.9
13 silty_clay_loam_(SICL)	28.16	34.1	1.94E-7	341	1	.43	.089	1.00	1.23	30	.3333	25	0.9
14 sandy_clay_loam_(SCL)	13.35	29.0	3.64E-6	290	1	.39	.010	5.90	1.48	30	.3333	25	0.9
15 rock	29.12	31.2	5.56E-7	312	1	.38	.068	0.80	1.09	30	.3333	25	0.9
30 ice	10.91	37.3	4.05E-5	373	1	.43	.057	12.4	2.28	30	.3333	25	0.9

## Appendix 3

### Data flow of WaSiM-ETH



Data flow chart for WaSiM-ETH version 2 (RICHARDS-equation), symbols see table

Description of the symbols in figure

Sym.	data name	description
	grids (*)	bold font in figures 2 and 6, output grids are marked with a *; otherwise, grids have no asterisk
$c, \gamma$	<b>ATB</b> <sup>1</sup>	topographic index $\ln(a/\tan\beta)$
-	<b>CLY</b> <sup>2</sup>	depth of a clay layer in m below surface, wenn no clay layer: -9999 or 0
-	<b>CH</b> <n>	constant head boundary (groundwater model) one grid for each aquifer [m]
-	<b>CQ</b> <n>	constant boundary flux (groundwater model), in m/s perpendicular to the cells surface (recharge or extraction by pumping in m/s); one grid for each aquifer
$T_H$	<b>DEP</b> <sup>2</sup>	river depths [m] (for exfiltration from groundwater into rivers), only those grid cells which have a river on it have valid values, the other: -9999 or 0
-	<b>DHM</b>	digital elevation model
-	<b>DIS</b> <sup>2</sup>	horizontal spacing between drainage tiles in m (no drainage: -9999 or 0)
-	<b>DRN</b> <sup>2</sup>	depth of the drainage tiles in m below surface (no drainage: -9999 or 0)
$\hat{\Omega}$	<b>EXP</b>	aspect of the grid cell: 0..360°, north=0, east=90, south=180, west=270
-	<b>FZT</b>	flow travel times for surface runoff to the subbasin outlet in seconds
-	<b>ICE</b> <sup>2</sup>	glacier grid: code 1 for ice, 2 for firm, alle other cells: nodata (-9999)
-	<b>IRR</b> <sup>2</sup>	codes for irrigation control (like land use or soil type codes), no irrigation: -9999 or 0
$K_S$	<b>K</b> <sup>1</sup>	hydraulic conductivities (generated internally or externally) in m/s
-	<b>KOL</b> <sup>2</sup>	colmation resistance of the river [ $s^{-1}$ ](for exfiltration from groundwater into rivers and vice versa), only those grid cells which have a river on it have valid values, the other: -9999 or 0
$K_X$	<b>KX</b> <n> <sup>2</sup>	horizontal saturated conductivity in m/s for each aquifer in x-direction in m/s
$K_Y$	<b>KY</b> <n> <sup>2</sup>	horizontal saturated conductivity in m/s for each aquifer in y-direction in m/s
-	<b>LAI</b>	leaf area index, interpolated from land use table entries, the actual data and the geodetic altitude (internally generated)
-	<b>LEAK</b> <n> <sup>2</sup>	leakage-faktors for leakage between aquifera in 1/s
-	<b>LNK</b> <sup>2</sup>	routing channel links of the river network as used in the model
$n_a$	<b>NA</b> <sup>1</sup>	fillable porosity (internally generated) in 1/1
$nFK$	<b>NFK</b> <sup>1</sup>	available field capacity (generated internally or externally) in mm
-	<b>PND</b> <sup>2</sup>	maximum capacity of the pond storage in mm
$S_0$	<b>S0</b> <n> <sup>2</sup>	specific storage coefficient in $m^3/m^3$ for each aquifer 1..n
-	<b>SBHI</b> <sup>2</sup>	soil moisture threshold for start irrigation (internally generated) in 1/1
-	<b>SBLO</b> <sup>2</sup>	soil moisture threshold for stop irrigation (internally generated) in 1/1
$\beta_i$	<b>SLP</b>	slope angle in grad (0..90)
-	<b>SOIL</b> <sup>2</sup>	soil type, corresponding to the soil table (control file)
-	<b>THCK</b> <n> <sup>2</sup>	aquifer thickness 1..n in m
-	<b>USE</b>	land use codes, corresponding to the land use table in the control file
-	<b>VBG</b>	vegetation coverage degree, interpolated from land use table entries, the actual data and the geodetic altitude (internally generated)
$B_h$	<b>WIT</b> <sup>2</sup>	river widths [m] (for exfiltration from groundwater into rivers), only those grid cells which have a river on it have valid values, the other: -9999 or 0
$z_w$	<b>WURZ</b>	root depth, interpolated from land use table entries, the actual data and the geodetic altitude (internally generated)
-	<b>ZON1</b>	zone grid for interpolation, radiation correction, evaporation, interception, and Snowmodel
-	<b>ZON2</b>	zone grid for soil model/infiltration, irrigation, groundwater, discharge routing
$\alpha$	❖ <b>ALBE</b>	albedo
-	❖ <b>CG1..9</b> <sup>2</sup>	tracer concentrations in the groundwater
-	❖ <b>CIN1..9</b> <sup>2</sup>	interpolated input tracer concentrations (for up to 9 tracers at a time)
-	❖ <b>CIR1..9</b> <sup>2</sup>	tracer concentrations in the irrigation water (for up to 9 tracers at a time)
-	❖ <b>CIZ1..9</b> <sup>2</sup>	tracer concentrations in the precipitation on the soil (for up to 9 tracers at a time)

<i>Sym.</i>	data name	description
-	❖CS1..9 <sup>2</sup>	concentrations in the snow melt
<i>EI</i>	❖EI	interception evaporation in mm/time step
<i>ETP</i>	❖ETP	potential evapo-transpiration in mm/time step
<i>ETR</i>	❖ETR	real evapo-transpiration in mm/time step
<i>f<sub>d</sub></i>	❖EXKO	result grid radiation correction factors
-	❖GWL <sup>2</sup>	index of the discretization layer the groundwater is located within
-	❖GWN <sup>2</sup>	groundwater recharge in mm/time step
-	❖GWEX <sup>2</sup>	exfiltration from groundwater into surface water in mm/ time step
-	❖GWIN <sup>2</sup>	infiltration from routing channels into groundwater or into the unsaturated zone in mm/time step
-	❖GWST <sup>2</sup>	groundwater table in m below surface (counts negative)
-	❖GWTH <sup>2</sup>	mean water content of the discretization layer the groundwater is located within
<i>Q<sub>D,I</sub></i>	❖INFX	infiltration excess (after GREEN-AMPT) in mm/time step
-	❖MAXP <sup>2</sup>	maximum pumpage amount from a grid cell for irrigation in mm/time step
-	❖NFKia <sup>1</sup>	available field capacity in the inactiv fraction of the soil (not rooted)
-	❖PEAK <sup>1</sup>	surface peak flow in mm/time step
-	❖POND <sup>2</sup>	content of the pond-storage in mm
<i>P</i>	❖PREC	interpolated precipitation in mm/time step
<i>Q<sub>B</sub></i>	❖QBAS	base flow in mm/time step
<i>Q<sub>D</sub></i>	❖QD	surface runoff in mm/time step
<i>q<sub>drain</sub></i>	❖QDRA <sup>2</sup>	drainage discharge in mm/time step
<i>Q<sub>FRN</sub></i>	❖QFRN	melt of firn (glacier model, only if a ICE grid is used)
-	❖QI	precipitation onto the soil from the interception storage in mm/time step
<i>Q<sub>ICE</sub></i>	❖QICE	melt of ice (glacier model, only if a ICE grid is used)
<i>Q<sub>I</sub></i>	❖QIFL	interflow in mm/time step
<i>M</i>	❖QSNO	snow melt or runoff from the snow cover (or precipitation, if snow is melted away) in mm/time step
<i>R<sub>G</sub></i>	❖RAD	interpolated global radiation in Wh/m <sup>2</sup>
-	❖SATT	saturated areas after applying GREEN-AMPT
-	❖SB	relative soil moisture in 1/1 (in version 1: root zone, in version 2: unsaturated zone)
-	❖SBia <sup>1</sup>	soil moisture in the inactive soil fraction (WP<nFK but not in the root zone)
<i>SD</i>	❖SD <sup>1</sup>	saturation deficit in mm
<i>SH</i>	❖SH <sup>1</sup>	content of the interflow storage in mm
-	❖SHAPE	result grid shadow
<i>SI</i>	❖SI	content of the interception storage in mm
-	❖SLIQ	water content of the snow storage (fraction of liquid water) in mm
<i>SSD</i>	❖SSD	interpolated relative sunshine duration in 1/1
-	❖SSNO	snow storage solid (fraction of frozen water) in mm
<i>SUZ</i>	❖SUZ <sup>1</sup>	content of the unsaturated zone (pore volume > nFK)
<i>T</i>	❖TEMP	interpolated temperature in °C
<i>T<sub>korr</sub></i>	❖TKOR	corrected temperature (after radiation correction)
<i>T<sub>Night</sub></i>	❖TNIGHT	Night temperature (at Δt > 720 min), like the uncorrected temperature
<i>e</i>	❖VAPO	interpolated vapour pressure in hPa (or relative air humidity in 1/1)
<i>u</i>	❖WIND	interpolated wind speed in m/s
<i>hydro-meteorologic input data</i>		
-	<i>CINI..9<sup>2</sup></i>	input-concentrations for modelled tracers (max 9, for each tracer one file) as station data (or, if the are constant in time, as a invariant grid)
-	<i>DISC</i>	observed discharge rates in mm/time step
<i>P</i>	<i>PREC</i>	station data of precipitation in mm/time step
<i>RG</i>	<i>RAD</i>	global radiation in Wh/m <sup>2</sup> as sum over the time step
<i>SSD</i>	<i>SSD</i>	relative sunshine duration in 1/1



Sym.	data name	description
<i>T</i>	<i>TEMP</i>	temperature in °C
<i>e</i>	<i>VAPO</i>	vapour pressure in mbar or hPa resp. relative air humidity
<i>u</i>	<i>WIND</i>	wind speed in m/s
	<i>statistic files</i> (Ø)	<i>table font</i> in figures 4 to 6 and prefixed with a Ø-symbol. These files contain spatially averaged results for separate zones and, if requested, for the entire model domain. Temporally accumulation can be done by summation or by averaging for a given number of time steps.
-	ØCG1..9 <sup>2</sup>	tracer concentrations in the groundwater
-	ØCGWNI..9 <sup>2</sup>	tracer concentrations in the groundwater recharge
-	ØCINI..9 <sup>2</sup>	input concentrations for each tracer
-	ØCIRI..9 <sup>2</sup>	tracer concentrations in irrigation water
-	ØCIZI..9 <sup>2</sup>	tracer concentrations in soil precipitation (outflow from the interception storage)
-	ØCROUT1..9 <sup>2</sup>	tracer concentrations in the river network
-	ØCSI..9 <sup>2</sup>	tracer concentrations in snow melt (or outflow from the snow cover resp. rain)
<i>EI</i>	ØEI	interception evaporation in mm/time step
<i>ETP</i>	ØETP	potential evaporation in mm/time step
<i>ETR</i>	ØETR	real evaporation (without interception evaporation, but including snow evaporation)
<i>Q<sub>exf</sub></i>	ØGWEX <sup>2</sup>	exfiltration from groundwater into surface water in mm/time step
<i>Q<sub>inf</sub></i>	ØGWIN <sup>2</sup>	infiltration from surface water into the groundwater in mm/time step
<i>GWN</i>	ØGWN <sup>2</sup>	groundwater recharge in mm/time step
<i>h<sub>GW</sub></i>	ØGWST <sup>2</sup>	groundwater table in m below surface
<i>Q<sub>D,I</sub></i>	ØINFX	infiltration excess in mm/time step
<i>IR<sub>GW</sub></i>	ØIRGW <sup>2</sup>	irrigation water taken from groundwater in mm/time step
<i>IR<sub>SW</sub></i>	ØIRSW <sup>2</sup>	irrigation water taken from surface water
<i>S<sub>P</sub></i>	ØPOND <sup>2</sup>	content in the ponds in mm
<i>P</i>	ØPREC	precipitation in mm/time step
<i>Q<sub>B</sub></i>	ØQBAS	base flow in mm/time step
<i>Q<sub>D</sub></i>	ØQD	surface runoff in mm/time step
<i>q<sub>drain</sub></i>	ØQDRA <sup>2</sup>	drainage runoff in mm/time step
<i>Q<sub>FRN</sub></i>	ØQFRN	melt of firn (if glaciers are modelled → ICE-grid)
<i>Q<sub>G</sub></i>	ØQGES	total runoff in mm/time step
<i>Q<sub>GLC</sub></i>	ØQGLC	total melt from glaciers (if glaciers are modelled → ICE-grid)
-	ØQI	outflow from interception storage = input into the soil model in mm/time step
<i>Q<sub>ICE</sub></i>	ØQICE	melt of ice (if glaciers are modelled → ICE-grid)
<i>Q<sub>I</sub></i>	ØQIFL	interflow in mm/time step
<i>Q<sub>out</sub></i>	ØQROUT	routed runoff in mm/time step
<i>M</i>	ØQSNO	outflow from the snow cover resp. rain (if snow storage is 0) in mm/time step
<i>RG</i>	ØRAD	global radiation in Wh/m <sup>2</sup>
<i>RG<sub>eff</sub></i>	ØRGEX	corrected global radiation in Wh/m <sup>2</sup>
<i>SB</i>	ØSB <sup>1</sup>	soil moisture in 1/1
<i>SB<sub>1</sub></i>	ØSB1 <sup>2</sup>	soil moisture in the root zone in 1/1
<i>SB<sub>2</sub></i>	ØSB2 <sup>2</sup>	soil moisture in the entire unsaturated zone in 1/1
<i>SD</i>	ØSD <sup>1</sup>	saturation deficit in mm
<i>SH</i>	ØSH <sup>1</sup>	interflow storage in mm
<i>SSD</i>	ØSSD	relative sunshine duration in 1/1
<i>S<sub>snow</sub></i>	ØSSTO	snow storage in mm
<i>S<sub>UZ</sub></i>	ØSUZ <sup>1</sup>	storage content of the unsaturated zone
<i>T</i>	ØTEMP	temperature in °C
<i>e</i>	ØVAPO	vapour pressure in mbar or hPa (or: relative air humidity)
<i>u</i>	ØWIND	wind speed in m/s

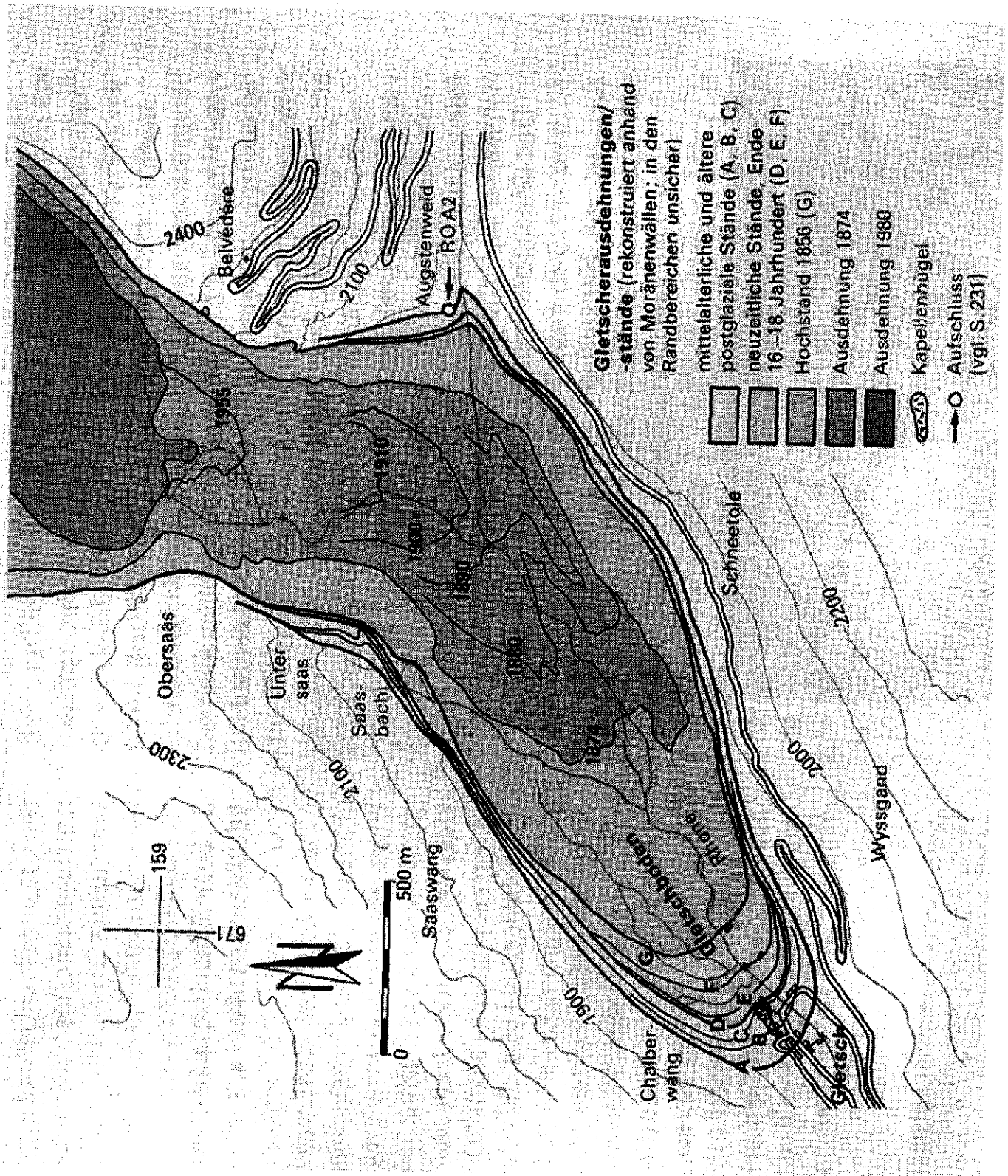
<i>Sym.</i>	data name	description
	<b>Stacks (☒)</b>	<b>bold font in figure 6 (for WaSiM-ETH version 2 only), prefixed with a ☒-Symbol</b>
	☒ <b>CU1..9</b> <sup>2</sup>	concentrations of all modelled tracers in all discretization layers
	☒ <b>HHYD</b> <sup>2</sup>	hydraulic heads in all discretization layers
	☒ <b>QBOT</b> <sup>2</sup>	fluxes between the discretization layers
	☒ <b>THET</b> <sup>2</sup>	water content in all discretization layers
	<b>Punktausgaben (*)</b>	<b>ASCII output files for state variables and fluxes in a single grid cell but for each soil discretization layer</b>
	• <b>CU1..9</b> <sup>2</sup>	concentrations of all modelled tracers in all discretization layers of the control point
	• <b>HHYD</b> <sup>2</sup>	hydraulische Heads in all discretization layers of the control point
	• <b>QBOT</b> <sup>2</sup>	fluxes between all discretization layers of the control point
	• <b>THET</b> <sup>2</sup>	water content in all discretization layers of the control point

<sup>1</sup> only in WaSiM-ETH version 1 (TOPMODEL-approach)

<sup>2</sup> only in WaSiM-ETH version 2 (RICHARDS-approach)

## Appendix 4

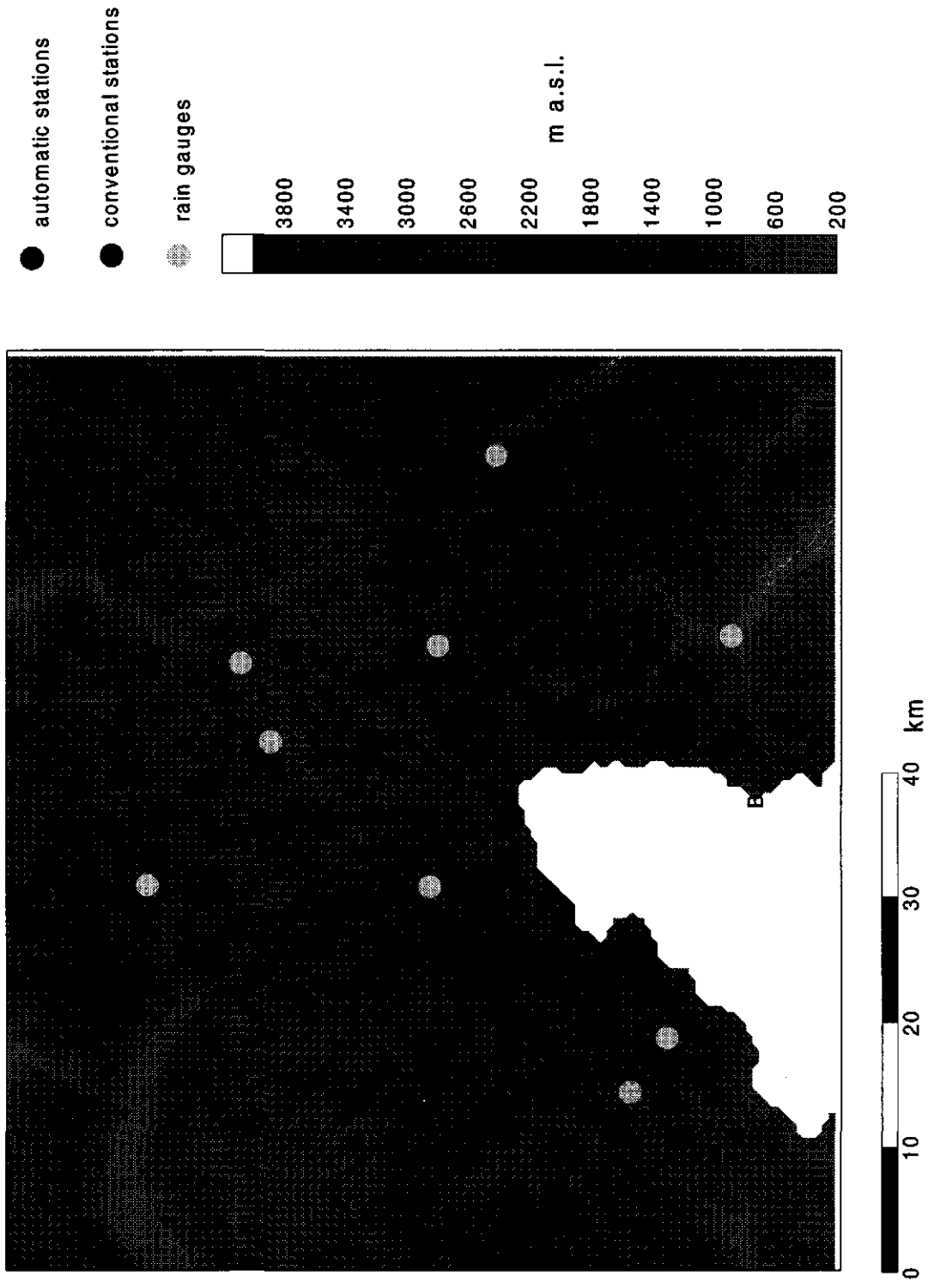
### Retreat of Rhone glacier



## Appendix 5

### Location of meteorological stations

# Meteorological stations in the Rhone/Gletsch catchment region

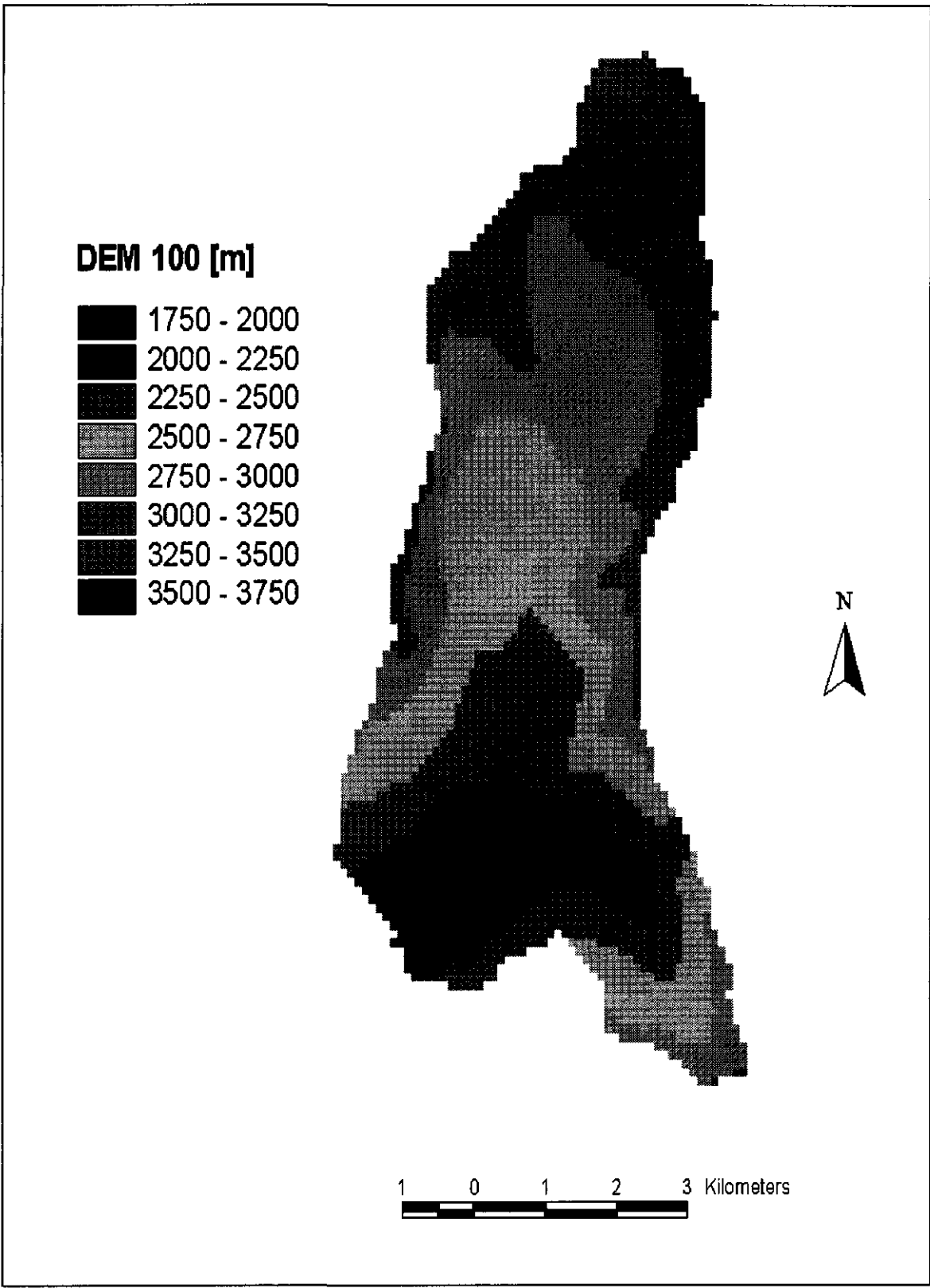




## Appendix 6

### Digital Elevation Model for the Gletsch catchment











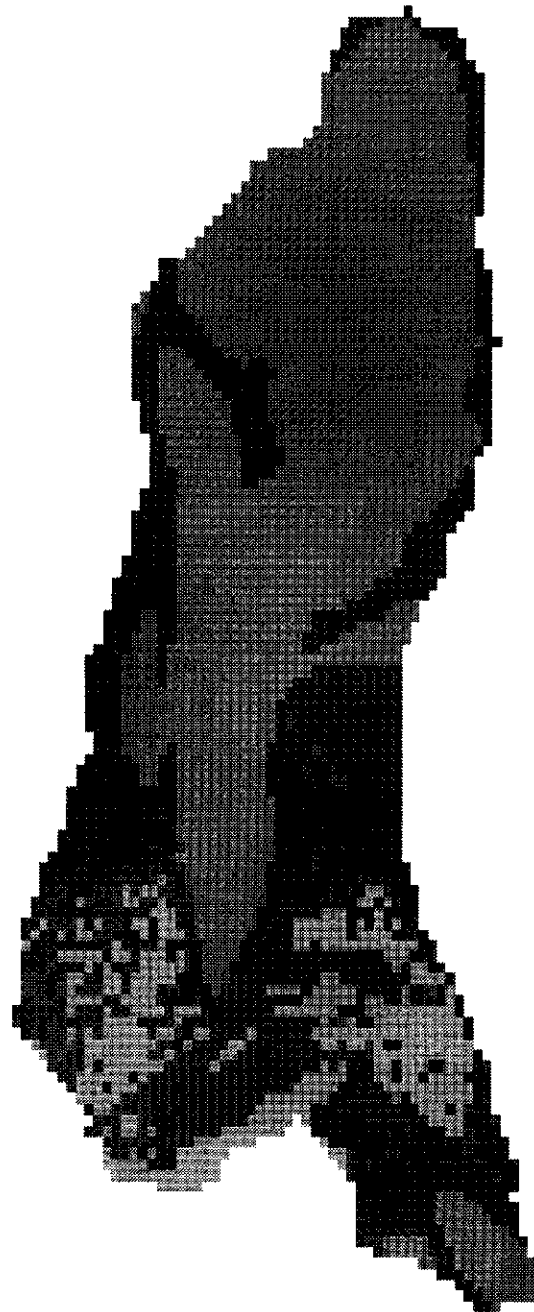


## Appendix 7

### Digital land use grid for the Gletsch catchment

### Landuse classes

-  water
-  settlements
-  forest
-  grass
-  bushes
-  rock
-  glacier (ice)
-  glacier (firn)



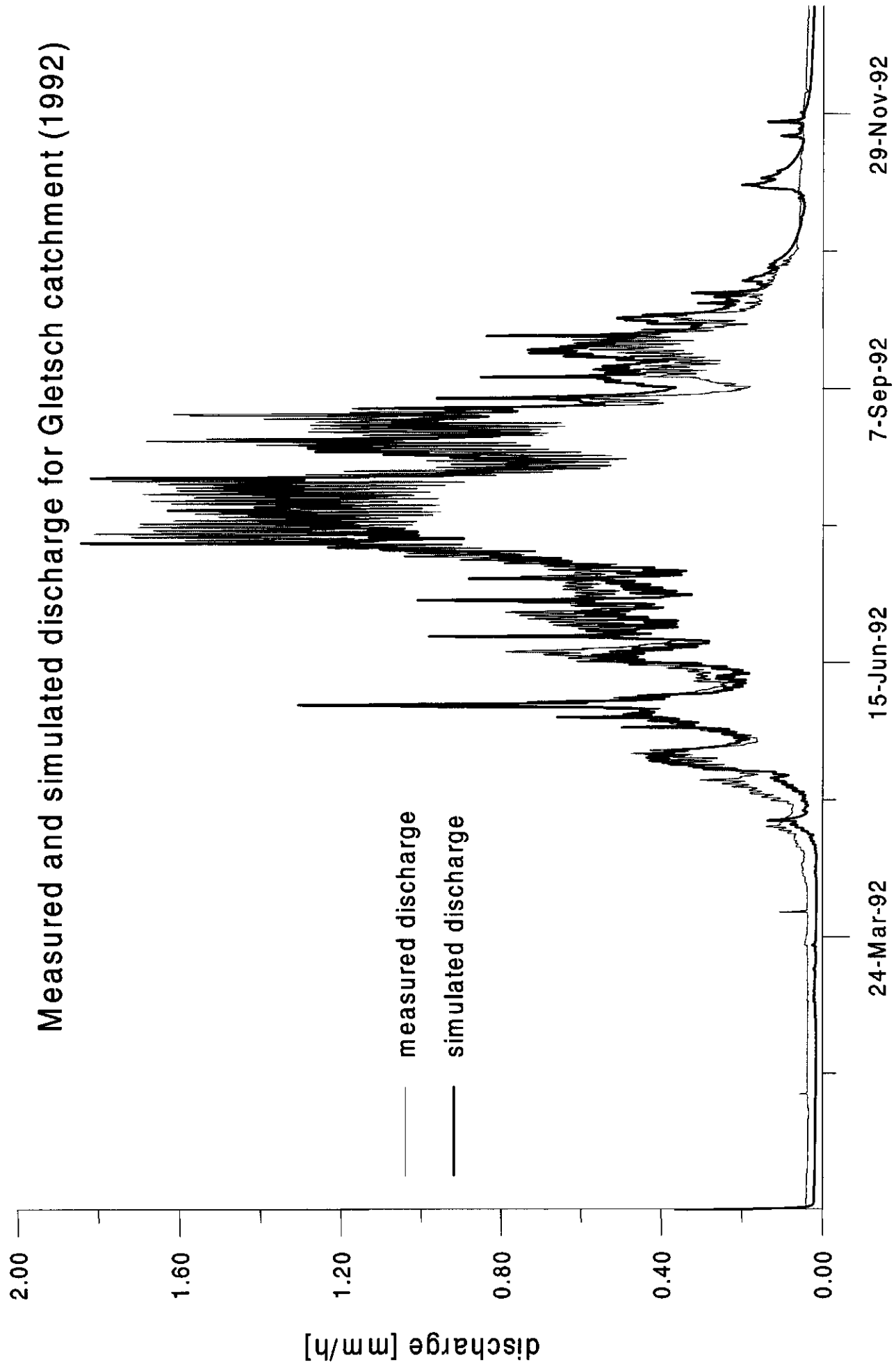
1 0 1 2 3 Kilometers



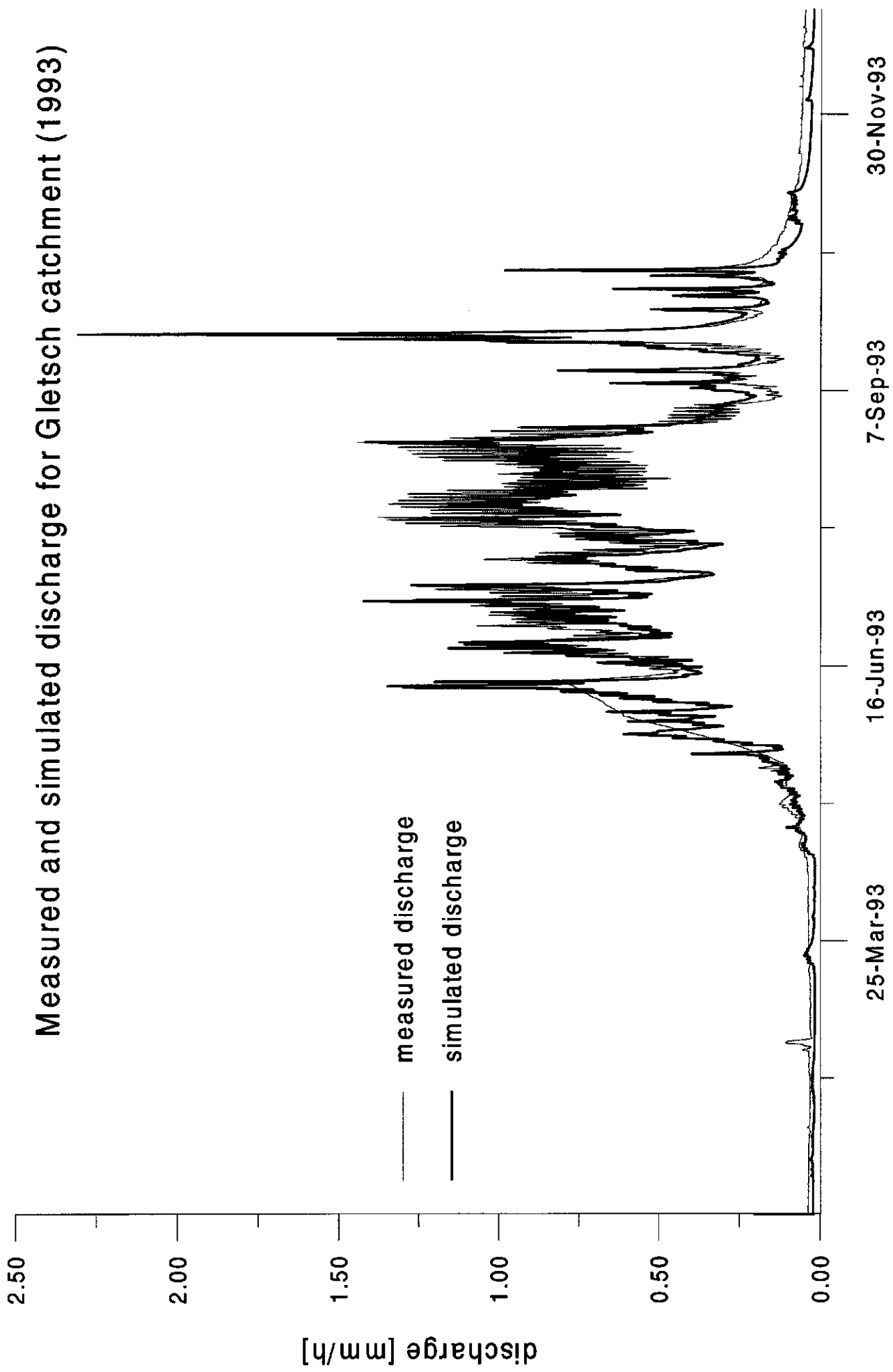
## Appendix 8

Time series for the validation years

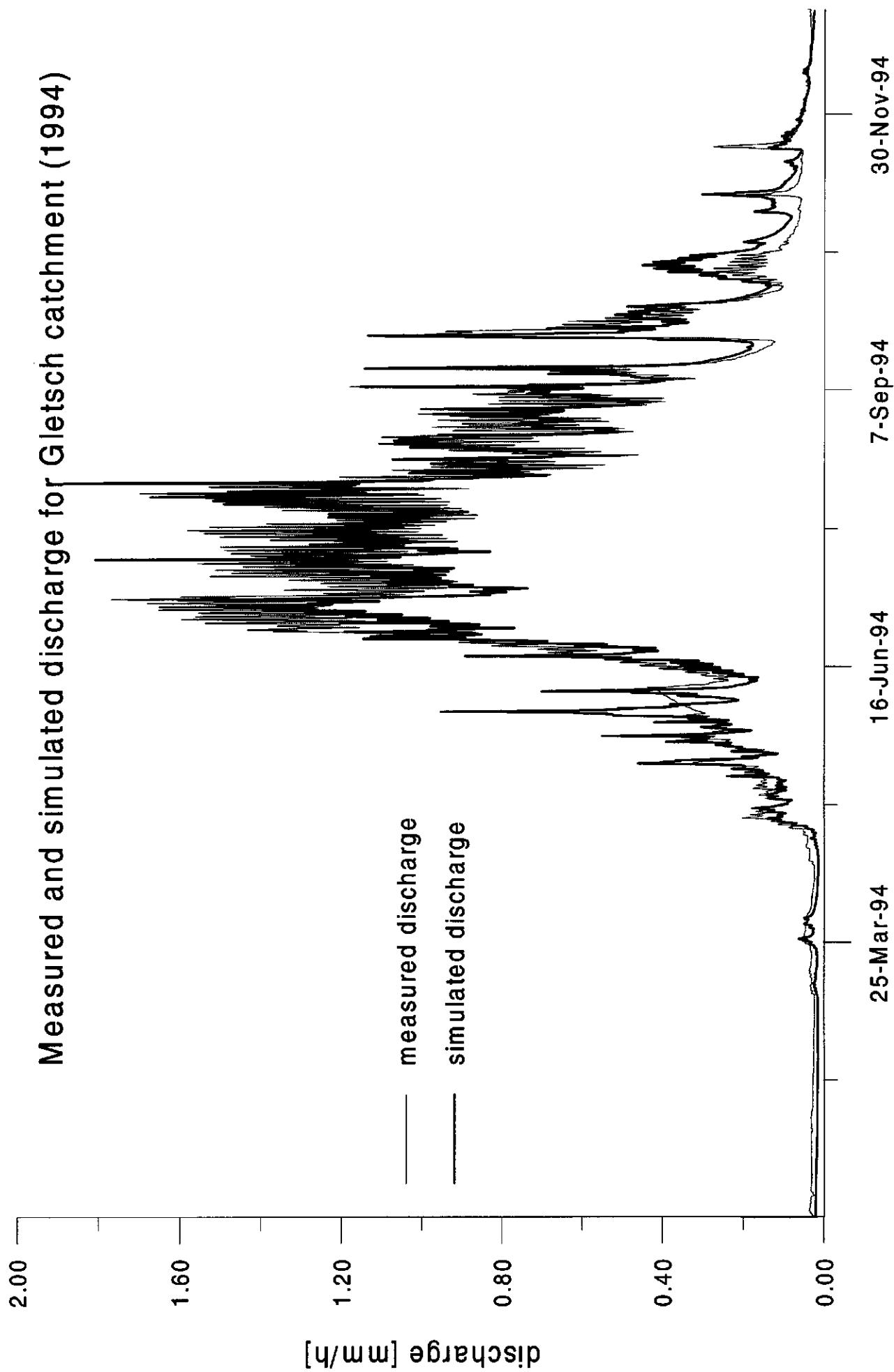
# Measured and simulated discharge for Gletsch catchment (1992)



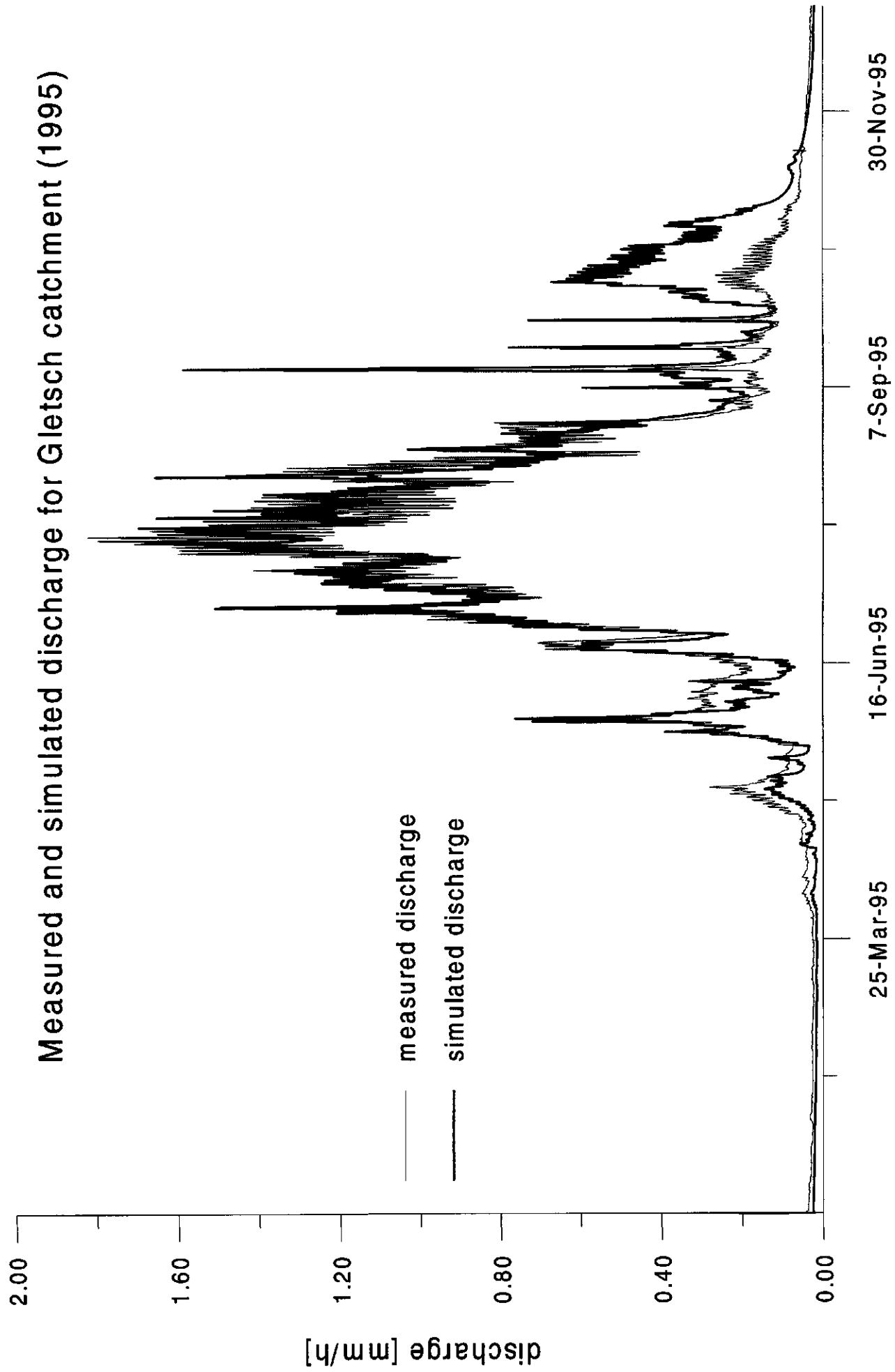
# Measured and simulated discharge for Gletsch catchment (1993)



# Measured and simulated discharge for Gletsch catchment (1994)



# Measured and simulated discharge for Gletsch catchment (1995)





# Measured and simulated discharge for Gletsch catchment (1996)

